

**Aus der Medizinischen Klinik und Poliklinik IV der Ludwig-Maximilians-
Universität München**

Direktor: Prof. Dr. med. Martin Reincke

**Extracellular Histones Cause Vascular Necrosis
in Severe Glomerulonephritis**

Dissertation

zum Erwerb des Doktorgrades der Humanbiologie

an der Medizinischen Fakultät der

Ludwig-Maximilians-Universität München

vorgelegt von

Santhosh Kumar Vankayala Ramaiah

aus Bangalore, Indien

2015

**Mit Genehmigung der Medizinischen Fakultät
der Ludwig-Maximilians-Universität München**

Berichterstatter : Prof. Dr. med. Hans-Joachim Anders

Mitberichterstatter : Prof. Dr. med. Reinhard Lorenz

Mitberichterstatter : Priv. Doz. Dr. Bärbel Lange-Sperandio

Mitberichterstatter : apl. Prof. Dr. Jürgen Scherberich

Dekan : Prof. Dr. med. dent. Reinhard Hickel

Tag der mündlichen Prüfung : 08.10.2015

Table of Contents

Acknowledgement	iv
Zusammenfassung	vi
Summary	viii
1. Introduction	1
1.1. Sterile inflammation.....	1
1.2. Mechanism of sterile inflammation.....	3
1.3. DAMPs and kidney diseases	4
1.4. Extracellular histones	6
1.5. Structure and functions of histones	8
1.6. Mode of histone release into the extracellular space.....	9
1.7. Pathogenic effects of extracellular histones	12
1.8. Contributions of extracellular histones in the disease setting	16
1.9. Extracellular histones as therapeutic target.....	20
1.10. Rapid progressive glomerulonephritis.....	22
2. Hypotheses	26
3. Materials and Methods	27
3.1 Instruments and Chemicals	27
3.2 Experimental procedures.....	33
3.3 Blood and urine sample collection	36
3.4 Urinary albumin to creatinine ratio	37
3.5 Cytokines ELISA	38
3.6 Immunostaining and confocal imaging	39
3.7 Periodic acid-Schiff staining	40
3.8 Histopathological evaluations	40
3.9 Immunohistochemistry in human tissues	42
3.10 Electron microscopy.....	43
3.11 RNA analysis.....	43
3.12 Flow cytometry	47
3.13 In-vitro methods	47
3.14 BWA3 hybridoma culture and anti-histone IgG purification.....	52
3.15 Statistical analysis	53

4. Results	54
4.1. Glomerular expression of TLR2 and TLR4 in human severe glomerulonephritis ...	54
4.2. Extracellular histones drive glomerular cell necrosis in-vitro	57
4.3. Neutrophil extracellular traps kill glomerular endothelial cells through histone release.....	61
4.4. Histones need TLR2/4 to trigger glomerular necrosis and microangiopathy	64
4.5. Extracellular histones contribute to severe glomerulonephritis	67
4.6. Delayed onset of histone neutralization still improves severe glomerulonephritis...	86
4.7. Delayed onset of histone neutralization using combination of histone blocking agents improves severe glomerulonephritis but had no additive effects.....	91
5. Discussion	92
6. Conclusion	97
7. Future Direction	99
8. References	100
9. Abbreviations	115
10. Appendix	116

Declaration

I hereby declare that all of the present work embodied in this thesis was carried out by me from 01/2012 until 01/2015 under the supervision of Prof. Dr. Hans Joachim Anders, Nephrologisches Zentrum, Medizinische Klinik und Poliklinik IV, Innenstadt Klinikum der Universität München. This work has not been submitted in part or full to any other university or institute for any degree or diploma.

Part of the work was supported by others, as mentioned below:

1. Prof. Dr. Christian Hugo and Prof. Dr. Bernd Hohenstein Division of Nephrology, Medizinische Klinik III, Technische Universität Dresden, Dresden, Germany.

They have performed the intra-renal administration of histones into wild type and *Tlr2/4* KO mice to study the involvement of TLRs in histones induced immunopathology. The data are presented in the results part section 4.5 of this thesis.

2. Dr. Helen Liapis, Department of Pathology & Immunology, Washington University School of Medicine, Saint Louis, MO, USA.

She has performed the electron microscopic examination of the kidneys and *in vitro* experiments.

Part of the work has been accepted for publication in *Journal of the American Society of Nephrology* (Feb-2015; doi: 10.1681/ASN.2014070673).

Date:

Signature:

Place: Munich, Germany

(Santhosh Kumar V.R)

Acknowledgement

There are many people who have helped and inspired me during my doctoral study and I would like to convey my gratitude to all of them.

Firstly, I would like to thank **God Almighty** for inspiring, guiding and accompanying me through good and bad times. Without his blessing I would have not come that far in my career.

I'm taking this opportunity to thank my mentor and guide **Prof. Hans-Joachim Anders**. He has patiently provided the vision, encouragement and advice necessary for me to proceed the doctoral program. Thank you very much for giving me the opportunity to work at the Klinische Biochemie, LMU Munich; instilling the confidence in me and your help with the transition to a new professional perspective. I would also like to thank **PD Dr. Volker Vielhauer**, **Prof. Bruno Luckow** and **Prof. Peter Nelson** for their constant encouragement regarding my research work and constructive suggestions throughout my stay at the Klinische Biochemie, LMU and **Prof. Helen Liapis** at the Department of Pathology and Immunology, School of Medicine, Washington University in Saint Louis, Saint Louis, Missouri for sharing her knowledge about microscopy and her cooperation to be able to complete this thesis.

I thank all my **lab friends**, especially **Steffi** for bringing my thesis into a better shape as well as Adriana, Alex, Dana, Jenny, Julian, Jyaysi, Khader, Kirstin, Maciej, Marc, Mi, Murthy, Shrikant, Simone, Xie and all medical students including Anais, George, Hauke, Lukas, Maia, Melissa, Michaela, Moying, Roman, Sophie and Vici for the wonderful time we had together. Special thanks to **Onkar and Supriya** for everything you have done for me both personal- and professional-wise, and for your constant support and guidance, which has helped me very much. You will always be remembered. The chain of gratitude would be incomplete if I would not thank Henny, Dan, Jana, Nuru and Ewa for providing skillful technical assistance to carry out the research work successfully.

There are no words to express my feelings, love and affectionate gratitude to **my family**, my mother and father without their support this would have never become true and my sister and brother-in-law for their faith, love, inspiration, selfless sacrifices and constant encouragement throughout my life.

I am grateful to everybody who has been part of my life and helped me in some ways or others, but if I failed to mention their name, **thank you all.**

It is my duty to express my tearful acknowledgement to the animals, which have been sacrificed for the betterment of human being.

(Santhosh Kumar VR)

Zusammenfassung

Die extrakapilläre proliferative Glomerulonephritis ist durch eine glomeruläre Nekrose gekennzeichnet. Sterbende Zellen setzen intrazelluläre Proteine frei, die als *damage-associated molecular patterns* agieren, um das angeborene Immunsystem zu aktivieren. Im Vorfeld haben wir bereits gezeigt, dass sterbende Tubuluszellen Histone freisetzen, welche Endothelzellen zerstören und den TLR2/4 Rezeptor aktivieren können. Dies führt zu einer tubulären-interstitiellen Entzündungsreaktion bei septischem oder post-ischämischem akuten Nierenversagen (ANV). Weiterhin haben andere Arbeitsgruppen bereits gezeigt, dass extrazelluläre Histone Organversagen bei akuter Lungenschädigung, Schlaganfall, Peritonitis und retinaler Dysfunktion verursachen können, und dass die Blockade von extrazellulären Histonen sich als ein vorteilhaftes Herangehen für das Fortschreiten der Erkrankung präsentiert. In dieser Doktorarbeit haben wir die pathogenen Effekte extrazellulärer Histone während nekrotisierender Glomerulonephritis untersucht. Dies wurde unter Verwendung eines Tiermodells, welches auf einen nekrotisierenden Typ der schweren Glomerulonephritis basiert, erforscht. Nekrotisierende Glomerulonephritis wurde mittels einer einzigen intravenösen Injektion von 100µl Schaf GBM Antiserum induziert. Um den Einfluss der Histon-Neutralisierung zu untersuchen, haben wir einen Antikörper verwendet, der von dem BWA-3 Klon isoliert wurde. Dieser Antikörper besitzt die Fähigkeit, extrazelluläre Histone *in-vitro* und *in-vivo* zu neutralisieren. Nach 7 Tagen wurden die Nieren zur weiteren Analyse entnommen.

Anti-GBM-behandelte Mäuse wiesen eine ansteigende Proteinurie (Albumin/Kreatinin Verhältnis), Plasma-Kreatinin und Harnstoff Werte auf. Dies war mit einer reduzierten Anzahl von Podozyten, ansteigender halbmondförmiger Glomeruli und infiltrierender Neutrophilen und Makrophagen in der Niere verbunden. Interessanterweise wurde die Proteinurie durch die Neutralisierung extrazellulärer Histone reduziert, was zu einem verminderten Podozytenschaden führte. Weiterhin war dies mit einer verbesserten renalen Funktionfähigkeit verbunden im Sinne von niedrigen Plasma-Kreatinin und Harnstoff Werten, und mit einer Abnahme der Neutrophilen und Makrophagen Infiltration und Aktivierung in der Niere. Die Blockade von Histonen reduzierten auch die renale mRNA Expression von TNF- α und Fibrinogen in den glomerulären Kapillaren signifikant, was mit geringeren Glomerulosklerose, Halbmonden und einer tubulären Atrophie assoziiert war. *In-vitro* Studien zeigten, dass extrazelluläre Histone und NETs-verbundene Histone glomeruläre

Endothelzellen, Podozyten und parietale Epithelzellen in einem Dosis-abhängigen Zusammenhang zerstören können. Histon-neutralisierende Mittel, wie Anti-Histon IgG, aktives Protein C oder Heparin unterdrückten diese zytotoxischen Effekte. Die Stimulation von BMDCs mit Histonen regulierte die Expression von Aktivierungsmarkern, einschließlich MHC-II, CD48, CD80 und CD86 hoch sowie steigerte die Produktion von TNF- α und IL-6.

Bisherig wurde von anderen sowie uns berichtet, dass es in Patienten mit ANCA-assoziiierter Vaskulitis zu einer Überexpression des TLR2/4 Rezeptors im Vergleich zu gesunden Glomeruli kommt. Die Histon Toxizität bei Glomeruli ex-vivo war abhängig von der TLR2/4 Rezeptor Achse, da das Ausschalten von TLR2/4 zur Abschwächung der Histon-induzierten renalen thrombotischen Angiopathie und glomerulären Nekrose in Mäusen führte. Anti-GBM Glomerulonephritis involviert NET Formation und vaskuläre Nekrose, während die Blockade von NETs durch PAD Inhibierung oder präventive Anti-Histon IgG Injektion signifikant alle Parameter der Glomerulonephritis reduzierten, einschließlich vaskuläre Nekrose, Podozytenverlust, Albuminurie, Produktion von Zytokinen, Rekrutierung und Aktivierung von glomerulären Leukozyten, und glomerulärer Halbmondformation. Um Histone als therapeutisches Ziel zu evaluieren, wurden Mäuse mit bereits etablierter Glomerulonephritis mit drei verschiedenen Histon-neutralisierenden Mitteln, wie Anti-Histon IgG, aktiviertes Protein C und Heparin, behandelt. Interessanterweise, weisen alle drei Mittel eine gleichwertige Effektivität auf, was zur reduzierten Glomerulonephritis beitrug, wohingegen die Kombinationstherapie keinen additiven Effekt hatte.

Zusammenfassend zeigen die Ergebnisse dieser Arbeit, dass NET-verbundene Histone, welche während der Glomerulonephritis freigesetzt werden, zytotoxische und immunostimulierende Effekte hervorrufen, und dass die Neutralisierung extrazellulärer Histone als potentielle Therapie bei bestehender Glomerulonephritis eingesetzt werden könnte.

Summary

Crescentic glomerulonephritis is characterized by glomerular necrosis. Dying cells release intracellular proteins that act as danger-associated molecular patterns to activate the innate immune system. Previously, we have demonstrated that dying tubular cells release histones, which can kill endothelial cells and activate the toll-like receptor 2/4 (TLR2/4). This drives tubulointerstitial inflammation in septic or post-ischemic acute kidney injury (AKI). Furthermore, other groups have also reported that extracellular histones cause organ damage during acute lung injury, stroke, peritonitis and retinal dysfunction, and that blocking extracellular histones represents a beneficial approach during the disease progression. In this thesis, we investigated whether extracellular histones can elicit similar pathogenic effects during necrotizing glomerulonephritis. To do so, we used an animal model based on the necrotizing type of severe glomerulonephritis. Necrotic glomerulonephritis was induced in mice by a single intravenous injection of 100 μ l sheep anti-GBM antiserum. The impact of histone neutralization was studied by using an antibody isolated from the BWA-3 clone, which had the capacity to neutralize released extracellular histones *in-vivo* and *in-vitro*. After 7 days, mice were sacrificed and kidneys were collected for further data analysis. Proteinuria was assessed in spot urine samples.

Anti-GBM treated mice showed increased proteinuria (albumin/creatinine ratio), plasma creatinine and BUN levels. This was associated with a reduced number of podocytes, increased crescentic glomeruli and the infiltration of neutrophils and macrophages into the kidney. Interestingly, neutralization of extracellular histones significantly reduced proteinuria leading to less podocyte damage. This was linked to an improved renal function defined by lower plasma creatinine and BUN levels, and with a decrease in neutrophil and macrophage infiltration and activation in kidney. Histone blockade also significantly reduced renal mRNA expression of TNF- α and fibrinogen in the glomerular capillaries, which was associated with less glomerulosclerosis, crescents and tubular atrophy. *In-vitro* studies demonstrated that extracellular histones and NETs-related histones kill glomerular endothelial cells, podocytes and parietal epithelial cells in a dose-dependent manner. Histone-neutralizing agents such as anti-histone IgG, activated protein C or heparin prevented this cytotoxic effect. Stimulation of BMDCs with histones upregulated the expression of the activation marker including MHC-II, CD48, CD80 and CD86 significantly as well as increased the production of TNF- α and IL-6.

It has been previously reported by others including us that in biopsies from patients with ANCA-associated vasculitis showed an over-expression of the TLR2/4 receptor compared to the healthy glomeruli. Histone toxicity on glomeruli *ex-vivo* was also dependent on the TLR2/4 receptor axis given that the lack of TLR2/4 attenuated histone-induced renal thrombotic microangiopathy and glomerular necrosis in mice. Anti-GBM glomerulonephritis involved NET formation and vascular necrosis, while blocking NET formation via PAD inhibitor or pre-emptive anti-histone IgG injection significantly reduced all parameters of glomerulonephritis including vascular necrosis, podocyte loss, albuminuria, cytokine induction, recruitment and activation of glomerular leukocytes, and glomerular crescent formation. Finally, to evaluate histones as a therapeutic target, mice with established glomerulonephritis were treated with three different histone-neutralizing agents such as anti-histone IgG, recombinant activated protein C and/or heparin. Interestingly, all agents were equally effective in abrogating severe glomerulonephritis, while combination therapy had no additive effect.

In summary, the results of this thesis indicate that NET-related histones released during glomerulonephritis elicit cytotoxic and immunostimulatory effects and that neutralizing extracellular histones, therefore, represents a potential therapeutic approach when applied during already established glomerulonephritis.

1. Introduction

1.1. Sterile inflammation

Inflammation is vital for host defence against invasive pathogens¹. In response to an infection, a cascade of signals leads to the recruitment of inflammatory cells by activating pattern recognition receptors (PRRs), particularly in innate immune cells such as neutrophils and macrophages. These cells, in turn, phagocytose infectious agents and produce additional cytokines and chemokines that lead to the activation of lymphocytes and adaptive immune responses. It is now evident that PRRs also recognize non-infectious material that can cause tissue damage and endogenous molecules that are released during cellular injury and death. These endogenous molecules have been termed damage-associated molecular patterns (DAMPs) (Table 1), as these host-derived non-microbial stimuli are released following tissue injury or cell death and have similar functions as pathogen-associated molecular patterns (PAMPs) in terms of their ability to activate pro-inflammatory pathways².

In 1994, Polly Matzinger proposed that the immune system is more concerned with ‘danger’ or ‘damage’ than with the distinction between self and non-self³. The model starts with the idea that the immune system defines danger as anything that causes tissue stress or destruction^{4,5}. In this model, antigen-presenting cells are activated by DAMPs from stressed and/or damaged tissues. Matzinger’s ‘danger model’ suggests why potent immune responses are initially elicited in the setting of sterile inflammation⁵.

DAMPs are cell-derived molecules that can initiate and perpetuate immunity in response to trauma, ischemia, cancer, and other settings of tissue damage in the absence of overt pathogenic infection. DAMPs are localized within the nucleus and cytoplasm (HMGB1), cytoplasm alone (S100 proteins), exosomes [heat shock proteins (HSP)], the extracellular matrix (hyaluronic acid), and in plasma components such as complement (C3a, C4a and C5a). Examples of non-protein DAMPs include ATP, uric acid, heparin sulfate, RNA, and DNA. DAMPs can also be mimicked by release of intracellular mitochondria consisting of formyl peptides and mitochondrial DNA (with CpG DNA repeats) to activate human polymorphonuclear neutrophils through activation of TLR9⁶.

Table: 1. List of the sterile inflammatory signals, its receptors and associated pathology². (The table is adapted from Chen *et al.* Nature Reviews Immunology, 2010)

Sterile inflammatory signal	Putative sensor	Associated pathology
<i>Endogenous</i>		
HMGB1	TLR2, TLR4, TLR9, RAGE and CD24	Cellular injury and necrosis
HSPs	TLR2, TLR4, CD91, CD24, CD14 and CD40	Cellular injury and necrosis
S100 proteins	RAGE	Cellular injury and necrosis
SAP130	CLEC4E	Cellular injury and necrosis
RNA	TLR3	Cellular injury and necrosis
DNA	TLR9 and AIM2	Cellular injury and necrosis
Uric acid and MSU crystals	NLRP3	Gout
ATP	NLRP3	Cellular injury and necrosis
Hyaluronan	TLR2, TLR4 and CD44	Cellular injury and necrosis
Biglycan	TLR2 and TLR4	Cellular injury and necrosis
Versican	TLR2	Cellular injury and necrosis
Heparan sulphate	TLR4	Cellular injury and necrosis
Formyl peptides (mitochondrial)	FPR1	Cellular injury and necrosis
DNA (mitochondrial)	TLR9	Cellular injury and necrosis
CPPD crystals	NLRP3	Pseudogout
β -amyloid	NLRP3, CD36 and RAGE	Alzheimer's disease
Cholesterol crystals	NLRP3 and CD36	Atherosclerosis
IL-1 α	IL-1R	Cellular injury and necrosis
IL-33	ST2	Cellular injury and necrosis
<i>Exogenous</i>		
Silica	NLRP3	Silicosis and pulmonary interstitial fibrosis
Asbestos	NLRP3	Asbestosis and pulmonary interstitial fibrosis

1.2. Mechanism of sterile inflammation

Despite the growing list of sterile immune stimuli, the mechanisms by which these stimuli trigger an inflammatory response are still not fully understood. Even though endogenously generated DAMPs are structurally heterogeneous, the outcome of inflammatory responses to these stimuli is generally uniform. The release of DAMPs from dying cells is illustrated in the Figure 1.

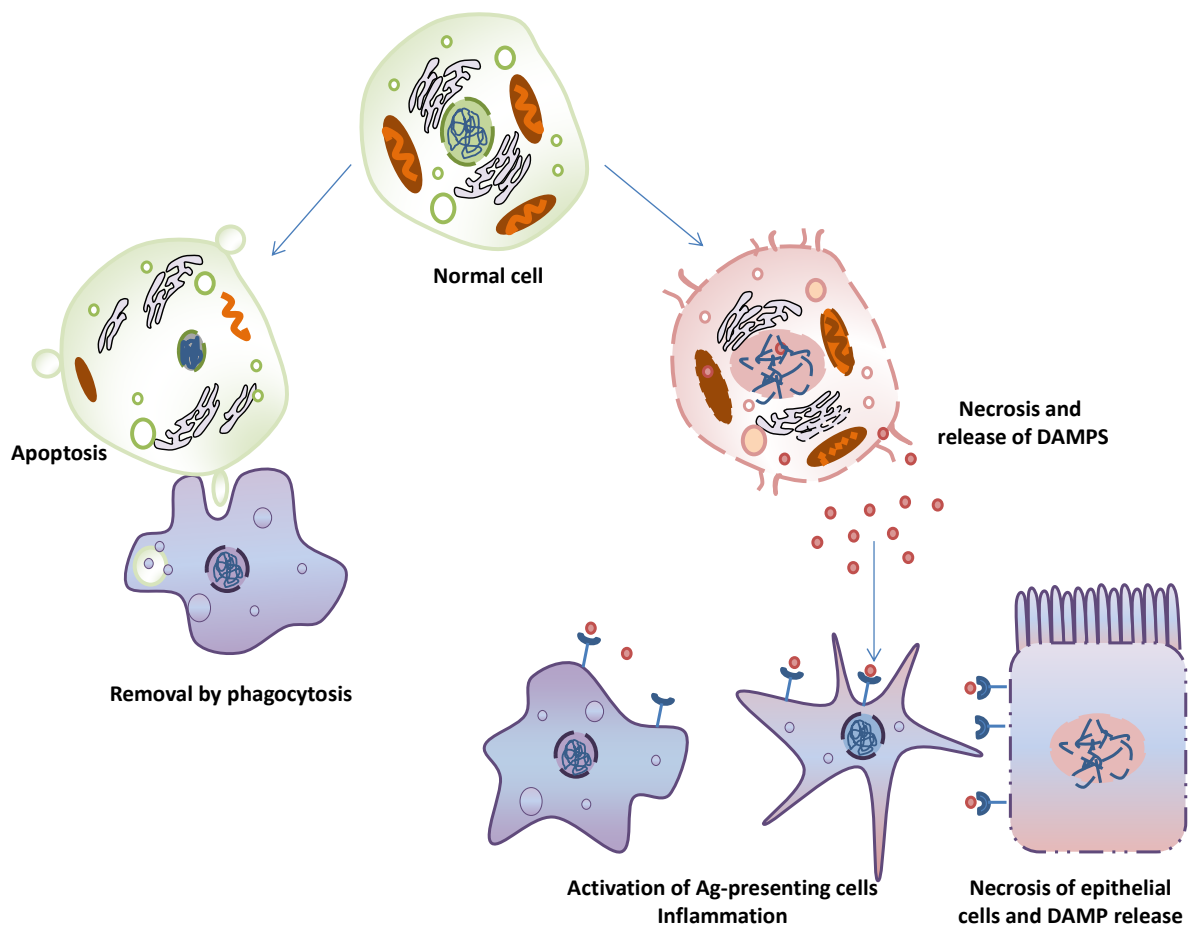


Figure: 1. During homeostasis most commonly cells in the body undergo apoptosis and they are removed by phagocytosis without any injury to the targeted organ and replaced by new cells of the same phenotype. When there is irreversible stress or toxin exposure, the cells undergo a pathogenic form of cell death such as necrosis that results in the release of cellular contents called damage-associated molecular patterns (listed in table 1). These damage-associated molecular patterns will be recognized by pattern recognition receptors on immune cells to activate the release of pro-inflammatory cytokines and chemokines. The released DAMPs can also kill cells within the targeted organs to cause severe inflammatory responses leading to organ failure.

Moreover, inflammatory responses during infection are very similar to responses induced by sterile stimuli including the recruitment of neutrophils and macrophages, the production of inflammatory cytokines and chemokines, and the induction of T cell-mediated adaptive immune responses⁷. This suggests that both infectious and sterile stimuli may function through common receptors and pathways. Based on the current understanding, there are three proposed mechanisms by which sterile endogenous stimuli trigger inflammation: (1) the activation of PRRs by mechanisms similar to those used by microorganisms and PAMPs, (2) the release of intracellular cytokines and chemokines, such as interleukin (IL)-1 α , that activates common pathways downstream of PRRs, and (3) the direct activation of receptors that are not typically associated with microbial recognition².

1.3. DAMPs and kidney diseases

Currently, most of the experimental data provide information about DAMPs playing an important role in the progression of kidney diseases. Indirect evidence from animal model, where mice lacking specific DAMP receptors showed protection of kidney diseases that will be further discussed within this section.

1.3.1. Acute kidney injury

Tubular necrosis

Compared to all other forms of kidney diseases, acute kidney injury (AKI) always linked to cells with abundant amounts of necrosis, which leads to inflammatory DAMPs release and activation of innate and adaptive immunity triggering inflammation with aggravated AKI. The injury is mainly caused due to the activation of DAMP receptors like toll-like receptors (TLRs) and receptor for advanced glycation end-products (RAGE).⁸ For example high-mobility group protein B1 (HMGB1), heat shock proteins (HSPs) and histones are well-known DAMPs that are released during tubular necrosis as in the case of septic, ischemic, or toxic forms of tubular necrosis. This further drives sterile inflammatory and immune pathologies that regulate organ failure⁹⁻¹⁵. Reports have shown that death during sepsis is mainly due to the release of DAMPs like HMGB1, histones, decorin, or biglycan^{10,13,16,17}. The lethality is based on DAMP-mediated endothelial dysfunction, which involves TLR2/4 receptors leading to increased vascular permeability and hypovolemic shock¹⁸. HSP and gp96

regulate the TLR2-mediated ERK pathway and inflammation during hypoxia or ischemic kidney conditions¹⁹. Geldanamycin, an inhibitor of Hsp90 and gp96, protects mice from IRI²⁰. Non-pathogenic and non-cellular DAMPs like high concentrations of uric acid accumulate during the ischemic kidney and activate the immune system leading to the severe inflammation in the kidney²¹.

Glomerulonephritis

Glomerular cells undergoing necrosis also release DAMPs during the necrotizing type of glomerulonephritis leading to AKI and glomerulonephritis (GN)²². Serum and tissue expression levels of HMGB1 are reported during experimental models of glomerulonephritis. Like in tubular necrosis, TLR2/4 deficiency reduces the complications of glomerulonephritis^{23,24}. Histones on the other hand are released from NETting neutrophils in necrotizing GN²⁵.

1.3.2. Chronic kidney injury

Diabetic nephropathy

Inflammatory responses mediated by activation of TLR2, TLR4 and the NLRP3 inflammasome play key roles in the progression of diabetic nephropathy (DN)^{26,27}. Reactive oxygen species or extracellular ATP can activate the NLRP3 inflammasome during diabetic conditions^{26,28}. The ATP receptor P2X4 is over expressed on renal TECs from patients with type 2 DN conditions; this is mainly due to the hyperglycaemic complications of diabetes, which correlates with the release of IL-1 cytokines²⁶. Biglycan and decorin are overexpressed in diabetic kidneys and may trigger inflammation by activating the TLR2/TLR4 receptors and the NLRP3 inflammasome²⁹⁻³¹. An increase in renal biglycan promotes LDL cholesterol, which leads to the infiltration of macrophages and upholds kidney injury³⁰.

There is expansive literature on the involvement of AGE and RAGE in podocytes, diabetes, and DN³²⁻³⁷. S100, a pro-inflammatory RAGE ligand, is involved in a novel pathway for leukocyte recruitment during inflammatory disorders and diabetic conditions in mice³⁸. RAGE and S100 are over-expressed in the podocytes of *db/db* mice, which contributes to both renal pathology and inflammation with increased infiltration of mononuclear phagocytes to the glomeruli. These effects can be blocked with the anti-RAGE antibody³⁹.

Lupus nephritis

Lupus nephritis is an inflammatory kidney disease caused by the autoimmune disorder systemic lupus erythematosus (SLE), which involves immune activation by nuclear DAMPs that share autoantigen and adjuvant qualities⁴⁰. The disease is mainly characterized by hyperproliferation of autoreactive lymphocytes, which enhance the autoantigen presentation. The effect is due to the activation of TLR7 and TLR9 receptor activating DAMPs like Ribonucleoproteins and hypomethylated dsDNA, respectively⁴¹. In addition, these TLR7- and TLR9-specific DAMPs trigger plasmacytoid dendritic cells to release IFN- α , which initiates antiviral gene transcription accounting for many of the unspecific (viral infection-like) symptoms of lupus⁴² and IFN-related glomerular pathology⁴³. TLR7 and TLR9 activation also leads to the generation and maturation of M1 type macrophages, which further activates the pathogenicity of lupus nephritis⁴⁴⁻⁴⁶. Biglycans has been shown to trigger lupus nephritis by activating TLR2 and TLR4 leading to the over expression of chemokines including CCL2, CCL3 and CCL5, and aggravated murine lupus nephritis⁴⁷.

Pathogenic effects of HMGB1 have been linked to a variety of pro-inflammatory and autoimmune diseases including SLE. Reports have shown that SLE patients have high levels of circulating HMGB1, which is also the case in mouse models of SLE⁴⁸⁻⁵⁰. The pathogenic effect of HMGB1 is mainly due to the antibody-induced immune complex deposition, a type of kidney damage in SLE⁵¹. In lupus-prone MRL-Fas(lpr) mice, p38 MAPK activation induced infiltration and maturation of dendritic cells (DCs) and secretion of HMGB1 from DCs has been implicated in autoimmune kidney diseases⁵².

1.4. Extracellular histones

Histones are important structural elements of the nuclear chromatin and can regulate gene transcription. In contrast, outside the cell histones elicit toxic and immunostimulatory effects. This becomes obvious when infectious organisms trigger granulocytes (and macrophages) to undergo a particular type of programmed cell death that catapults the chromatin outside the cell to cover and kill pathogens, e.g. NETosis. Pro-inflammatory cytokines also have the ability to induce the process of NETosis, which contributes to sterile forms of inflammation

and tissue injury. As illustrated in figure 2, which describes in more detail how the histone component of extracellular chromatin mediates injury and triggers innate immunity including activation of TLRs or inflammasomes (Figure 2). Furthermore, we discuss how to target extracellular histones to improve disease outcomes using different histone blocking agents.

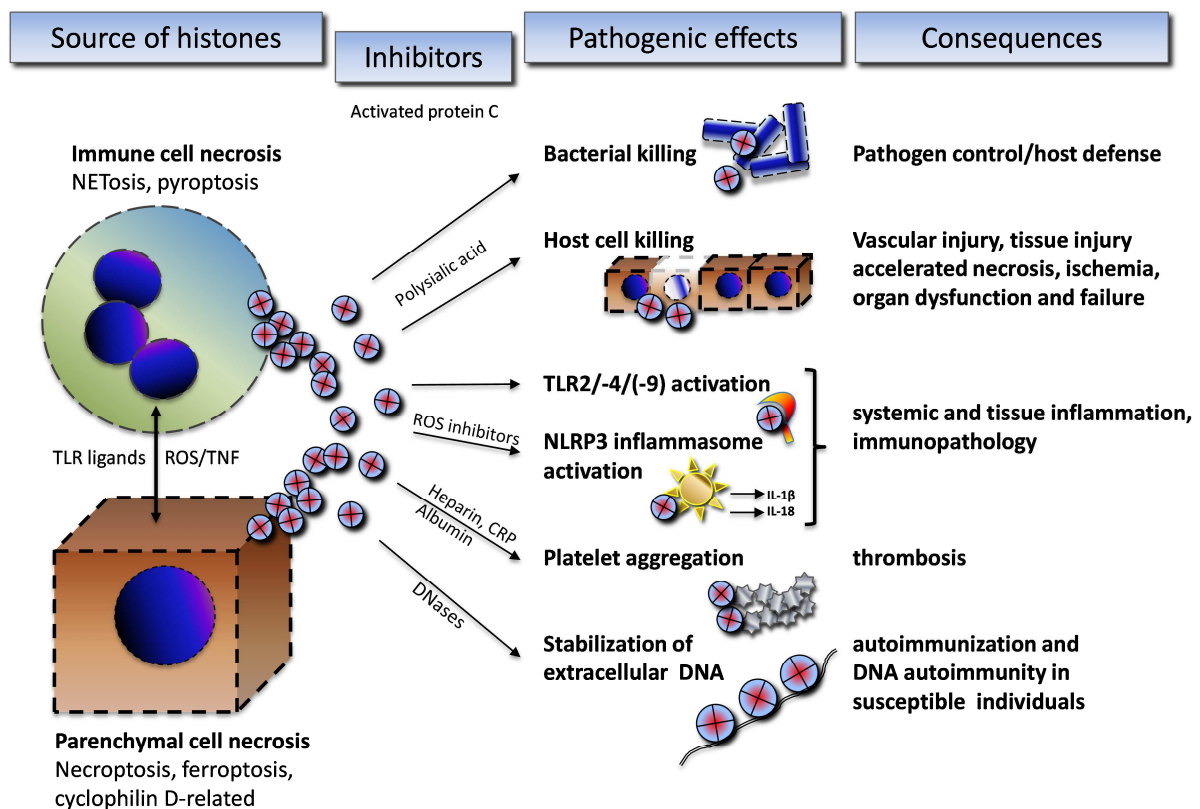


Figure: 2. How histones trigger tissue injury and inflammation. Various forms of cell necrosis release chromatin into the extracellular space. Histone-specific effects and their consequences for the disease. A number of molecules inhibit histone effects such as, Activated protein C degrades histones in the extracellular space. Other elements can also neutralize the specific effects without degrading the histone structure like heparin, albumin and neutralizing histone antibody⁵³.

1.5. Structure and functions of histones

The eukaryotic cell nucleus maintains DNA and histones in a highly organized chromatin format, which is conserved across species. There are five classes of histones: H2A, H2B, H3 and H4 that are known as ‘core histones’, while H1 represent ‘linker histones’⁵⁴. Structurally, all core histones share a common structural motif consisting of a long central helix flanked by a helix-strand-helix motif on each end. This “histone fold” exhibits high hydrophobic interactions to form dimers and tetramers within the core histones (Figure 3). The organizational unit of chromatin, the nucleosome consists of one H3/H4 tetramer and two H2A/H2B dimers also called the “histone octamer”, coiling 147bp of DNA in approximately two parallel strands, while H1 binds to non-nucleosomal DNA to form higher-order chromatin structures. These octamers are stabilized by C-terminal helices of core histones. The basic nature of the histone proteins neutralizes the acidic residues of the DNA. Each histone has its N-terminal tail rich in lysine and arginine residues that extend out from the core structure. These amino-terminal sites are flexible and undergo numerous post-translational modifications such as acetylation, phosphorylation, methylation, ubiquitination, sumoylation, and ADP ribosylation, which play a key role in gene replication and regulation⁵⁵.

Histone methylation, phosphorylation and acetylation serve as markers for the transcriptional state of genes in several diseases and distinct post-translational modification patterns are linked to certain inflammatory diseases⁵⁶. While histones are completely inert within the nucleus, they elicit pathogenic effects outside the cell. Histones are released from dying cells and contribute to antimicrobial defence responses during infection^{10,57}.

However, extracellular histones are a double-edged sword because they also damage host tissue and may cause death. But when and how histones access the extracellular space? This is discussed in the next section.

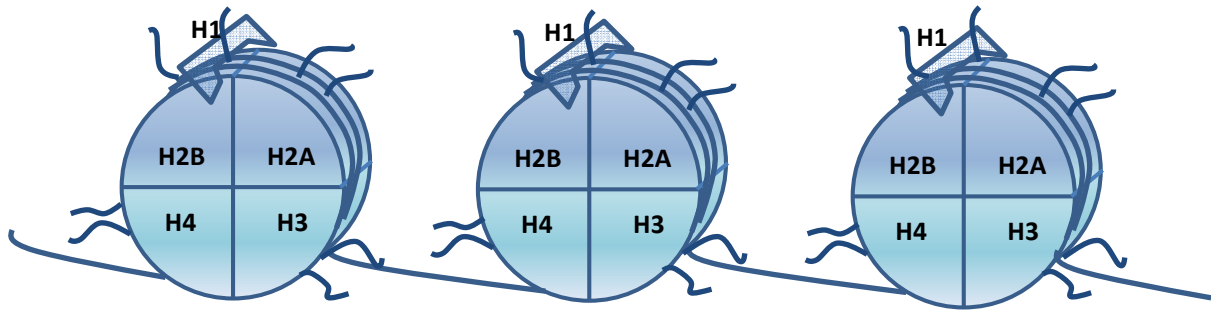


Figure: 3. Structure of histone octamer with the core histones H2A, H2B, H3 and H4 and the linker histone H1. Coiled dsDNA surrounds the histones, which forms the complete nucleosome.

1.6. Mode of histone release into the extracellular space

Releasing chromatin requires rupture of the nuclear and outer cell membrane, e.g. during cell death⁵⁸. Apoptosis avoids membrane disintegration, therefore apoptosis was considered a ‘silent death’ that rather contributes to cell turnover and lymphocyte selection during homeostasis⁵⁹. However, histones have been reported to accumulate in and leak also from membrane blebs of apoptotic cells⁶⁰. In contrast, disruption of the outer plasma membrane, as it occurs during necrotic cell death, massively releases intracellular components that have the capacity to activate innate immunity, referred to as danger/damage-associated molecular patterns (DAMPs) or alarmins. Later the histones reach the extracellular space and act as DAMPs to activate innate immunity⁶¹. The forms of necrosis that exist in the biological system will be described in more detail within this section.

1.6.1. Necrosis

Necrosis is an active form of cell death and occurs predominantly due to the irreversible stress on tissue cells, e.g. hypoxia, radiation, changes in pH or toxic chemicals. Necrosis leads to the complete destruction of the cell integrity resulting in the release of DAMPs followed by the loss of function.

1.6.2. Passive necrosis

Mechanical trauma or charge- or detergent-related toxicity passively disrupt the plasma membrane⁵⁹. In view of recent data on regulated forms of necrosis, it is fair to speculate that passive necrosis is a rather rare event in clinical medicine⁶². Regulated necrosis is defined as a genetically controlled cell death process that eventually results in cellular leakage, and it is morphologically characterized by cytoplasmic granulation, as well as organelle and/or cellular swelling ('oncosis')⁶². The different forms of regulated necrosis are as follows.

NETosis/ETosis

NETosis/ETosis is a regulated form of necrosis that is restricted to immune cells like neutrophils (NETosis) and other granulocytes or macrophages (ETosis)⁶². Pro-inflammatory cytokines such as IL-8 or TNF- α can activate neutrophils to undergo regulated burst, a process that takes up to 6 hours and spreads all chromatin to the outside of the cells in a net-like structure NETs (neutrophil extracellular traps)⁶³. Akt- and NOX2-dependent reactive oxygen species facilitate and trigger NETosis⁶⁴ as well as the activation of TLR2, TLR4, complement, and platelet^{65,66}. NETosis results in the release of histones from cells that are present at sites of infection as well as during sterile inflammation^{25,62}.

Pyroptosis

Pyroptosis is mechanistically distinct from other forms of cell death. Caspase 1 dependence is a defined feature of pyroptosis, and caspase 1 is the enzyme that mediates this process of cell death^{67,68}. However, caspase 1 is not involved in apoptotic cell death that was confirmed in caspase 1-deficient mice, which had no defects in apoptosis and developed normally. Pyroptosis also involves the involvement of a Caspase 11-dependent form of regulated necrosis downstream of inflammasome activation⁶⁹. Until now, pyroptosis has mainly been described in infected macrophages and as being responsible for the loss of T cells in patients with AIDS^{70,71}. Its role in tissue necrosis remains to be explored. The apoptotic caspases including caspase 3, caspase 6 and caspase 8 are not involved in pyroptosis^{72,73}, and substrates of apoptotic caspases including poly (ADP-ribose) polymerase and inhibitor of caspase-activated DNase (ICAD) do not undergo proteolysis during pyroptosis^{67,68,74,75}.

Necroptosis

Necroptosis is a mechanism of necrotic cell death induced by external stimuli leading to the engagement of death domain receptors (DRs) with their respective ligands such as TNF- α , Fas ligand (FasL) and TRAIL. This happens under conditions when apoptotic cell death execution is prevented, e.g. by caspase inhibitors. Although it occurs under regulated conditions, necroptotic cell death is characterized by the same morphological features as unregulated necrotic death. RIP1 kinase activity is a key step in the necroptosis pathway, followed by the activation of RIP3 kinase and phosphorylation of MLKL, which form a complex known as the necroptosome. Necroptosis may be a central mode of regulated necrosis under inflammatory conditions⁷⁶⁻⁷⁸.

Cyclophilin D-mediated regulated necrosis

Cyclophilin D-mediated regulated necrosis disrupts the mitochondrial transmembrane potential, which opens mitochondrial membranes and translocates NAD⁺ to the cytosol^{79,80}. Mitochondrial dysfunction is the first step in ischemia-associated forms of regulated necrosis⁸¹.

Ferroptosis

The oncogenic RAS-selective lethal small molecule erastin triggers a unique iron-dependent form of non-apoptotic cell death, called ferroptosis. Ferroptosis is dependent on intracellular iron, but not other metals, and is morphologically, biochemically and genetically distinct from apoptosis, necrosis and autophagy⁸². Oxidative stress is also a trigger for ferroptosis, a recently described iron-dependent form of regulated necrosis. Under normal conditions, glutathione peroxidase 4 levels inhibit ferroptosis, and its depletion during oxidative stress can set off the cell death event⁸³.

Podoptosis

Podoptosis is another regulated cell death pathway occurs mainly in non-dividing cells like podocytes, it is mainly due to the p53-overactivation-dependent cell death, thus, referred as podoptosis. Podoptosis is associated with cytoplasmic vacuolization, endoplasmic reticulum stress, and dysregulated autophagy leading to the release of DAMPs⁸⁴.

1.7. Pathogenic effects of extracellular histones

Some of the reported pathogenic effects of released extracellular histone are illustrated in the Figure 4 and will be further discussed in this section.

1.7.1. Bactericidal effects

In late 1950s, James G. Hirsch first reported that the arginine-rich fraction of calf thymus histone (histone B) exerts bactericidal activity on various coliform bacilli and micrococci under certain conditions *in-vitro*⁵⁷. Concentrations less than 1µg/ml histones kill susceptible microbes without detectable morphological alteration or lysis. This was later confirmed by other groups^{63,85-87}. Microorganisms which are highly susceptible to histone toxicity are *Escherichia*, *Salmonella*, *Shigella*, *Pseudomonas*, *Klebsiella*, and *Micrococcus pyogenes var. albus*. Less susceptible or completely resistant are *Proteus*, *Serratia*, *Micrococcus pyogenes var. aureus*, and various types of hemolytic streptococci. but the mode of this bactericidal effect remained unknown⁵⁷. It has been suggested that their basic charge and their capacity to bind strongly to anionic moieties of the bacterial cell wall damage the osmotic barrier⁵⁷.

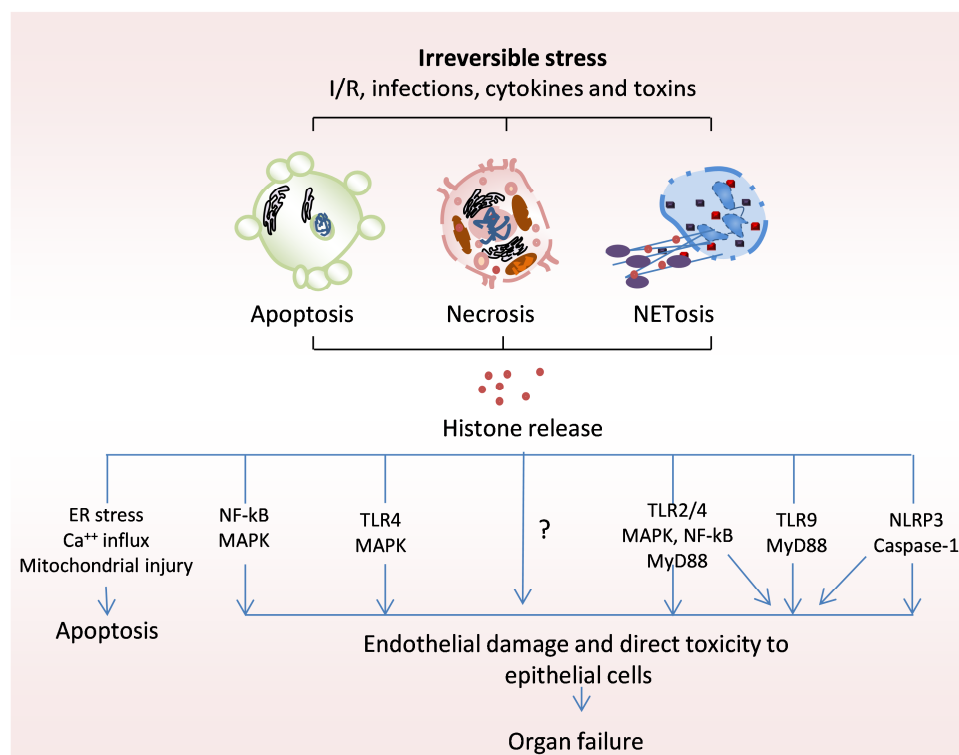


Figure: 4. Release and activity of histones in response to stress⁸⁸ and its pathogenic effects on different organs

1.7.2. Cellular toxicity

Xu *et al.* reported for the first time that the unspecific cytotoxic effects of extracellular histones on the host leading to lethal effects during sepsis¹⁰. Histone release in sepsis or major trauma primarily affects endothelial cells that can cause fatal organ dysfunction^{10,89}. Intravenous injection of recombinant histones kills healthy mice within a few minutes due to severe endothelial damage in the microvasculature of the lungs¹⁰. Similarly, injection of histones into the renal artery causes microvascular injury and ischemic renal necrosis⁹. Histone-induced endothelial permeability and death is a non-regulated form of necrosis that is mediated through a charge-dependent mechanism resulting in disruption of junctional protein expression and cell death⁹⁰. In fact, the anionic molecule polysialic acid can abrogate NET-mediated alveolar epithelial injury⁹¹. However, despite having a similar charge only histone H1, but not H2A, H2B, H3, and H4 is neurotoxic⁹², which suggests cell type-specific effects. For example, histone H1 kills neurons but not astrocytes or microglia⁹². In addition, it is currently not known whether histones trigger any of the recently described forms of regulated necrosis⁶².

1.7.3. TLR activation

Xu *et al.* has recently shown that histones specifically induce TLR2- and TLR4-mediated reporter gene expression in a cell line overexpressing different classes of TLRs¹⁰. Histones can also bind and activate the TLR2 and TLR4 receptors leading to the activation of the Myd88 pathway, which further results in an inflammatory response by activating NF- κ B and mitogen activated protein kinase target gene expression^{9,93,94}. Furthermore, histone-induced tissue injury is partially dependent on TLR2/4^{9,94} that is to other cell-derived extracellular DAMPs, which activate predominantly TLR2/4 receptors and show immunogenic actions⁹⁵. Whereas, Huang *et al.* reported that extracellular histones activate TLR9 and contribute to postischemic liver failure in a TLR9-dependent manner⁹⁶. In this study, anti-histone IgG had almost a comparable protective effect on organ function as TLR9 gene deletion, yet in gene-deleted mice. These antibodies did not show any additional effect⁹⁶. However, in our *in-vitro* studies, Allam *et al.* could not confirm the data from Huang and colleagues that TLR9 acts as a receptor for histones⁹, possibly this maybe because of residual TLR9-agonistic DNA complexes within histones, which normally occur *in-vivo*.

1.7.4. NLRP3 inflammasome activation

The Nod-like receptor (NLR) family is characterized by the presence of a central nucleotide-binding and oligomerization (NACHT) domain, which is commonly flanked by C-terminal leucine-rich repeats (LRRs) and N-terminal caspase recruitment (CARD) or pyrin (PYD) domains. LRRs are believed to function in ligand sensing and autoregulation, whereas CARD and PYD domains mediate homotypic protein-protein interactions for downstream signaling⁹⁷. The NACHT domain, which is the only domain common to all NLR family members, enables activation of the signaling complex via ATP-dependent oligomerization. The NLRP3 inflammasome is a cytosolic platform, activated upon cellular infection or stress that integrates various danger signals into the caspase-1-dependent maturation of pro-inflammatory cytokines such as IL-1 β to initiate innate immune defences⁹⁷.

Allam R *et al.* has recently reported that cytosolic uptake of necrotic cell-derived histones trigger mechanisms of sterile inflammation, which involve NLRP3 inflammasome activation and IL-1 β secretion via oxidative stress⁹⁸. This may be due to the existence of histones in its particle nature, as it is observed by many crystals and microparticles that are capable of activating NLRP3 inflammasome complexes^{99,100}. Intraperitoneal injection of histones into *Nlrp3* gene deficient mice significantly reduces IL-1 β production and recruitment of neutrophils causing attenuated histone-induced peritonitis⁹⁸.

1.7.5. Platelet activation

Fuchs *et al.* has published for the first time an interactions of extracellular histones with platelets. Histones that have bound to platelets induced calcium influx and recruited plasma adhesion proteins such as fibrinogen to induce platelet aggregation^{93,101-103}. Hereby, fibrinogen cross-linked histone-bearing platelets and triggered micro-aggregation. Whereas the interaction of fibrinogen with α IIb β 3 integrins were not required for this process, but were necessary for the formation of large platelet aggregates. Intravenous administration of histones caused the profound thrombocytopenia within minutes after administration *in vivo*¹⁰¹. Mice lacking platelets or α IIb β 3 integrins were protected from histone-induced death but not from histone-induced tissue damage. In contrast, heparin and albumin prevented histone interactions with platelets and protected mice from histone-induced thrombocytopenia, tissue damage and death^{101,103}. Extracellular histones also induced platelet

aggregation and clotting that was dependent on the presence of TLR2/4 and downstream signaling via ERK, p38, AKT and NF- κ B^{93,104}.

1.7.6. Protecting DNA degradation

DNA in chromatin is arranged in form of arrays of nucleosomes, highly conserved nucleoprotein complex. The X-ray crystal structure of the nucleosome core particle of chromatin shows in atomic detail how the histone protein octamer is assembled and how 146 base pairs of DNA are organized into a superhelix around it¹⁰⁵. Von Hahn *et al.* reported that histones stabilize the extracellular DNA against the thermal degradation *in-vitro*¹⁰⁶. Histones in form of nucleosomes protect the DNA from further degradation by nucleases, which leads to the stabilization of DNA within the system and contributes to autoimmune complications. For example, in SLE, where genetic variants often compromise phagocytic dead cell and chromatin clearance and the persistence of extracellular chromatin fosters immunization against DNA and histones^{107,108}. SLE patients who cannot dismantle NETs might be a useful indicator of the renal involvement¹⁰⁸. To be protected from lupus, autoantigens such as dsDNA from degradation inside injured organs will need to remain accessible to circulating anti-dsDNA antibodies, a process that is involved in the pathogenesis of lupus nephritis^{40,109}. However, this mechanism can explain the (transient) occurrence of anti-nuclear antibodies in numerous forms of tissue injury. As mentioned before, the TLR9 agonistic activity of histones might relate to residual DNA components⁹⁶. Finally, histones can even act as a DNA transfectant by shuttling DNA inside cells¹¹⁰.

1.8. Contributions of extracellular histones in the disease setting

The pathogenic roles of extracellular histones are demonstrated in both infectious and non-infectious disease conditions, as illustrated in Figure 5 and Table 2, and are described in more detail within this section.

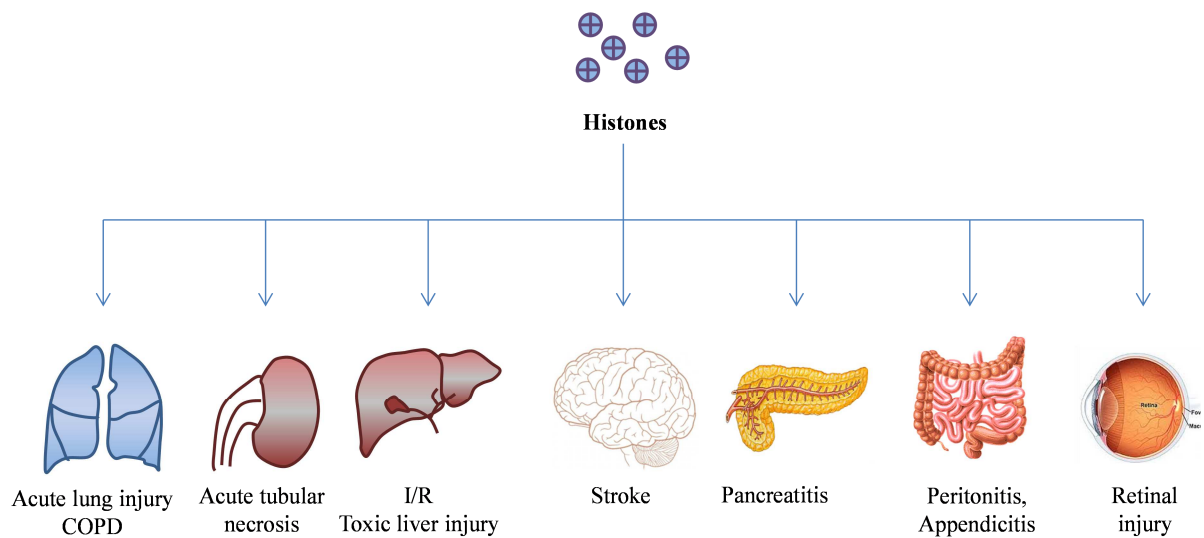


Figure: 5. The diagram represents the different pathogenic effects of extracellular histone on variety of internal organs like lungs: acute lung injury and COPD; kidneys: acute kidney injury; liver: ischemia reperfusion and toxic liver injury; brain: stroke; pancreases: pancreatitis; GIT: peritonitis and appendicitis; eye: retinal injury.

Table: 2. Current evidence for a functional role of extracellular histones in disease⁵³.

Disorder	Pathomechanism	Ref.
Infectious disease		
Sepsis	Histone release promotes sepsis-related endothelial dysfunction, tissue hypoxia and death.	10,111
Peritonitis/Appendicitis	Histones trigger peritoneal inflammation directly by activating PRRs and indirectly by inducing cell necrosis causing local cytokine production.	63,112
Non-infectious disease		
Trauma	Dying cells release histones that injure lung endothelial cells causing microvascular thrombosis and haemorrhage.	89,113,114
Thrombosis/embolism	Histones trigger thrombosis by inducing endothelial activation and by directly inducing thrombin generation and platelet aggregation via TLR2 and TLR4.	93,101,115
Brain		
Stroke	Histone neutralization reduces infarct size, while histone infusion increases infarct size.	116
Atherogenesis	Histones bind to LDL.	117
Lung		
Acute lung injury	Histones from NETting neutrophils that injure endothelial cells cause microvascular thrombosis and haemorrhage.	91,113,118
COPD	Hyperacetylated H3 resists degradation and causes injury.	119
Liver		
Toxic liver injury	TLR9-mediated hepatotoxicity.	94,120,121
Kidney		
Acute kidney injury	Microvascular endothelial injury and TLR2/4-mediated inflammation leading to acute tubular necrosis.	9,122
Glomerulonephritis	NETosis leading to vascular injury in glomeruli.	25
Autoimmunity		
Rheumatoid arthritis/ Felty`s syndrome	Citrullinated/deiminated histones serve as autoantigens within joint immune complexes.	123,124 125
Systemic lupus	Extracellular histones protect self-DNA from degradation, promote auto-immunization together with genetic dead cell clearance deficits.	108,126
Others		
Blood transfusion	NETosis leading to transfusion of histones, DNA and other DAMPs that may cause reactions in recipients.	127
Sickle cell disease	NETs and its components involved in the pathogenesis vaso-occlusive painful sickle cell crisis	128
Hair growth	Histones kill hair follicle progenitor cells.	129

1.8.1. Sepsis

Sepsis is a systemic inflammatory response syndrome primarily caused by bacterial infections. In 1958, Hirsch *et al.* observed that histones have a stronger ability to kill bacteria than many canonical antimicrobials⁵⁷. Hyper-inflammatory responses can lead to a variety of diseases including sepsis. Esmon CT group reported that extracellular histones released in response to inflammatory challenges contribute to endothelial dysfunction, organ failure and death during sepsis¹⁰. Significant amounts of the histone H3 were increased when *E.coli* was injected into Baboons intravenously, which was associated with septic kidney injury¹⁰. In the same way, lipopolysaccharide (LPS)-induced AKI also involves the contribution of histones because this effect can be completely reversed by the administration of the neutralizing histone antibody or activated protein c (aPC)⁹. Antibodies for histones can reduce the mortality of mice in LPS, TNF or cecal ligation and puncture models of sepsis¹⁰.

1.8.2. Thrombosis and intravascular coagulopathy

Coagulation is the biological process by which blood forms clots. A control mechanism, which fails to coagulate blood results in an increased risk of bleeding (haemorrhage) or obstructive clotting (thrombosis). Several studies report that extracellular histones were cytotoxic to endothelial cells, which further contributes to the formation of clots and thrombosis in the microvasculature during many disorders. This was confirmed when histones were intravenously injected into mice, which resulted in complications such as thrombocytopenia, prolonged prothrombin time, decreased fibrinogen, fibrin deposition in the microvasculature and bleeding^{101,115}. Histone-induced TLR2/4 receptor activation is one of the main reasons by which platelets aggregate and plasma thrombin is generated⁹³. This process can be inhibited by recombinant thrombomodulin that binds to histones and protects against thrombosis¹¹⁵. It is possible that in platelets histones raise the intracellular calcium concentrations triggering the activation of α IIb β 3, which further activates the aggregation of platelets¹⁰¹. As, because histones are able to bind the platelet adhesion molecules fibrinogen and vWF, they are well equipped to stimulate platelet aggregation¹⁰¹. Platelet-deficient mice are protected from histone-induced indicating that platelet thrombi contribute to fatal lung injury upon intravenous injection of histones¹⁰¹.

1.8.3. Lung diseases

Approximately half of the patients with ALI/ARDS show the presence of histones in their bronchial alveolar fluid (BALF). Ward PA group showed that injection of calf thymus histones directly into the lungs via the intratracheal route activates the complement system leading to increased histone levels in ALI. They further reported that histones outside of cells were highly cytotoxic for alveolar epithelial cells promoting tissue damage and inflammation; such effects were reversed by the blockade of histones *in-vivo*¹¹⁸. A recent study has linked circulating histones with trauma-associated ALI/ARDS and mortality¹¹³. These findings were consistent with mouse trauma models that displayed pulmonary oedema, haemorrhage, microvascular thrombosis and neutrophil congestion¹¹³. The dying airway cells also release extracellular histones, which further contributes to the development of chronic obstructive pulmonary disease. Several nuclear proteins that are known to affect gene expression are elevated in the lungs of subjects with COPD, the most notable being those that belong to the core histones, especially H3.3. Relative to control subjects, the lung samples from subjects with COPD showed increased H3.3 in the extracellular spaces, cellular debris, airway lumen mucous, BALF and plasma¹¹⁹.

1.8.4. Brain, liver and kidney disease

The mechanisms of histone release into the circulation is a consequence of cell death of neurons, liver cells or kidney parenchymal cells, either due to the ischemia reperfusion or toxic injury of the organs. The locally released histones further promote the microvascular and parenchymal injury. Blocking released extracellular histones using the neutralizing histone antibody or other histone blocking agents protects from post ischemic injury in the brain, liver and kidney^{9,96,116,130}. Histones released through NETs formation usually cause microvascular complications in organs such as liver, brain and kidneys, but a direct effect has not been proven yet¹²². Previous experiments have demonstrated a role for NETs-associated toxicity during glomerulonephritis, a mechanism that has been shown for ANCA-associated small vessel vasculitis affecting the glomerular compartment of the kidney²⁵. In these organs histones mediate their toxic effects by partially activating TLRs and also mediate its immunopathology via the activation of NLRP3 inflammasome^{9,98}.

1.8.5. Autoimmune disorders

A recent report has shown the involvement of NETs and its components in activating plasmacytoid dendritic cells during the pathogenesis of SLE¹³¹. In SLE patients, NETs that are released following infection do not rapidly get degraded and cleared from the circulation, which could further lead to increased lupus precipitations^{108,132}. NETting neutrophils also induce endothelial damage, infiltrate tissues and release immunostimulatory molecules during SLE¹³³. Persistent chromatin particles in the extracellular space not only provide immunostimulatory DAMPs but also act as autoantigens. Histones are important lupus autoantigens, mainly within the nucleosomes; hence, extracellular histones enforce autoantigen-presentation and activation of autoreactive lymphocyte clones^{42,131}. Histone H1 constitutes a major B cell and T cell autoantigens in SLE triggering a pro-inflammatory Th1 response and driving autoantibody production¹³⁴. Histones have also been reported to stimulate and accelerate the progression of rheumatoid arthritis, whereby protein microarray and tandem mass spectrometry analysis of the synovial joint tissue from patients with rheumatoid arthritis identified histone H2A and H2B within immune complex deposits along the cartilage surface¹²⁵. Deimination and citrullination of histones by the hydrolase family of enzymes like protein arginine deiminases present in the NETs increase the antigenicity of NETosis-derived histones^{123,135,136}. Elevated levels of TNF- α drive the citrullination of histone H3, which plays an important role in multiple sclerosis¹³⁷. Besides acting as direct autoantigens in autoimmune disorders, extracellular histones can prevent DNA degradation through formation of histone–DNA complex, which enhance autoimmune responses¹⁰⁸.

1.9. Extracellular histones as therapeutic target

Amongst many DAMPs, histones represent one of the major danger signals during tissue injury and disease progression. However, their potential to amplify tissue injury by killing other cells in addition to their agonistic activity on TLRs and the NLRP3 inflammasome provides a rationale to target histones for therapy. Three histone-neutralizing agents have been identified to degrade and neutralize extracellular histone toxicity and of being able to prevent histone-related pathologies *in-vitro* and *in-vivo*: the histone-neutralizing antibody BWA3^{9,10,90,91,138}, the serum protease activated protein C (aPC)^{9,10,90} and heparin^{93,101,139,140}.

1.9.1. Histone-neutralizing antibody BWA3

A histone neutralizing monoclonal antibody was obtained by culturing BWA3 hybridoma cells that was first described and confirmed by M. Monestier in 1993¹⁴¹. Since then several experimental studies were carried out using the neutralizing antibody from the BWA3 clone and showed its effect in several disease models. BWA3 binds to an epitope corresponding to a region of high sequence similarity between H2A and H4. The therapeutic effect of the histone antibody was first reported by Xu J *et al.* during sepsis¹⁰. Since then other groups have reported the therapeutic property of BWA3 in many other diseases, which have been discussed in section 1.8.

1.9.2. Activated protein C

aPC is classified as a serine protease because it contains a residue of serine at its active site¹⁴². aPC is a vitamin K-dependent plasma protein zymogen that is synthesized in the liver, whose genetic, mild or severe deficiencies are linked with a risk for venous thrombosis or neonatal purpura fulminans, respectively¹⁴²⁻¹⁴⁴. Over the past decades, studies have shown that aPC inactivates factor Va and VIIIa to down-regulate thrombin generation. More recently, basic and preclinical research on aPC has characterized the direct cytoprotective effects that involve gene expression profile alterations, anti-inflammatory and anti-apoptotic activities and endothelial barrier stabilization^{145,146}. These protective functions of aPC are mainly due to the activation of the angiopoietin/Tie2 axis and the modulation of EPCR-bound lipids^{145,146}. Many studies reported that aPC has the capacity to cleave the released extracellular histones indicating that aPC has cytoprotective and anti-inflammatory actions^{89,90,147}, for example, during sepsis¹⁰ and ischemic injury in the brain, liver and kidney^{9,96,116}. However, the activity of aPC *in-vivo* seems limited in blocking NETosis-induced histone toxicity, even though this protease has certainly additional biological effects⁹¹. A clinical trial in children with meningococcal sepsis, histone plasma levels correlated with the disease severity, but recombinant aPC therapy did not affect these levels¹⁴⁸. Although recombinant aPC had first been approved by the FDA for the treatment of human sepsis, it was later withdrawn from the market due to a lack of efficacy in reducing sepsis mortality in a subsequent randomized controlled trial¹⁴⁹.

1.9.3. Heparin

Heparin is a highly sulphated glycosaminoglycan that is widely used as an injectable anticoagulant and has the highest negative charge density of any known biological molecule. As histones carry a strong positive charge, it is possible that histones have a strong affinity to the negatively charged heparin triggering the formation of a complex due to the electrostatic interactions of the high affinity¹⁵⁰. It is, however not known whether binding of heparin to histones also protects against the cytotoxic effect of histones on endothelial cells. In this thesis and this was reported before by several groups that, heparin has beneficial effects on histone neutralization and elicits cytoprotective effects. Only moderate doses of heparin can attenuate injuries, whereas high doses of heparin are harmful due to the complication of disseminated hemorrhage¹⁵¹⁻¹⁵³. It is reasonable to suggest that chemically modified heparin derivatives, devoid of anticoagulant activity, may be more useful than heparin for controlling inflammation caused by histones.

1.10. Rapid progressive glomerulonephritis

Rapidly-progressive glomerulonephritis (RPGN) encompasses a heterogeneous group of disorders resulting in severe glomerular inflammation and injury. Clinically, RPGN is characterized by a rapid loss of glomerular filtration rate, haematuria and proteinuria caused by characteristic glomerular lesions such as capillary necrosis and hyperplasia of the parietal epithelial cells (PEC) along Bowman`s capsule forming crescents. The pathogenesis of RPGN involves autoantibodies, immune complex-mediated activation of complement, the local production of cytokines and chemokines, and glomerular leukocyte recruitment¹⁵⁴.

RPGN often manifests as necrotizing and crescentic GN, such as seen in anti-neutrophil cytoplasmic antibody (ANCA)-associated renal vasculitis or anti-GBM disease (e.g. Goodpasture syndrome). All these forms are associated with neutrophil-induced glomerular injury^{24,155-157}. In situations where the stimuli persistently trigger inflammation, an increasing number of leucocytes and neutrophils will infiltrate into the injured area¹⁵⁸. In the presence of local cytokines released due to the inflammatory or infectious stimuli, these infiltrated neutrophils gets activated and form NETs, these are comprised of extracellular fibrillary material containing chromatin and granule proteins and numerous DAMPs including histones will be released^{159,160}.

Necrotizing injury to vessel walls results in haemorrhage and the release of plasma proteins into the vessel walls and adjacent extravascular tissue¹⁶¹ (Figure 6). These proteins include coagulation factors, which are activated by thrombogenic cellular and tissue debris, and tissue factors, which result in the formation of fibrin within areas of fibrinoid necrosis¹⁶². This leads to severe platelet activation and fibrotic clot formation within the microvasculature causing hypoxia in the local areas of the glomeruli, which can further lead to cell death-associated release of DAMPs and continues during the necrotizing or crescentic glomerulonephritis. It is possible that the fibrin formation is facilitated by tissue factors present in NETs in glomeruli. Foci of segmental fibrinoid necrosis develop adjacent cellular reactions (as in crescents) composed predominantly of monocytes, macrophages and activated epithelial cells¹⁵⁷.

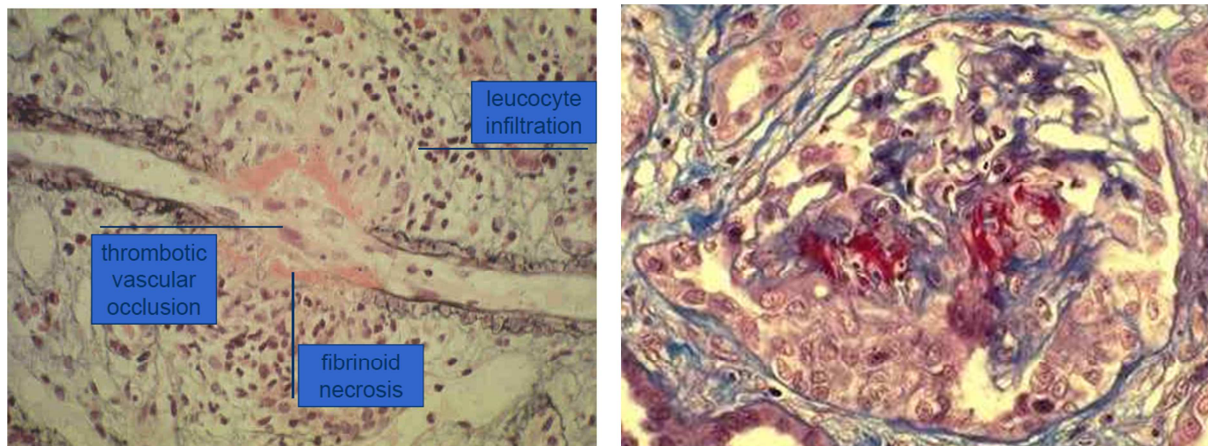


Figure: 6. Leukocytoclastic vasculitis caused due to the infiltrating leukocytes cause endothelial damage by fibrinoid necrosis resulted in thrombotic vascular occlusions this further leads to the hypoxia and organ failure (left image). Necrotizing glomerulonephritis involves vascular damage and sclerosis (right image)

1.10.1. Anti-GBM glomerulonephritis

Anti-GBM disease also called “Goodpasture's disease” is one of the three major forms of RPGN. Here, the loss of tolerance with production of GBM autoantibodies described against the noncollagenous-1 (NC1) domain of type 4 collagen of GBM membrane and kill the glomerular cells in a complement-dependent manner^{163,164}. Although some patients present initially with relatively mild renal insufficiency, the disorder is typically associated with severe renal injury that, if left untreated, progresses quickly to end-stage renal disease (ESRD)^{165,166}.

1.10.2. Epidemiology

It's been reported that, the disease has an estimated incidence of one case per 2 million per year in European caucasian populations. It is responsible for 1 to 5% of all types of GN and is the cause in 10 to 20% of patients with crescentic GN. All age groups are affected but the peak incidence is in the third decade in young men with a second peak in the sixth and seventh decades affecting men and women equally. Lung haemorrhage is more common in younger men, while isolated renal disease is more frequent in the elderly with near equal gender distribution.

1.10.3. Diagnosis

- The diagnosis of Goodpasture's disease is dependent on the detection of anti-GBM antibodies either in the circulation or in kidney tissue.
- Renal biopsy to detect the severity of the lesions. The antibodies can also be detected on renal biopsy specimens with characteristic linear staining for IgG and frequently C3 detected along the GBM

1.10.4. Treatment

It has been observed that neither steroids nor immunosuppressive drugs had an influence on the renal outcome. However, the recommended treatment approaches are listed in the table below (Table: 3).

Table: 3. Recommended treatment approaches for GN¹⁶⁷

Treatment	Description
Plasma exchange	4-L exchanges daily with human albumin as replacement solution. Where there is risk of hemorrhage FFP should be given at the end of the procedure.
Corticosteroids	Prednisolone 1 mg/kg for first week then reduce at weekly intervals to 45, 30, 25, 20, 15, 10, and 5 mg.
Cytotoxic drugs	Cyclophosphamide 3 mg/kg rounded down to nearest 50 mg. In patients over 55 yr of age, use 2 mg/kg rounded down to nearest 25 mg

^aFFP, fresh frozen plasma.

There have been many studies that have explored the functional role of the immune complex deposition and/or chemokines and cytokines involved in the progression of severe glomerulonephritis¹⁶⁸⁻¹⁷⁰. However, limited research has been undertaken to establish new and effective methods to control the progression of glomerulosclerosis. This thesis will addresses novel pathomechanisms involved in the progression of glomerulosclerosis and provide important insights into the development of effective and safe treatments.

2. *Hypotheses*

An important characteristic feature of severe GN is necrosis of the glomerular tuft cells, so we hypothesized that there will be extensive release of DAMPs including histones. The disease is also characterized by infiltration of neutrophils and release of cytokines, in this condition we speculated the formation of NETs and release of more histones in to the extracellular space.

Accordingly, the specific objectives and aims of this study were:

1. To investigate, whether extracellular histones elicit toxic effects on glomerular endothelial cells (GEnC) and whether they promote tuft necrosis, proteinuria and crescent formation during experimental glomerulonephritis.
2. To investigate the effect of extracellular histones using histone blocking agents such as neutralizing anti-histone antibody, heparin and aPC during severe glomerulonephritis.
3. To evaluate NETs-related histones and to determine the efficacy of blocking NETosis using the Peptidylarginine deiminase (PAD)-4 inhibitor during the progression of severe glomerulonephritis.

3. *Materials and Methods*

3.1 *Instruments and Chemicals*

3.1.1 Instruments

Balance:

Analytic Balance, BP 110 S	Sartorius, Göttingen, Germany
Mettler PJ 3000	Mettler-Toledo, Greifensee, Switzerland

Cell Incubator:

Type B5060 EC-CO ₂	Heraeus Sepatech, München, Germany
-------------------------------	------------------------------------

Centrifuges:

Heraeus, Minifuge T	VWR International, Darmstadt, Germany
Heraeus, Biofuge primo	Kendro Laboratory Products GmbH, Hanau, Germany
Heraeus, Sepatech Biofuge A	Heraeus Sepatech, München, Germany

ELISA-Reader:

Tecan, GENios Plus	Tecan, Crailsheim, Germany
--------------------	----------------------------

Fluorescence Microscopes:

Leica DC 300F	Leica Microsystems, Cambridge, UK
Olympus BX50	Olympus Microscopy, Hamburg, Germany

Spectrophotometer:

Beckman DU® 530 Beckman Coulter, Fullerton, CA, USA

TaqMan Sequence Detection

System:

ABI prism™ 7700 sequence detector PE Biosystems, Weiterstadt, Germany

qRT-PCR syber green LC-480 Roche, Mannheim, Germany

Other Equipments:

Nanodrop PEQLAB Biotechnology GMBH, Erlangen, Germany

Cryostat RM2155 Leica Microsystems, Bensheim, Germany

Cryostat CM 3000 Leica Microsystems, Bensheim, Germany

Homogenizer ULTRA-TURRAX IKA GmbH, Staufen, Germany
T25

Microtome HM 340E Microm, Heidelberg, Germany

pH meter WTW WTW GmbH, Weilheim, Germany

Thermomixer 5436 Eppendorf, Hamburg, Germany

Vortex Genie 2™ Bender & Hobein AG, Zürich, Switzerland

Water bath HI 1210 Leica Microsystems, Bensheim, Germany

3.1.2 Chemicals and Reagents

RNeasy Mini Kit Qiagen GmbH, Hilden, Germany

RT-PCR primers Metabion, Munich, Germany

Cell culture:

DMEM-medium Biochrom KG, Berlin, Germany

RPMI-1640 medium GIBCO/Invitrogen, Paisley, Scotland, UK

FCS	Biochrom KG, Berlin, Germany
Dulbecco's PBS (1×)	PAN Laboratories GmbH, Cölbe, Germany
Trypsine/EDTA (1×)	PAN Laboratories GmbH, Cölbe, Germany
CD hybridoma media	GIBCO/Invitrogen, Paisley, Scotland, UK
FBS, ultralow IgG	PAN Laboratories GmbH, Cölbe, Germany
Glutamine	PAN Laboratories GmbH, Cölbe, Germany
Penicillin/Streptomycin (100×)	PAN Laboratories GmbH, Cölbe, Germany
Matrigel	BD biosciences, Heidelberg, Germany

Drugs and treatment:

Heparin	Ratiopharma, Ulm, Germany
Cl-amide (PAD inh)	Millipore, Darmstadt, Germany
aPC	Lilly, UK

Antibodies:

Anti-histone antibody	Homemade BWA3 clone
Neutrophil elastase	Abcam, Cambridge, UK
MPO	Abcam, Cambridge, UK
Fibrinogen	Abcam, Cambridge, UK
TNF- α	Abcam, Cambridge, UK
WT-1	Cell signaling, Danvers, MA
Mac-2	Cedarlane, ON, Canada
HRP linked Anti-Rabbit secondary Ab	Cell signaling, Danvers, MA
HRP linked Anti-Mouse secondary Ab	Cell signaling, Danvers, MA

HRP linked Anti-Goat secondary Ab	Dianova, Hamburg, Germany
β -Actin	Cell signaling, Danvers, MA
α -tubulin	Cell signaling, Danvers, MA
Tamm–Horsfall protein	Santa Cruz Biotechnology, Santa Cruz, CA
Lotus tetragonolobus lectin	Vector Labs, Burlingame, CA
rat anti-mouse neutrophils	Serotec, Oxford, UK
CD3+	AbD Serotec, Düsseldorf, Germany
F4/80+	AbD Serotec, Düsseldorf, Germany
Claudin	Bioworld technology, CB8 7SY England
Nephrin	Acris Antibodies GmbH, Herford, Germany
Ki-67	Dako Deutschland GmbH, Hamburg, Germany
α -SMA	Dako Deutschland GmbH, Hamburg, Germany

Elisa and assay Kits:

mouse IL-6	R &D Systems, Minneapolis, MN, USA
mouse TNF- α	Biologend, San Diego, CA
mouse Albumin	Bethyl Laboratories, TX, USA
Creatinine FS	DiaSys Diagnostic System, GmbH, Holzheim, Germany
Urea FS	DiaSys Diagnostic System, GmbH, Holzheim, Germany

Chemicals:

Acetone	Merck, Darmstadt, Germany
AEC Substrate Packing	Biogenex, San Ramon, USA
Bovines Serum Albumin	Roche Diagnostics, Mannheim, Germany

Skim milk powder	Merck, Darmstadt, Germany
DEPC	Fluka, Buchs, Switzerland
DMSO	Merck, Darmstadt, Germany
Diluent C for PKH26 dye	Sigma-Aldrich Chemicals, Germany
EDTA	Calbiochem, SanDiego, USA
30% Acrylamide	Carl Roth GmbH, Karlsruhe, Germany
TEMED	Santa Cruz Biotechnology, Santa Cruz, CA
Eosin	Sigma, Deisenhofen, Germany
Ethanol	Merck, Darmstadt, Germany
Formalin	Merck, Darmstadt, Germany
Hydroxyethyl cellulose	Sigma-Aldrich, Steinheim, Germany
HCl (5N)	Merck, Darmstadt, Germany
Isopropanol	Merck, Darmstadt, Germany
Calcium chloride	Merck, Darmstadt, Germany
Calcium dihydrogenphosphate	Merck, Darmstadt, Germany
Calcium hydroxide	Merck, Darmstadt, Germany
MACS-Buffer	Miltenyl Biotec, Bergisch Gladbach, Germany
Beta mercaptoethanol	Roth, Karlsruhe, Germany
Sodium acetate	Merck, Darmstadt, Germany
Sodium chloride	Merck, Darmstadt, Germany
Sodium citrate	Merck, Darmstadt, Germany
Sodium dihydrogenphosphate	Merck, Darmstadt, Germany
Penicillin	Sigma, Deisenhofen, Germany
Roti-Aqua-Phenol	Carl Roth GmbH, Karlsruhe, Germany
Streptomycin	Sigma, Deisenhofen, Germany
Tissue Freezing Medium	Leica, Nussloch, Germany

Trypan Blue	Sigma, Deisenhofen, Germany
Oxygenated water	DAKO, Hamburg, Germany
Xylol	Merck, Darmstadt, Germany

Miscellaneous:

Cell death detection (TUNEL) kit	Roche, Mannheim, Germany
Microbeads	Miltenyl Biotech, Germany
Cell Titer 96 Proliferation Assay	Promega, Mannheim, Germany
LS+/VS+ Positive selection columns	Miltenyl Biotec, Bergish Gladbach, Germany
Preseparation Filters	Miltenyl Biotec, Bergish Gladbach, Germany
Super Frost® Plus microscope slides	Menzel-Gläser, Braunschweig, Germany
Needles	BD Drogheda, Ireland
Pipette's tip 1-1000µL	Eppendorf, Hamburg, Germany
Syringes	Becton Dickinson GmbH, Heidelberg, Germany
Plastic histocassettes	NeoLab, Heidelberg, Germany
Tissue culture dishes Ø 100x20mm	TPP, Trasadingen, Switzerland
Tissue culture dishes Ø 150x20mm	TPP, Trasadingen, Switzerland
Tissue culture dishes Ø 35x10mm	Becton Dickinson, Franklin Lakes, NJ, USA
Tissue culture flasks 150 cm ²	TPP, Trasadingen, Switzerland
Tubes 15 and 50 mL	TPP, Trasadingen, Switzerland
Tubes 1.5 and 2 mL	TPP, Trasadingen, Switzerland

All other reagents were of analytical grade and are commercially available from Invitrogen, SIGMA or ROCH.

All the FACS antibodies were used from BD Biosciences, eBiosciences or BIO-RAD.

3.2 Experimental procedures

3.2.1 Animals

C57BL/6N wild-type mice obtained from Charles River (Sulzfeld, Germany). All mice were housed in poly-propylene cages under standard conditions with the temperature of $22\pm 2^{\circ}\text{C}$ with 12 hours light and dark cycle. Water and standard chow diet (Sniff, Soest, Germany) were available *ad libitum* for the complete duration of the study. Cages, bedding, nestles, food, and water were sterilized by autoclaving before use. All the aspects of animal handling and experiments were approved by the *Regierung von Oberbayern*.

3.2.2 Animal models

*GBM anti-serum induced glomerulonephritis*¹⁶⁸

Glomerulonephritis was induced in the wild type C57BL/6N mice by a single intravenous injection of 100 μl of GBM anti-serum (Probetex, San Antonio, TX). The induction of the disease can be seen by increased albuminuria within 24 hours after anti-serum injection. All the animals were sacrificed on day 7, urine and blood were collected for the analysis of functional parameters and kidneys were harvested for histology, protein, mRNA and FACS analysis. Anti-serum contains antibodies against the GBM, this directly binds GBM and micro-vasculature in the glomeruli leading to the activation of the complement system followed by glomerular and endothelial cell death, as illustrated in Figure 7. This leads to the release of abundant amounts of intracellular contents including DAMPs like histones and results in the infiltration of immune cells especially neutrophils and macrophages leading to the secretion of inflammatory cytokines and chemokines¹⁶⁸.

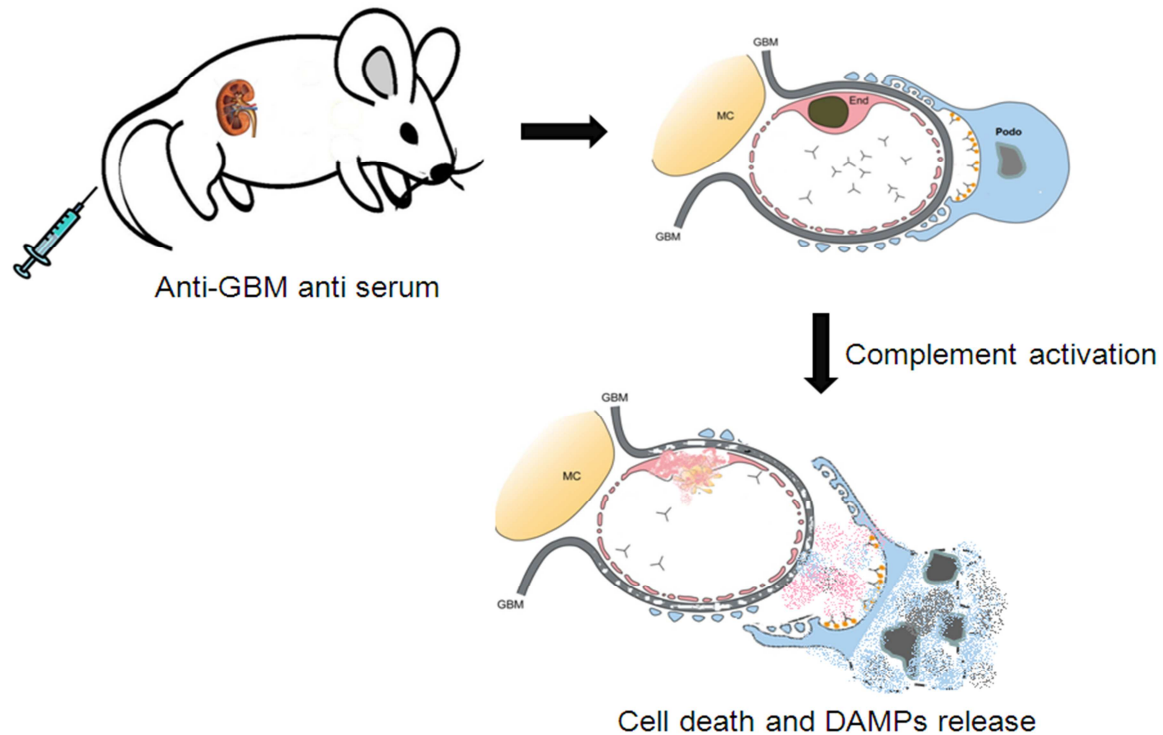


Figure: 7. Schematic represents of stages of GBM antiserum induced glomerulonephritis and DAMPs release.

3.2.3 Experimental design

To study the effect of histone neutralization in the anti-GBM glomerulonephritis model, we used anti-histone IgG as a potential therapy, which has capacity to neutralize extracellular histones. To do so we used different strategies:

- a) Prophylactic of anti-histone IgG
- b) Therapeutic administration of anti-histone IgG
- c) Other histone neutralizing agents such as heparin, aPC or blocking NETosis with Cl-amide
- d) A combination of anti-histone IgG, heparin and aPC.

The therapeutic and prophylactic administration schedules are illustrated in figure 8.

a) *Prophylactic administration with anti-histone IgG*

In this experimental setting, mice received an i.p. injection of 20 mg/kg anti-histone IgG or control IgG 24h prior to the administration of anti-GBM serum followed by treatment with anti-histone IgG on day 1 and 3 (Figure 8). On day 7, urine and blood were collected to analyze the functional parameters, like BUN, plasma creatinine and albuminuria, later mice were sacrificed and kidneys harvested for histology, mRNA and FACS analysis.

b) *Therapeutic administration with anti-histone IgG*

For the therapeutic treatment, mice were injected with anti-GBM serum (100 µl/animal) and treatment with anti-histone IgG was initiated only after the onset of GN (i.e., after induction of proteinuria) on day 2, 4 and 6. On day 7, urine and blood were analyzed for functional parameters as well as albuminuria, and the kidneys harvested for histology, mRNA and FACS analysis.

c) *Therapeutic administration with heparin, aPC or Cl-amide*

Mice received an injection of 100 µl anti-GBM serum prior to the daily administration of heparin (50 IU/mice, i.p.), aPC (5 mg/kg, i.p.) or Cl-amide (10 mg/kg, i.p.) for up to 7 days. Sample analysis was performed as stated in the Prophylactic treatment of anti-histone IgG regime (section 3.2.3 a).

d) *Combination of anti-histone IgG, heparin and aPC*

Here, mice were treated with a combination of anti-histone IgG (20 mg/kg, i.p. on day 2, 4 and 6), heparin (50 IU/mice, i.p., daily) and/or aPC (5 mg/kg, i.p., daily) 48 hours after the injection of anti-GBM serum (100 µl). Samples were collected on day 7 and prepared like in section 3.2.3 a).

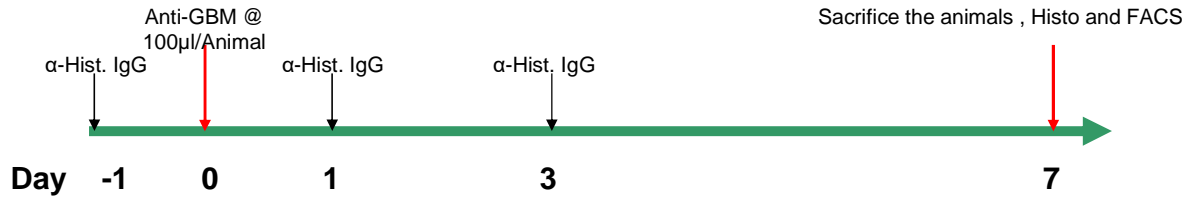
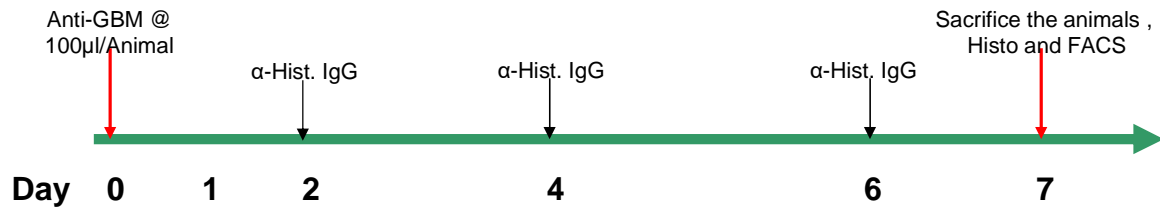
Prophylactic administration (n=6) α -Histone IgG 20 mg/kg, i.p.**Therapeutic administration (n=6)** α -Histone IgG 20 mg/kg, i.p.

Figure: 8. Schematics showing the treatment schedules for prophylactic and therapeutic treatment with anti-histone IgG

3.3 Blood and urine sample collection

Mice were anesthetized using isoflurane at a rate of 2.5 % with an oxygen flow of 2 l/h and blood was drawn from the facial vein using micro lancet and blood collected into centrifuge tubes containing EDTA (10 μ l of 0.5 M solution per 200 μ l of blood). Blood samples were centrifuged at 8000 rpm for 5 min and plasma collected and stored at -20°C until further use.

Urine samples were collected at different times during the experimental time course as well as at the end of the study. All samples were stored at -20°C until used for further analysis.

3.4 Urinary albumin to creatinine ratio

3.4.1 Urinary albumin

Urinary albumin levels were determined using an albumin ELISA kit from Bethyl Laboratories according to manufacturer's instructions. One hallmark of the glomerular disease is the abundant amount of protein excreted through the urine due to the loss of endothelial cells and glomerular basement membrane barrier leading to increased excess levels of albumin in the urine. In this study, urine samples were diluted 10^4 to 10^6 times with the assay diluent before estimation. Briefly, capture antibody (goat anti-mouse albumin, 1:100) was diluted in coating buffer (carbonate-bicarbonate, pH 9.6) and coated with 100 μ l of diluted antibody onto a Nunc Maxisorb flat bottom 96-well plate and incubated overnight at 4⁰C. Plate was then washed 3 times with wash buffer (Tris NaCl with Tween 20) and blocking solution (Tris, NaCl with 1% BSA, pH 8) added for 1 hour at room temperature. Following blocking, the plate was washed 3 to 5 times with wash buffer and diluted samples/standards were then added in the respective wells and incubated for 1 hour. After incubation, each well was washed 5 times with wash buffer and HRP-conjugated detection antibody (dilution of 1:75000) was added and the plate was incubated in dark for 1 hour. After HRP-conjugate incubation, each well was washed 5 to 7 times with wash buffer and TMB reagent (freshly prepared by mixing equal volumes of two substrate reagents) was added and the samples incubated in dark until color reaction was completed (for 5 minutes) followed by addition of the stop solution (2 M H₂SO₄). The absorbance was read at 450 nm within 10 minutes following addition of the stop solution. The albumin content in each sample was determined using the equation of regression line generated by plotting absorbance of different standards against their known concentrations.

3.4.2 Urinary creatinine, plasma creatinine and plasma BUN

Urinary creatinine and plasma creatinine levels were measured by Jaffe's enzymatic reaction using a Creatinine FS kit (DiaSys Diagnostic system, GmbH, Holzheim, Germany). Urine samples were diluted 10 times with distilled water, whereas plasma samples were used undiluted. Serial dilutions of the standard were prepared using the stock provided in the kit. Working monoreagent was prepared by mixing 4 part of reagent 1 (R1) and 1 part of reagent 2 (R2). Then, 10 μ l of each of the diluted samples and standards were added to a 96-well flat

bottom plate (Nunc maxisorb plate). The monoreagent (200 μ l) was added to each well and the reaction mixture incubated for one minute before measuring the absorbance at 492 nm immediately (1 (A1) and 2 (A2) minutes after addition) using an ELISA plate reader. The change in absorbance (ΔA) was calculated as $\Delta A = [(A2 - A1) \text{ sample or standard}] - [(A2 - A1) \text{ blank}]$. And creatinine content in the samples was calculated as:

$$\text{Creatinine (mg/dl)} = \Delta A \text{ sample} / \Delta A \text{ standard} \times \text{Concentration of standard (mg/dl)}$$

Plasma BUN levels were measured using a Urea FS kit (DiaSys Diagnostic system, GmbH, Holzheim, Germany). Serial dilutions of standard were prepared using the stock provided with the kit. Working monoreagent was prepared by mixing 4 part of reagent 1 (R1) and 1 part of reagent 2 (R2) provided in the kit. Then, 2 μ l of each of the sample and standards were added to a 96-well flat bottom plate (Nunc maxisorb plate). The monoreagent (200 μ l) was added to each well and the reaction mixture incubated for one minute before measuring the absorbance at 360 nm immediately after 1 (A1) and 2 (A2) minutes using an ELISA plate reader. The change in absorbance (ΔA) was calculated as $\Delta A = [(A1 - A2) \text{ sample or standard}] - [(A1 - A2) \text{ blank}]$. And BUN content in the samples was calculated as:

$$\text{BUN (mg/dl)} = \Delta A \text{ sample} / \Delta A \text{ standard} \times \text{Concentration of standard (mg/dl)} \times 0.467$$

The urinary albumin to creatinine ratio was calculated after converting values for albumin and creatinine to similar units (mg/dl). Albumin content for each sample calculated (mg/dl) was divided by creatinine content (mg/dl) for the same sample.

3.5 Cytokines ELISA

All cytokine levels in the supernatants collected from *in-vitro* cell stimulation assays were measured using ELISA kits in accordance with the manufacturer's instructions. Briefly, the NUNC ELISA plates were captured with the capture antibody in coating buffer overnight at 4°C. On the next day, the plates were washed 3 times with washing buffer and non-specific binding blocked with either the blocking solution or assay diluent for 1 hour. Following washing, the standards, samples and sample diluent (blank) were added into the wells and incubated at RT for 2 hours. After 2 hours, plates were washed 5 times and the HRP/AP conjugated secondary antibody diluted in assay diluent was added and incubated for 1 hour. The plates were washed 5-7 times and incubated with 100 μ l of substrate A and B (1:1

mixture) for 25-30 minutes in the dark. The reaction was stopped by addition of 100 μ l of 1 M H_2SO_4 . The absorbance was measured at 450 nm and the reference wavelength was 620 nm using a spectrophotometer (TECAN-Genios Plus).

3.6 Immunostaining and confocal imaging

For immunohistological analysis, the middle part of the kidney from each mouse was fixed in formalin (10 % in PBS or Saline) over night, than processed using tissue processors (Leica) and the paraffin blocks prepared. 2 μ m thick paraffin-embedded sections were cut. De-paraffinization was carried out using xylene (3x 5 minutes) followed by re-hydration, which was carried out by incubating the sections in 100% absolute ethanol (3x 3 minutes), 95% ethanol (2x 3 minutes) and 70% ethanol (1x 3 minutes) followed by washing with PBS (2x 5 minutes). Blocking of endogenous peroxidase was carried out by incubating sections in H_2O_2 and methanol mixture (20 ml of 30% H_2O_2 in 180 ml of methanol) for 20 minutes in dark followed by washing in PBS (2x 5 minutes). For unmasking of antigen, sections were dipped in antigen unmasking solution (3 ml of antigen unmasking solution + 300 ml of distilled water) and cooked in the microwave for 10 minutes (4x 2.5 minutes, every 2.5 minutes water level was checked and made up to the initial levels with distilled water every time). After microwave cooking, the sections were cooled to room temperature for 20 minutes and then washed with PBS. Blocking endogenous biotin, we incubated the sections with one drop of Avidin (Vector) for 15 minutes followed by incubation with Biotin (Vector) for an additional 15 minutes. After incubation, sections were washed with PBS (2x 5 minutes).

Next, sections were incubated with different primary antibodies either for 1 hour at room temperature or overnight at 4⁰C in a wet chamber followed by wash steps with PBS (2x 5 min). After washing, sections were incubated with the appropriate biotinylated secondary antibodies (1:300, dilution in PBS) for 30 minutes followed by wash steps with PBS (2x 5 minutes). Substrate solution (ABC solution, Vector) was added and sections were incubated for 30 minutes at room temperature in a wet chamber followed by wash steps with PBS (1x 5 minutes). Tris buffer saline (1x 5 minutes) and sections were stained for DAB followed by counter staining with methyl green (Fluka). Then sections were washed with alcohol (96 %) to remove excess stain and xylene and then dried and mounted with VectaMount (Vector).

The primary antibodies used in the study are mentioned above (section 3.1.2). For each immunostaining, negative controls were performed by incubation with the respective isotype antibody instead of the primary antibody.

For confocal imaging, the sections, prepared as described above, were incubated with the following primary antibodies: pig anti-mouse nephrin (1:100, Acris Antibodies, Herford, Germany), rabbit anti-mouse WT1 (1:25, Santa Cruz Biotechnology, Santa Cruz, CA) and rabbit anti-mouse MDM2 (1:100, Abcam, Cambridge, UK) and biotinylated lotus tetragonolobus lectin (Vector Labs, CA, USA) for 1 hour in PBS or 0.1 % milk solution at room temperature. After washing, the sections were incubated with the secondary antibodies: guinea pig Alexa Fluor 488 (1:100, Invitrogen, Carlsbad, CA) or rabbit Cy3 (1:200, Jackson ImmunoResearch Laboratories, West Grove, PA) for 30 minutes at room temperature. The antibody staining of the sections were evaluated using the confocal microscope LSM 510 and the LSM software (Carl Zeiss AG).

3.7 Periodic acid-Schiff staining

Formalin-fixed tissues were processed using tissue processors (Leica) and the paraffin blocks were prepared. 2 μ m thick paraffin-embedded sections were cut. De-paraffinization was carried out using xylene (3x 5 minutes) followed by re-hydration by incubating the sections in 100% absolute ethanol (3x 3 minutes), 95% ethanol (2x 3 minutes) and 70% ethanol (1x 3 minutes) followed by washing with distilled water (2x 5 minutes). Re-hydrated sections were incubated with Periodic acid (2 % in distilled water) for 5 minutes followed by washing with distilled water (1x 5 minutes). Then sections were incubated with Schiff solution for 20 minutes at room temperature followed by washing with tap water (1x 7 minutes) and counter staining with Hematoxylin solution (1x 2 minutes). This was followed by washing with tap water (1x 5 minutes) and finally sections were dipped in 90% alcohol, dried and the sections closed with cover slips.

3.8 Histopathological evaluations

3.8.1 PAS staining

All kidney sections were quantified for PAS scoring and values were expressed as mean \pm SEM. Glomerular sclerotic lesions were assessed using a semi quantitative score (as in figure 9) by a blinded observer as follows, after assessing 50 glomeruli from each section:

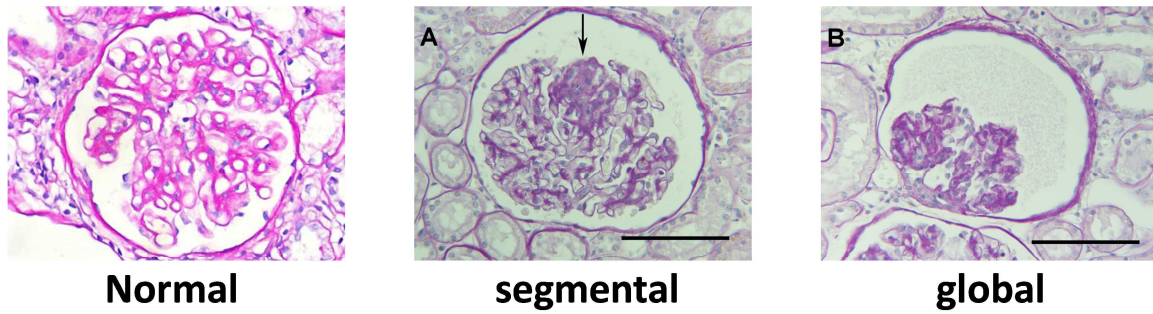


Figure: 9. Representative images of glomerular lesions

<u>Score</u>	<u>Lesion in Glomeruli</u>
No lesion (0)	None
Segmental Lesion (1)	$\leq 50 \%$
Global Lesion (2)	$\geq 50 \%$

All sections in each group were quantified as percentage of glomeruli with each score (mean \pm SEM).

Tubular injury also was scored in the PAS sections, percentage of tubules in the corticomedullary junction that displayed cell necrosis, loss of brush border, cast formation, and tubular dilatation as follows:

<u>Score</u>	<u>Injury level</u>
0	None
1	$\leq 10\%$
2	21 % to 40 %
3	41 % to 60 %
4	61 % to 80 %
5	81 % to 100 %

3.8.2 Mac-2 staining

The number of infiltrated macrophages into the glomeruli was counted in the sections stained with Mac-2 (pan marker for macrophage) antibodies. Mac-2 positive cells were counted manually in 50 glomeruli from each kidney section and reported as the percentage of Mac-2 positive cells in each group.

3.8.3 Neutrophils

The number of infiltrated neutrophils in the glomeruli was counted in the sections stained with the Ly-6B.2 antibody. Positive cells were counted manually in 50 glomeruli from each kidney section and reported as percentage Ly-6B.2 positive cells per group.

3.8.4 Podocytes

Kidney sections were staining with the WT-1/Nephrine antibody, which were labeled with Alexa and FITC conjugated secondary antibodies respectively. Double positive cells were counted manually in 50 glomeruli and the average number of podocytes was reported in each group. Representative pictures were taken on the confocal microscope to support the counting.

3.8.5 Myeloperoxidase and CD31

Kidney sections were stained with Myeloperoxidase (MPO) and CD31 antibody to show the presence of NETs within the MPO positive area, which was in close association with endothelial cells (CD31 positive area). This staining method shows the cytotoxicity associated with NETs on endothelial cells.

3.9 *Immunohistochemistry in human tissues*

Formalin-fixed paraffin-embedded sections of renal biopsies from five subjects with ANCA-positive RPGN, newly diagnosed in 2013, were drawn from the files of the Institute of Pathology at the Ludwig-Maximilians-University of Munich. Informed consent was obtained in all cases before renal biopsy. The renal biopsies were fixed in 4 % PBS-buffered formalin

solution and embedded in paraffin. Biopsies contained normal glomeruli and glomeruli exhibiting cellular, fibrocellular or fibrous crescents. Controls consisted of normal kidney tissue from tumor nephrectomies. TLR2 and TLR4 expression was assessed by using specific antibodies (TLR2-LS Bio, Seattle, WA, TLR4- Novus, Littleton, CO).

3.10 Electron microscopy

Kidney tissues and endothelial cell monolayers were fixed in 2.0 % paraformaldehyde/ 2.0 % glutaraldehyde, in 0.1 M sodium phosphate buffer, pH 7.4 for 24 hours, followed by 3 washes x15 min in 0.1 M sodium phosphate buffer, pH 7.4 and distilled water. For transmission EM kidneys were post-fixed, in phosphate cacodylate-buffered 2 % OsO₄ for 1h, dehydrated in graded ethanols with a final dehydration in propylene oxide and embedded in Embed-812 (Electron Microscopy Sciences, Hatfield, PA). Ultrathin sections (~90-nm thick) were stained with uranyl acetate and Venable's lead citrate. For scanning EM, after rinsing in distilled H₂O, cells on coverslips were treated with 1 % thiocarbohydrazide, post-fixed with 0.1 % osmium tetroxide, dehydrated in ethanol, mounted on stubs with silver paste and critical-point dried before being sputter coated with gold/palladium. Specimens were viewed with a JEOL model 1200EX electron microscope (JEOL, Tokyo, Japan).

3.11 RNA analysis

3.11.1 RNA isolation

Another part of the kidney from each mouse was preserved in RNA-later immediately after kidney isolation and stored at -20⁰C until processed for RNA isolation. RNA isolation was carried out using RNA isolation kit from Ambion (Ambion, CA, USA). In short, tissues (30 mg) preserved in RNA-later were homogenized using blade homogenizer for 30 seconds at speed 4 in lysis buffer (600 μ l) containing β -mercaptoethanol (10 μ l/ml). The homogenate was centrifuged at 6000 rpm for 5 minutes and 350 μ l of supernatant was transferred into a fresh DEPC-treated tube and 70 % ethanol was added and mixed gently. The whole mixture was then loaded on a RNA column and processed for RNA isolation as per manufacturer's instruction. Isolated RNA was measured, checked for purity as follows and stored at -80⁰C.

3.11.2 RNA quantification and purity check

The isolated RNA samples were quantified using a Nano drop (PEQLAB Biotechnology GMBH, Erlangen, Germany). The ratio of optical densities at 260 nm and 280 nm is an indicator for RNA purity (indicative of protein contamination in the RNA samples). Only samples with a ratio of 1.8 or more were considered to be of acceptable quality.

3.11.3 RNA integrity check

A further quality check (if necessary) was performed using a denaturing RNA gel. Briefly, 2% Agarose gel with Ethidium-bromide was casted, RNA samples were mixed with RNA loading buffer (4:1 ratio) (Sigma Aldrich, Germany) and the samples were loaded onto the gel. Electrophoresis was carried out at constant volt (70-100 V) using MOBS running buffer for 1 hour and the gel was imaged on a gel documentation apparatus under a UV lamp. RNA samples that show a single bright band were considered to be of good quality. Loss of RNA integrity could be detected as smear formation in the Agarose gel (Figure 10).

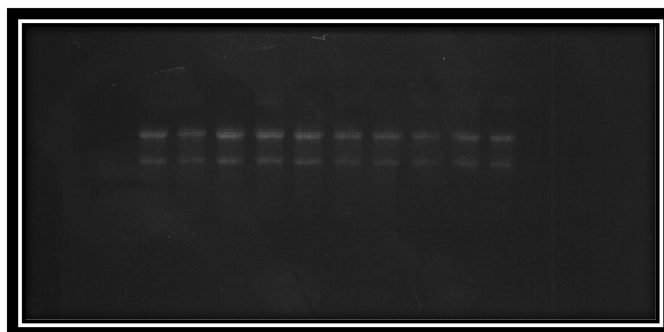


Figure: 10. RNA integrity check

3.11.4 cDNA synthesis and real-time RT-PCR (SYBR Green)

The isolated RNA samples were quantified and processed for cDNA conversion using reverse transcriptase II (Invitrogen, Karlsruhe, Germany). RNA samples were diluted in DEPC treated tubes containing water to get a final concentration of 2 µg / 30 µl. To the diluted RNA samples, 13.9 µl of master mix* was added and the tubes were incubated at 42⁰C for 1 hour

and 30 minutes on a thermal shaker. Upon completion of incubation, cDNA samples were stored at -20°C until used for RT-PCR analysis using SYBR green. The cDNA samples prepared as described above were diluted 1:10 for the real-time RT-PCR. 2 μl of diluted cDNA samples were mixed with SYBR green master mix (10 μl), forward primer (0.6 μl) and reverse primer (0.6 μl), that are specific for the gene of interest, Taq polymerase (0.16 μl) and distilled water (6.64 μl). The real-time RT-PCR was performed using Light Cycler480.

*The master mix was prepared by mixing 9 μl of 5x buffer (Invitrogen, Karlsruhe, Germany), 1 μl of 25 mM dNTP mixture (Amersham Pharmacia Biotech, Freiburg, Germany), 2 μl of 0.1 M DTT (Invitrogen, Karlsruhe, Germany), 1 μl of 40U/ μl RNAsin (Promega, Mannheim, Germany), 0.5 μl of Hexanucleotide (Roche, Mannheim, Germany), 1 μl of Superscript (Invitrogen, Karlsruhe, Germany) or ddH₂O in the case of the control cDNA (RT minus).

3.11.5 Real time PCR

SYBR Green Dye detection system (SYBR Green I 96 protocol LC480 Roche running program) was used for amplification. Quantitative real-time PCR was performed on Light Cycler 480 (Roche, Mannheim, Germany). Each amplification step included initiation phase 95°C , annealing phase 60°C and amplification phase 72°C and was repeated 45 times. Gene-specific primers (300 nM, Metabion, Martinsried, Germany) were used as listed in table 4. Controls consisting of ddH₂O were negative for target and housekeeper genes. Primers were designed to be cDNA specific and to target possibly all known transcripts of genes of interest. In silico specificity screen (BLAST) was performed. The lengths of amplicons were between 80 and 130 bp. The kinetics of the PCR amplification (efficiency) was calculated for every set of primers. The efficiency-corrected quantification was performed automatically by the LightCycler 480 based on external standard curves describing the PCR efficiencies of the target and the reference gene [ratio = $E_{\text{target}}\Delta C_{\text{Ptarget}}(\text{control} - \text{sample})/E_{\text{ref}}\Delta C_{\text{Pref}}(\text{control} - \text{sample})$]. To reduce the risk of false positive Cp the high confidence algorithm was used. All the samples that during the amplification reaction did not rise above the background fluorescence (crossing point Cp or quantification cycle Cq) of 40 cycles were described as not detected (n.d. = not detected in the figures). Crossing points between 5 and 40 cycles were considered as detectable. The melting curves profiles were analyzed for every sample to detect unspecific products and primer dimers. Products were visualized on agarose gels, extracted and analyzed for sequence.

3.11.6 Oligonucleotide primers used for SYBR-Green RT-PCR

The following oligonucleotide primers were used in this thesis.

Table: 4. Oligonucleotide primer sequences used in the study

Gene	Sequence
18s	Forward: GCAATTATTCCCATGAACG
	Reverse: AGGGCCTCACTAAACCATCC
Ccl2	Forward: CCTGCTGTTACAGTTGCC
	Reverse: ATTGGGATCATCTTGCTGGT
Cxcl10	Forward: GGCTGGTCACCTTTCAGAAG
	Reverse: ATGGATGGACAGCAGAGAGC
IL-6	Forward: TGATGCACTTGCAGAAAACA
	Reverse: ACCAGAGGAAATTTCAATAGGC
Nphs1 (Nephrin)	Forward: TTAGCAGACACGGACACAGG
	Reverse: CTCTTTCTACCGCCTCAACG
Nphs2 (Podocin)	Forward: TGACGTTCCCTTTTTCCATC
	Reverse: CAGGAAGCAGATGTCCCAGT
Nos2 (iNos)	Forward: TTCTGTGCTGTCCCAGTGAG
	Reverse: TGAAGAAAACCCCTTGTGCT
Tnf- α	Forward: CCACCACGCTCTTCTGTCTAC
	Reverse: AGGGTCTGGGCCATAGAACT
Wt-1	Forward: CATCCCTCGTCTCCCATTTA
	Reverse: TATCCGAGTTGGGGAAATCA
CXCL2	Forward: CGGTCAAAAAGTTTGCCTTG
	Reverse: TCCAGGTCAGTTAGCCTTGC
CD44	Forward: AGCGGCAGGTTACATTCAA

	Reverse:	CAAGTTTGGTGGCACACAG
BAD	Forward:	GTACGAACTGTGGCGACTCC
	Reverse:	GAGCAACATTCATCAGCAGG
FGL-2	Forward:	AGGGGTA ACTCTGTAGGCC
	Reverse:	GAACACATGCAGTCACAGCC
BID	Forward:	GTGTAGCTCCAAGCACTGCC
	Reverse:	GCAAACCTTTGCCTTAGCC
NOXA	Forward:	ACTTTGTCTCCAATCCTCCG
	Reverse:	GAAGTCGCAAAAGAGCAGGA
PUMA	Forward:	CACCTAGTTGGGCTCCATTT
	Reverse:	ACCTCAACGCGCAGTACG

3.12 Flow cytometry

Flow cytometric analysis of cultured and renal immune cells was performed on a FACS Calibur flow cytometer (BD) as described 52. Every isolate was incubated with binding buffer containing either anti-mouse CD11c, CD11b, CD103, F4/80, and CD45 antibodies (BD) for 45 min at 40C in dark were used to detect renal mononuclear phagocyte populations. Anti-CD86 (BD) was used as activation marker. Anti-CD3 and CD4 (BD) were used to identify the respective T-cells population.

3.13 In-vitro methods

3.13.1 Cell freezing and thawing

At earlier passages, large amounts of cells were grown under standard culture conditions and were frozen for future use. For freezing cells, cells were detached from the culture plates and spun down under sterile conditions for 3 minutes at 1000 rpm. The cell pellet was maintained on ice and carefully re-suspended in cold freezing medium (90 % FCS and 10 % DMSO) by

pipetting the suspension repeatedly up and down. 1.5 ml aliquots were quickly dispensed into freezing vials (4⁰C) and the cells were slowly frozen at -20⁰C for 1 hour and then at -80⁰C overnight. The next day, all aliquots were transferred into liquid nitrogen.

In order to thaw cells, a frozen vial was removed from liquid nitrogen and put into the water bath at 37⁰C. The cells were then dispensed in 5 ml of warm complete growth medium and spun down at 1000 rpm for 5-7 minutes. The old medium was then removed and the cells were re-suspended in fresh medium and transferred into a new culture plate. The medium was changed once more after 24 hours.

3.13.2 Cell culture

GEnCs were cultured using standard cell culture techniques. Briefly, cells were thawed from liquid nitrogen and immediately seeded into 150cm² cell culture plates containing 20 ml of complete RPMI media with 10 % FCS and 1 % PS. Cells were allowed to grow until they became confluent, fresh media was supplied every 2 days. For growing podocytes and mPECs specified media was used, in which RPMI containing 1 % P/S and 5 % FCS and if required for controlling pH we used 1% Sodium pyruvate, 1 % HEPES and 1 % Sodium Bicarbonate. When cells reached 80-90% confluence, they were split or detached from the plate by adding 2 ml of trypsin solution and the cells incubated at 37⁰C for 2-3 minutes. Once the cells were detached from the plate, trypsin was neutralized by adding complete media, and then the cells were centrifuged at 1200 rpm for 5 minutes. The cells were re-suspended in normal media and exact number of cells counted using a Neubauer chamber. The required number of cells was used for the different experiments like cytotoxicity assay using MTT dye, angiogenesis assay etc.

3.13.3 Assessment of histone induced toxicity on GEnC

For cytotoxicity experiments, 10 to 15x10⁴ GEnCs were seeded in 96-well plates and allowed to adhere overnight. Once the cells adhered to the plates, different concentrations of histones were added to the cells in the absence or presence of anti-histone IgG, whereas control groups were only stimulated with Control IgG for 18 to 24 hours. Cytotoxicity was detected by non-radioactive cell proliferation assay kit. Briefly, after the stimulation cells were supplemented

with 15 μl of the MTT dye solution and incubated at 37°C for 4-6 hours. During this time, live cells were converting the MTT dye into colored formazon crystals and these crystals were then dissolved using 100 μl of stop solution. The color change can be detected using a photometer at $\lambda=570$ nm. The color is directly proportional to the live cells.

3.13.4 Podocyte culture and detachment assay

Podocytes are terminally differentiated highly specialized cells with a complex cellular architecture. Podocytes do not have the ability to divide and multiply, therefore we used immortalized podocytes (from H-2K^b-tsA58 mice) that were cultured in the presence of recombinant mouse IFN- γ (100 U/ml) at 33°C in collagen-1 coated plates using DMEM media containing 1% of HEPEs, sodium bicarbonate and sodium pyruvate (to maintain the pH of the medium). The cells were trypsinized once they were 80% confluent. For the differentiation of podocytes, cells were grown in collagen-I coated plates at 37°C without IFN- γ for 14 days and then used for experiments. For detachment assays, a specific number of podocytes were plated in 10 cm dishes and allowed to differentiate. These differentiated cells were stimulated with histones (100 $\mu\text{g}/\text{ml}$) for 24 hours with or without anti-histone IgG. In the case, podocytes detach from the plate, it is a sign that these cells are dead. This was determined by counting the detached cells in the supernatants and the ratio was reported as live and detached cells (Figure 11). Further results were also confirmed by an MTT assay.

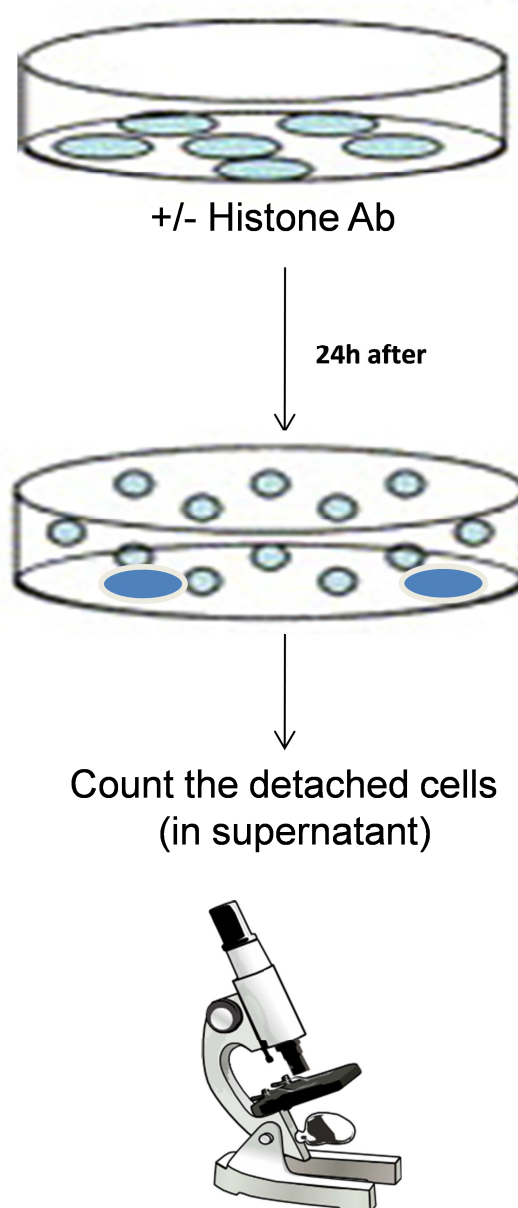


Figure: 11. Schematic diagram showing the procedure employed to perform the podocyte detachment assay.

3.13.5 Neutrophil isolation and NETs formation and cytotoxicity assay

Neutrophils were isolated from mouse the peripheral blood. Whole blood was collected into heparin tubes from the facial vein and mixed with 1,25% of high molecular weight dextran (molecular weight 450K-650K), and RBCs were allowed to settle at 4⁰C. The upper clear yellowish leucocyte rich layer was separated and lysed for the remaining RBCs using hypotonic lysis (ddH₂O) and tonicity was maintained by adding 0,15M KCl. Resultant leucocytes were enriched for neutrophils by gradient centrifugation with Biocoll solution (density of 0,177). As the neutrophils were very sensitive to the external stimuli, care was taken not to activate them by aggressive shaking and all the procedure were performed at 4⁰C. No glass material was used as neutrophils sticks to the glass surface.

Once the pure neutrophils were isolated, suspended in plane RPMI media and then incubated at 37⁰C in CO₂ incubator for 30 minutes to rest, the NETosis experiments were carried out. We hypothesized that NETs can kill endothelial cells, therefore we performed co-culture experiments with GEnC and neutrophils followed by in-situ NETs formation using TNF- α or PMA (known agonists for NETs formation, concentrations used did not have any direct killing effect on GEnC). The cytotoxicity of NETs was analyzed by MTT assay, in which only survived GEnC were able to convert the MTT salt. The results were confirmed by immuno-fluorescence staining and scanning electron microscopy (SEM).

3.13.6 Intra-renal administration of histones

To check the cytotoxic effect of histones on glomerular cells, histones were injected directly into the renal artery of WT and *Tlr2/4 KO* mice as illustrated in figure 12. One group of mice received histones after treating with anti-histone IgG, whereas the control mice were administered with Control IgG. In the case of *Tlr2/4 KO* mice, histones were only injected to check the cytotoxic effects compared to WT mice. After 24 hours, mice were sacrificed and kidneys fixed in formalin and taken for histological evaluation using PAS and fibrinogen staining to check the effect on glomerular cells and endothelial cell damage.



Figure: 12. Histone injection into the renal artery, the abdominal aorta and the left renal artery was prepared and a microcannula was placed into the left renal artery (left) for histone injection. The puncture site was mounted with glue before closure of the wound (right)⁹.

3.13.7 Isolation of glomeruli

To further confirm the cytotoxic effects of histones on glomerular cells, we isolated pure glomeruli from WT and *Tlr2/4 KO* mice. The glomerular fraction was isolated by using magnetic isolation using perfusion of paramagnetic beads. Briefly, animals were anesthetized by an intraperitoneal injection of narcosis mix. Animals were cut open by midline incision and kidneys excised along with the intact arteries and veins and then taken for microsurgery using Leica, WILD M10 microscope with the help of micro scissors and forceps. Renal arteries were cut open to locate the arterial entrance into the kidney. Using a 1 ml syringe containing paramagnetic beads were slowly administered into the kidney containing 2×10^6 magnetic beads (Dnabeads, M-450 Epoxy). Successful perfusion will turn the kidney pale. After completion of the perfusion, kidneys were minced into fine pieces. Kidney samples were then digested with collagenase A for 30 minutes at 37°C and the digested tissue was passed through a $100 \mu\text{m}$ cell strainer on ice. Digested and filtered tissue was passed through cell separation magnet (BD IMagnet, BD) and washed 5 times to isolate the glomeruli fractions. The first wash elutes the tubulointerstitial part of the kidney, the second wash eluted predominantly the tubular fraction and the remaining fractions were washed carefully until a 95 % to 98 % purity of glomeruli was obtained upon microscopic observation. The uniform glomeruli were seeded in 96-well plates and stimulated with histones to check the cytotoxic effects on the entire glomeruli, which can be measured by the release of LDH. The results were compared between WT and *Tlr2/4 KO* glomeruli. In another set of experiment,

following histone stimulation with or without α -Histone IgG for 6 hours all fractions were lysed using RNA lysis buffer to prepare mRNA and stored at -20°C until further use.

3.13.8 *In-vitro* tube formation assay

To study the cytotoxic effects of histones on formed microvasculature, we setup the tube formation assay in which the cells were grown on 3D-matrix made of basement membrane protein called matrigel. Matrigel was thawed overnight at 40°C to make it liquid and $10\ \mu\text{l}$ was added into each well of the μ -slide angiogenesis (ibidi, Munich, Germany) allowing solidifying at 37°C . GEnCs were seeded at 1×10^4 cells/well and stimulated with VEGF and b-FGF as positive control or with histones in the absence or presence of histone antibody. Tube formation as a marker of angiogenesis was assessed by light microscopy by taking series of pictures at 0 hour, 4 hours, 8 hours and 24 hours. The cell covered area was calculated using the software photoshop. Angiogenic score was determined by blinded technique.

3.14 *BWA3 hybridoma culture and anti-histone IgG purification*

Anti-histone IgG was isolated from the culture supernatants of monoclonal BWA-3 hybridoma cells. Initially BWA-3 cells were revived from liquid nitrogen and cultured in normal growth medium (DMEM) containing 10 % FBS and 1 % PS until the cells attain confluence. Cells were collected by centrifugation and seeded in CD hybridoma media containing 5 % ultra-low IgG serum, 1 % PS and 2 mM glutamine into cell culture flasks (Monestier *et al*, 1993). Cells were allowed to grow and during this time, hybridoma cells secreted α -Histone IgG in the supernatants. After 7-8 days, the supernatant was centrifuged to separate the cells and debris, and suspension was filter through $0.22\ \mu\text{m}$ membranes and stored at 4°C in SCOTH bottles. To purify and concentrate anti-histone IgG, hybridoma culture supernatants were passed through high trap protein GHP columns. Initially, columns were activated by passing 20 mM sodium phosphate buffer (pH 7.0) through followed by the hybridoma culture supernatant. During this process, antibodies bind to protein GHP columns and this can be eluted using low pH (0,1M glycine hydrochloride buffer (pH 2,7)) into 2 mL Eppendorf tubes and the acidic pH can be neutralized to 7 using the appropriate amount of 1M Tris-HCl buffer (pH 9,0).

The obtained antibody can be quantified for its concentration by measuring the absorbance (optical density O.D) using a UV-visible spectrophotometer at a wave length of 280 nm for total protein concentration. For determining the actual concentration of the anti-histone IgG, the O.D values were multiplied with the factor 0.7 and the antibody was then stored at -20⁰C until further use. Binding efficiency of the antibody was confirmed by western blotting using total histones as positive control.

Note: avoid repeated freezing and thawing of anti-histone IgG

3.15 Statistical analysis

Data are presented as mean \pm SEM. For multiple comparisons of groups one way ANOVA was used with post-hoc test using GraphPad prism (CA, USA). Paired Student`s t-test was used for the comparison of single groups. A value of $p < 0.05$ was considered to indicate statistical significance.

4. Results

4.1. Glomerular expression of TLR2 and TLR4 in human severe glomerulonephritis

Allam *et.al* have previously shown that extracellular histones can act as ligands for TLR2 and TLR4 leading to the tubular injury after AKI⁹. Therefore we studied the expression of these receptors in the glomeruli of both healthy and severe glomerulonephritis in human kidneys. To investigate this, we performed immunohistological staining using TLR2 and TLR4 antibodies in healthy human kidney (Biopsy taken during kidney transplantation) and kidney biopsies from patients with ANCA-vasculitis, a severe form of glomerulonephritis. TLR2/4 immunostaining of normal human kidney showed only a weak granular positivity in all glomerular cells, whereas TLR4 positivity was clearly observed in the glomerular endothelial cells (Figure 13A). In addition, TLR2 was strongly expressed in the cytoplasm of epithelial cells of the proximal and distal tubule, while the TLR4 expression was less prominent (Figure 13A).

However, immunostaining of kidney biopsies from patients with ANCA-associated necrotizing and crescentic GN revealed a strong expression of TLR2 and TLR4 also in parietal epithelial cells (PECs) along the inner aspect of the Bowman's capsule (Figure 13B). Furthermore, glomerular crescents are known to be predominantly formed by PECs^{171,172}. As shown in Figure 13C, glomerular crescents were positive for both receptors TLR2 and TLR4, and the isotype IgG staining confirmed the specificity as this control staining was negative in all tissues (Figure 14). Together, TLR2 and TLR4 expression was observed in the cells of the normal glomerulus and ligands for the TLR2/4 can activate PECs proliferation and responsible for the induction of crescentic GN.

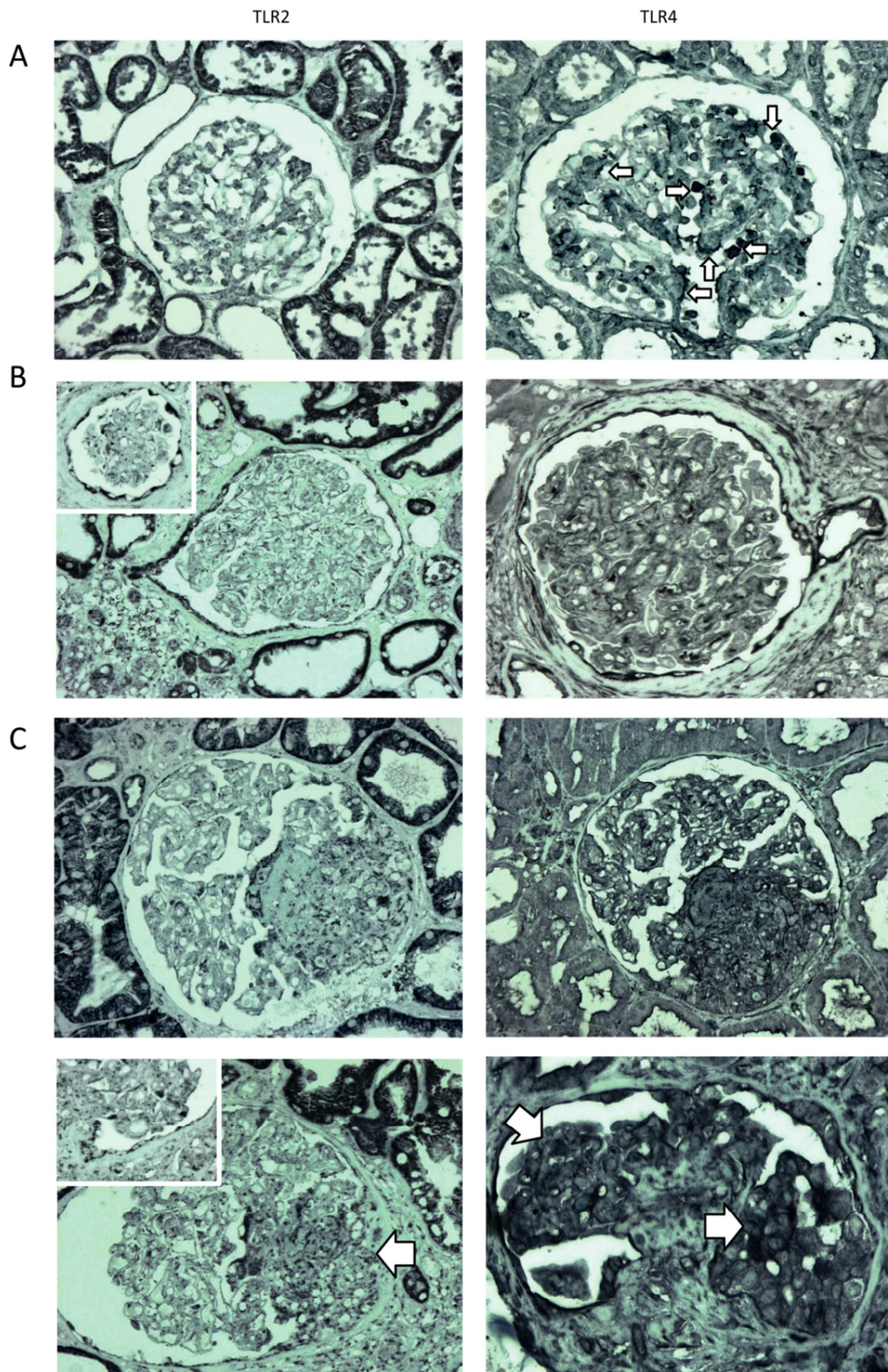


Figure: 13. TLR2 and TLR4 expression in human crescentic glomerulonephritis. Toll-like receptor (TLR)-2 and -4 immunostaining was performed on healthy kidney tissue (A) or on kidney biopsies from patients with recently diagnosed ANCA vasculitis and clinical signs of glomerulonephritis (B and C). (B) Glomeruli were unaffected by loop necrosis or crescent formation, while glomeruli affected by such lesions are shown in (C). Original magnification x400.

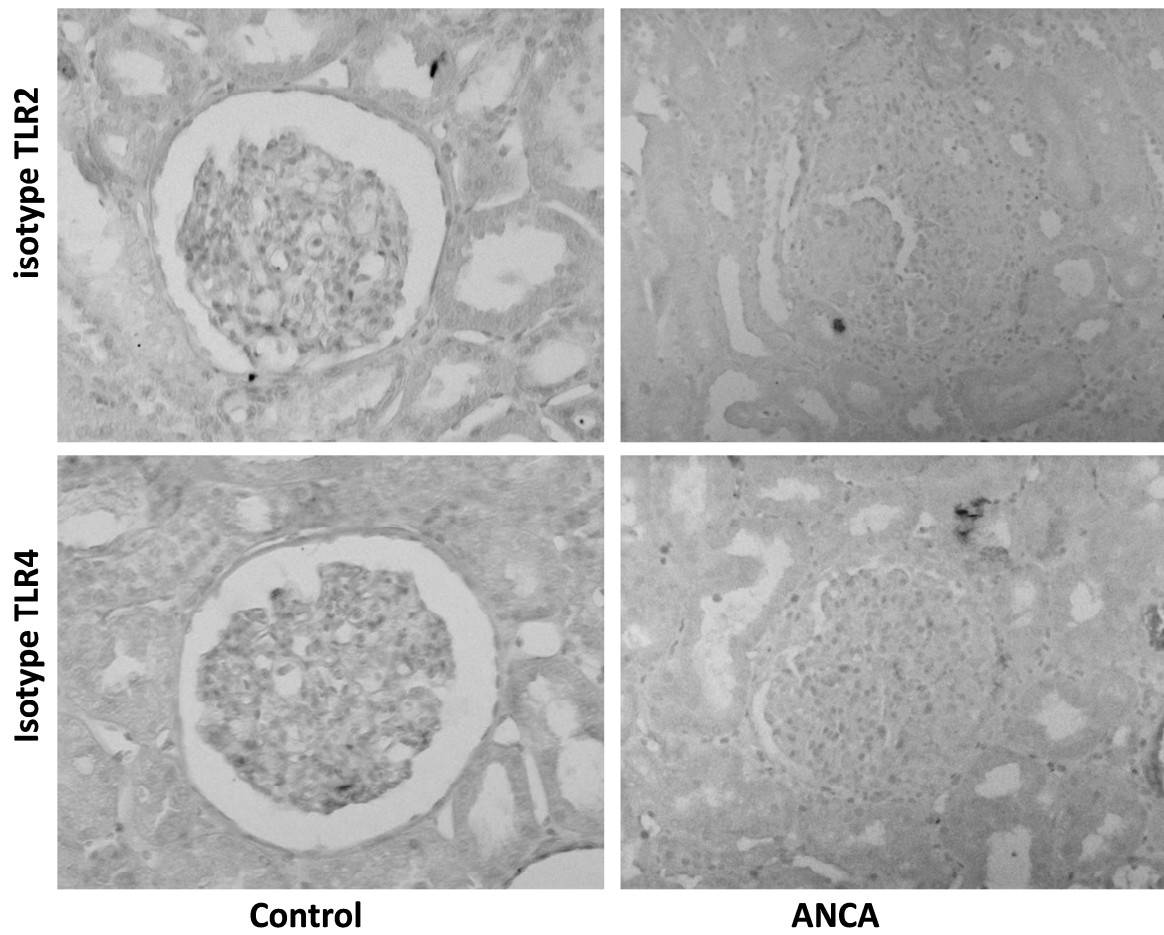


Figure: 14. Isotype staining were negative in both control and ANCA kidney sections.

4.2. Extracellular histones drive glomerular cell necrosis *in-vitro*

4.2.1. Anti-histone IgG prevents histone toxicity on glomerular cells

It has been previously reported that extracellular histones can cause toxicity and kill different types of cells including tubular epithelial cells and pulmonary endothelial cells *in-vitro* and *in-vivo*⁹. To confirm the cytotoxic effect of extracellular histones on cultured glomerular endothelial cells (GEnCs), we cultured GEnCs in 96 well plates at a cell density of 10.000 to 15.000 cells/well in the presence of different concentration of histones and with or without the neutralizing histone antibody to block the action of histones. The cells were stimulated for 24 hours and the OD measured via a photospectrometer at 570nm. As shown in Figure 15A, treatment of GEnCs with the histone preparation resulted in a decrease in the absorbance (OD) indicating that histones were cytotoxic on GEnCs. This cytotoxic effect of histones on GEnCs occurred in a dose-dependent manner. Previously, anti-histone IgG derived from BWA3 hybridoma has been demonstrated to be able to neutralize the cytotoxic and immunostimulatory effect of extracellular histones^{10,94,141}. To test this, GEnCs were incubated with anti-histone IgG (at 100µg/ml concentration) following treatment with different concentration of histones. The data show that anti-histone IgG almost entirely prevented histone toxicity in glomerular endothelial cells up to a histone concentration of 30µg/ml (Figure 15A).

Next, we wanted to investigate whether histones had a cytotoxic effect on other glomerular cells such as PECs and podocytes. To do so, these cells were cultured with different histone concentration in the absence or presence of anti-histone IgG. Histones also induced toxicity in cultured PECs and podocytes, but occurred at much higher histone concentrations (Figure 15B and 15C) compared to the toxic dose required for killing endothelial cells (Figure 15A). Neutralization of histones with anti-histone IgG prevented the killing action of histones on PECs and podocytes in an efficient manner (Figure 15B and 15C). The findings confirmed the cytotoxic effects of histones on glomerular cells that were inhibited following treatment with anti-histone IgG.

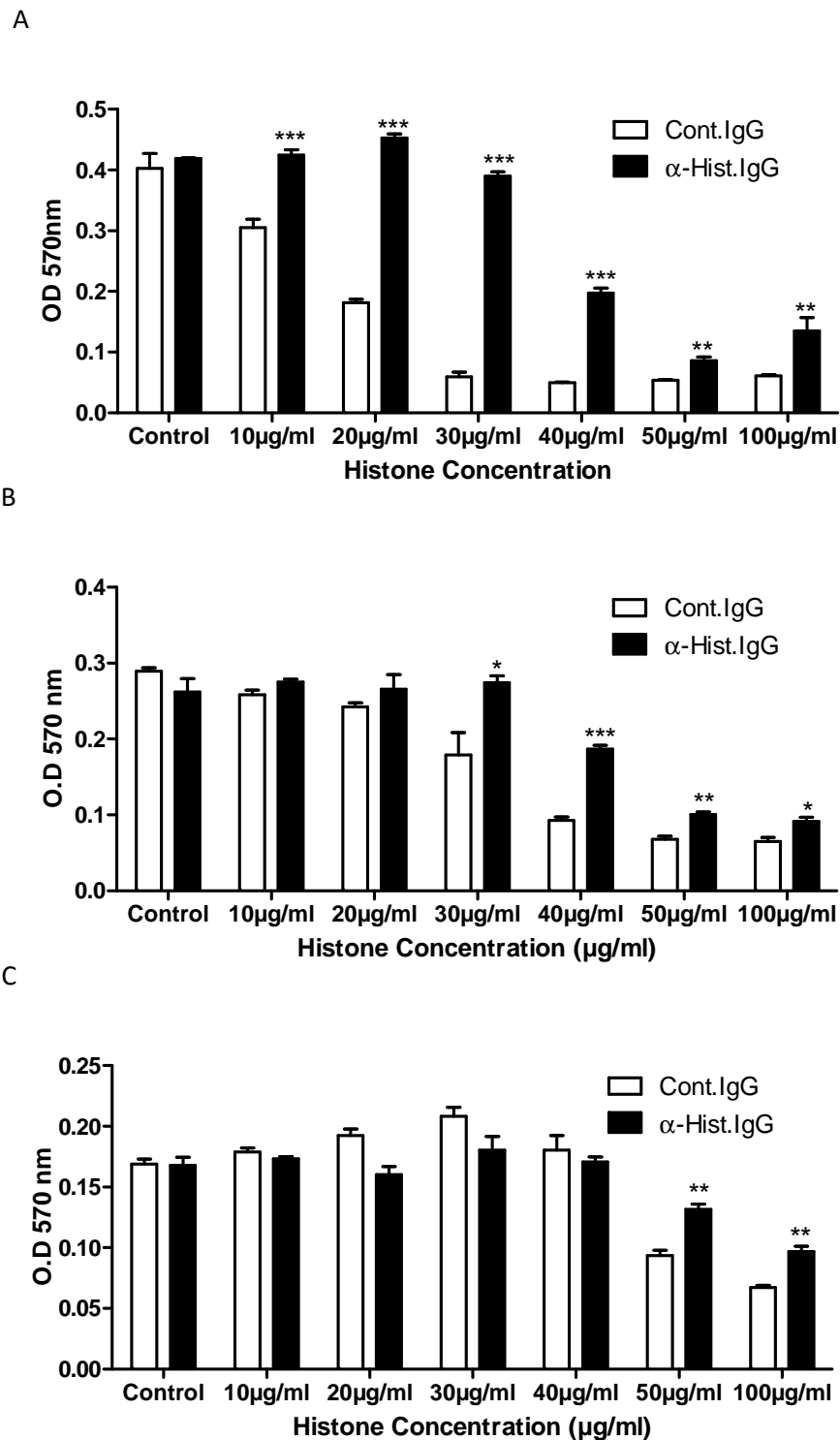


Figure: 15. (A) Murine glomerular endothelial cells (GENC), (B) podocytes, and (C) parietal epithelial cells (PECs) were incubated with increasing doses of histones together with either control IgG or anti-histone IgG. Cell viability was determined after 24 hours by MTT assay. Values are the mean \pm SEM of three independent experiments. * = $P < 0.05$, ** = $P < 0.01$, *** = $P < 0.001$.

4.2.2. Anti-histone IgG prevents histone toxicity on neovascularization and microtubules

Endothelial cells have been shown to grow on matrigel surface, which resembles the microvasculature of the glomeruli. Therefore, this model seemed to be suitable to mimic the *in-vivo* conditions of glomerular capillary system and to study the cytotoxic effects of histones on the microvasculature.

In our next *in-vitro* experiments, GEnCs were grown on a Matrigel surface to form neovascularization or microtubules, which resembles the microvasculature similar to that observed in the glomerular tuft. The addition of histones (40 μ g/ml) induced destruction of a microtubule formation within 12 hours, whereas treatment with anti-histone IgG prevented histone-induced GEnC microtubule destruction after 8 and 24 hours, as illustrated in Figure 16A. Treatment of endothelial cells with anti-histone IgG resulted in an increase in the cell covered area (Figure 16B) and a significant high angiogenesis score (Figure 16C) compared to control IgG.

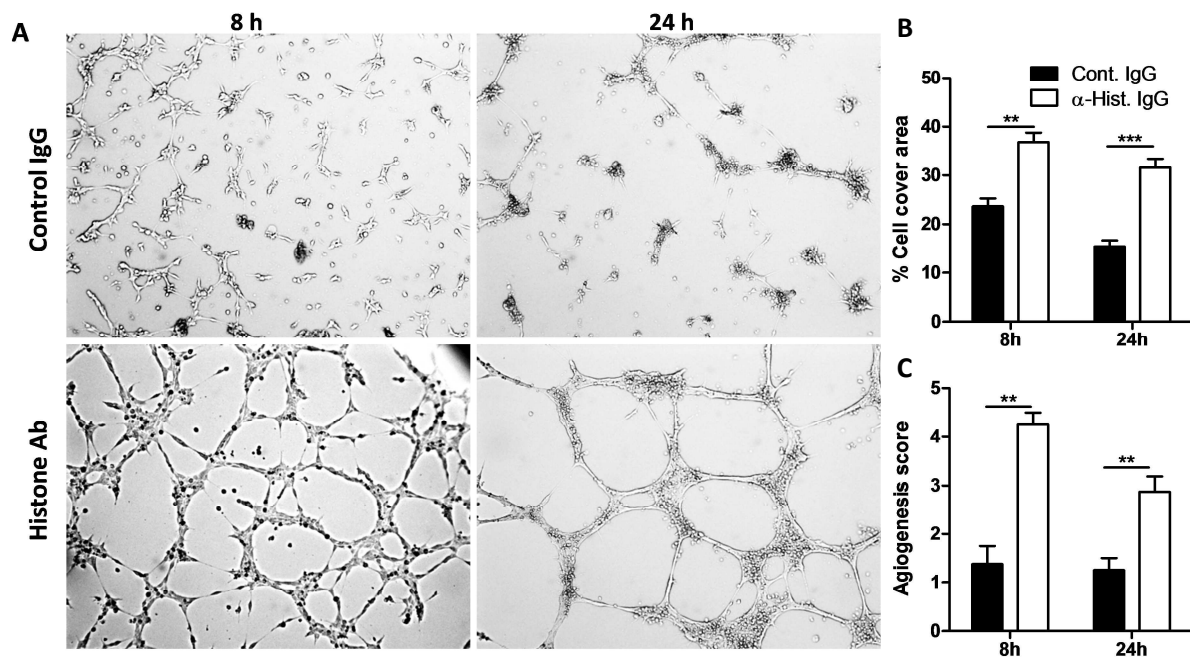


Figure: 16. Histones and endothelial cell microtubules *in vitro*. (A) Murine glomerular endothelial cells were seeded into a matrigel matrix for angiogenesis experiments as described in methods (section 3.10.8) treated with histones, with or without anti-histone IgG. After 8 hours and 24 hours of stimulation, the control IgG group shows complete GEnC death, whereas the anti-histone IgG group shows a well preserved microvasculature. (B) Cell covered area and (C) angiogenic score are demonstrated. Values are the mean \pm SEM of two independent experiments. ** = $P < 0.01$, *** = $P < 0.001$.

Next, we allowed the formation of microtubules for 12 hours on a matrigel surface. After the microtubule formation was completed, we stimulated the microtubules with histone (40 μ g/ml) in the presence or absence of anti-histone IgG after 8 hours (as 0 hour control). The data in Figure 5 demonstrate that prior to the stimulation with histone both groups showed well-formed microtubules with the same percentage of cell covered area and angiogenesis score. After 12 hours of histone treatment, the microtubule structure was destroyed in the control IgG groups (Figure 17A) and the percentage of the cell covered area and the angiogenesis score decreased (Figure 17B and 17C), which was completely rescued by treatment with anti-histone IgG. The data confirmed that histones also had the ability to kill already formed microtubules, which is most likely to occur in *in-vivo* settings as well. Therefore, neutralization of histones was beneficial to protect the microvasculature.

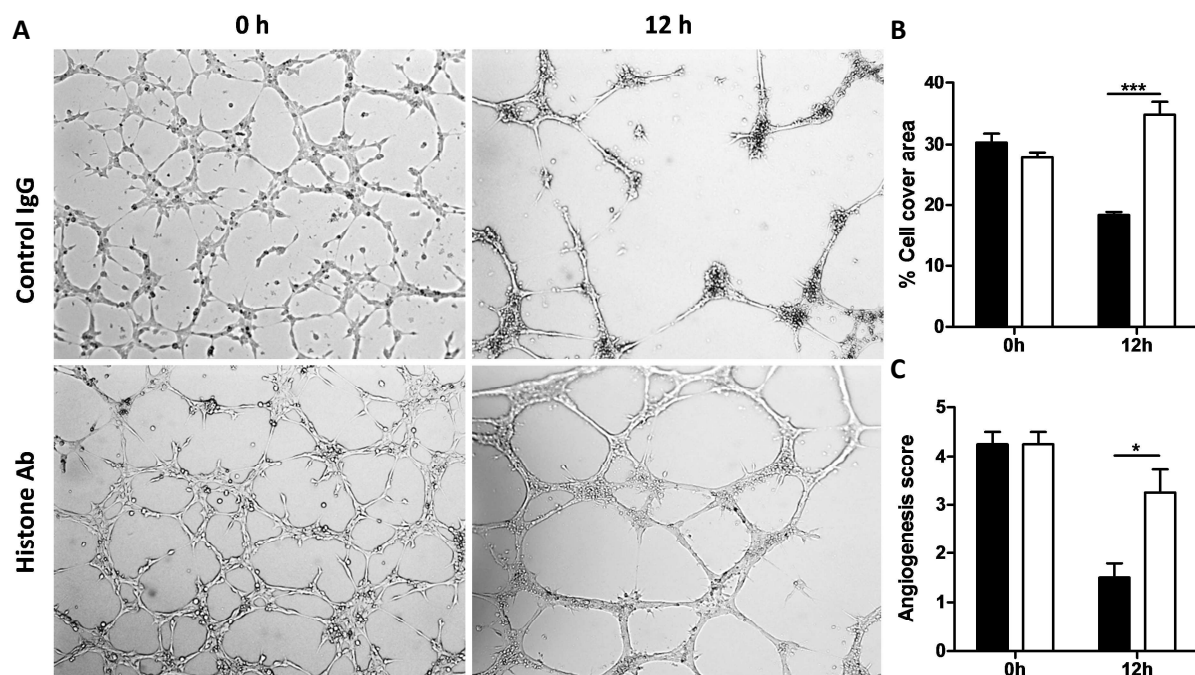


Figure: 17. Histones and endothelial cell microtubules *in-vitro*. (A) Murine glomerular endothelial cells were seeded into a matrigel matrix for angiogenesis experiments as described in methods (section 3.10.8) treated with histones, in the presence or absence of anti-histone IgG. After 0 hour and 12 hours of stimulation, control IgG showed GEnC death, whereas treatment with anti-histone IgG preserved the microvasculature. (B) The percentage of cell covered area and (C) angiogenic score. Values are the mean \pm SEM of two independent experiments. * = $P < 0.05$, *** = $P < 0.001$.

4.3. Neutrophil extracellular traps kill glomerular endothelial cells through histone release

4.3.1. Histones were released during NETosis

Previously, it has been reported that during severe GN neutrophils can undergo NETosis¹⁷³. NETosis is a form of programmed cell death that occurs in the presence of cytokines released from dying cells due to a severe inflammatory insult^{160,174}. As a consequence nuclear chromatin including histones and DNA are released from NETting neutrophils within the glomerular capillaries²⁵. We hypothesized that histones present within the chromatin structure were functionally pathogenic during GN. To investigate this in more detail, we performed *in vitro* experiments to demonstrate the formation of NETs from isolated neutrophils. Neutrophils were stimulated or left untreated for 8 hours and then stained for elastase (red) and histones (green). Fluorescent microscopy showed that PMA-activated neutrophils released chromatin material including histones compared to unstimulated cells (Figure 18) indicating that activated neutrophils were forming NETs and released their nuclear material including histones.

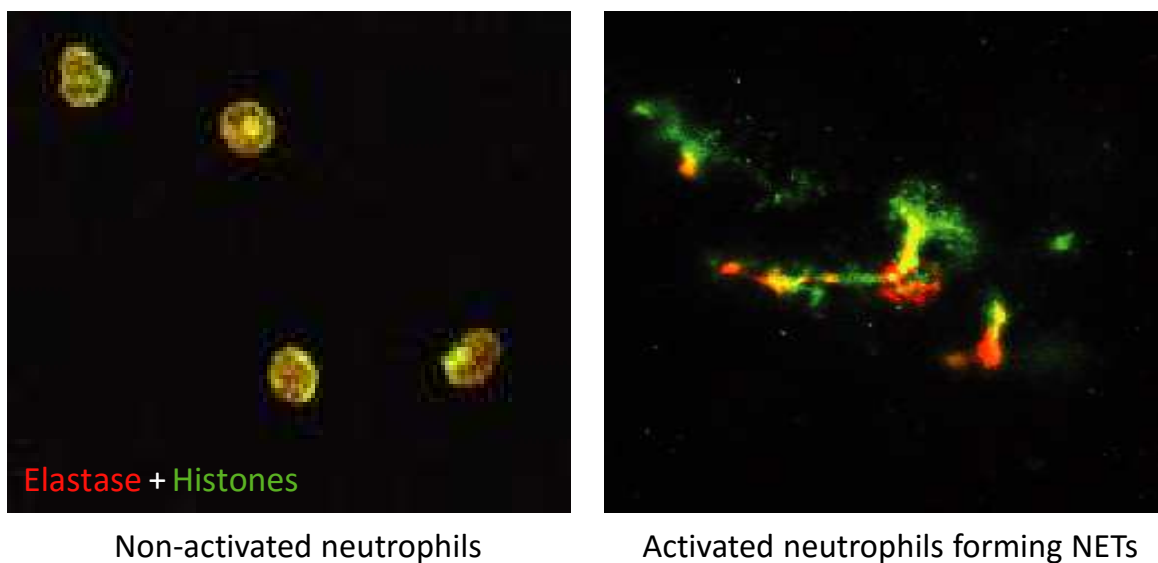


Figure: 18. Non-activated neutrophils did not form NETs (left image). Right image, neutrophils formed NETs following activation with PMA and released nuclear material including the granular protein elastase (red) and the nuclear proteins histones (green) into the extracellular space.

4.3.2. Histones in the formed NETs kill GEnC *in-vitro*

To further investigate the killing action of histones, we set up an experiment where we added neutrophils onto a monolayer of GEnCs and incubated the cells in the presence of TNF- α or PMA in 4 well permonax microslides to induce NETosis. The killing action of NET related histones was evaluated by scanning electron microscopy (SEM). After inducing NETs on a monolayer of GEnC using TNF- α in the absence of presence of anti-histone IgG, the cells were fixed using electron microscopic fixative (2 % glutaraldehyde and 2 % paraformaldehyde) and analyzed for the pathogenic changes induced by NETs on GEnC. The SEM results showed that TNF- α treatment alone did not affect the morphology of GEnC (Figure 19, left). However, TNF- α activated neutrophils formed NETs that killed the monolayer of GEnC as illustrated by blebs formation on the cell surface (Figure 19, middle). In the group where anti-histone IgG was added to the cells, the GEnC were completely protected from the cytotoxic effects exhibited by the NETs (Figure 19, right), whereby the GEnC showed normal cell morphological features similar to the control group (Figure 19, left).

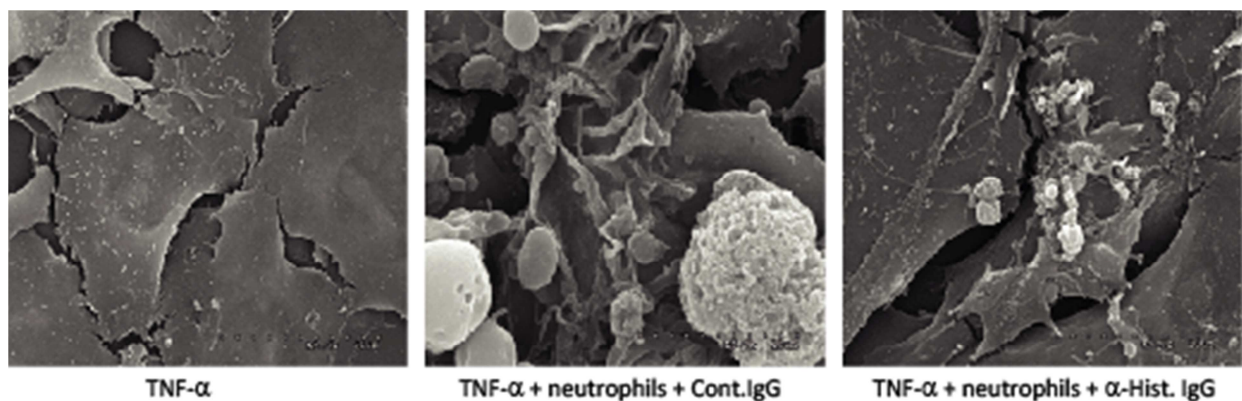


Figure: 19. Scanning electron microscopy was performed on monolayers of glomerular endothelial cells, which appeared flat and evenly laid out (left image). However, neutrophil ETosis caused severe injury and death of endothelial cells appearing as bulging white balls with corrugated surfaces adjacent to TNF α -activated NETs (middle image). This effect was almost entirely prevented by anti-histone IgG treatment demonstrated by a significant reversal of the structural integrity of the endothelial cell monolayer (right image).

The killing actions of NETs-related histones were further investigated by immunostaining of fixed cells. The data showed that neutrophils that were undergoing TNF- α -induced NETosis destroyed the monolayer of glomerular endothelial cells by inducing endothelial cell death, which can be seen by reduced DAPI staining (Figure 8A, middle) compared to treatment with TNF- α alone (Figures 20A, left). Interestingly, the observed NETosis-related endothelial cell toxicity was entirely prevented by anti-histone IgG treatment (Figure 20A, right) that did not affect NET formation as illustrated by clumping of elastase (red) and histones (green) and preserved DAPI staining (blue). Together, we conclude that NETting neutrophils damage glomerular endothelial cells via the release of histones. These findings were confirmed using a colorimetric MTT assay to measure endothelial cell viability. As shown in Figure 20B, addition of anti-histone IgG resulted in a significant increase in the O.D values compared to the control IgG-treated group when neutrophils were stimulated with the NETosis inducing stimuli TNF- α or PMA indicating that anti-histone IgG prevented death of GEnC. Non-activated neutrophils did not induce GEnC death that was independent of anti-histone IgG treatment.

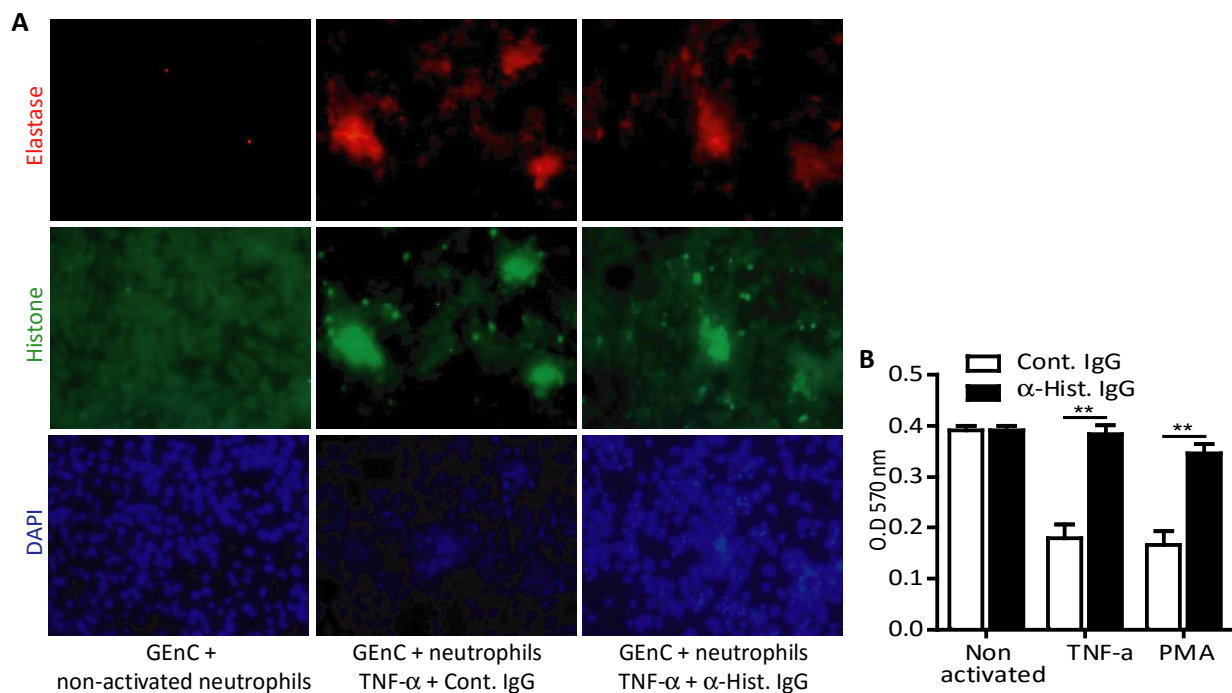


Figure: 20. Anti-histone IgG prevents cell death in glomerular endothelial cells. Glomerular endothelial cells were co-cultured with TNF- α -activated neutrophils in the presence of anti-histone IgG or control IgG. (A) Immunostaining for elastase, histone, and DAPI. (B) Neutrophils were activated with the NETosis stimulus TNF- α and PMA and the MTT assay analysis of endothelial cell viability was used to measure the O.D at 570 nm. Values are the mean \pm SEM of two independent experiments. ** = $P < 0.01$.

4.4. Histones need TLR2/4 to trigger glomerular necrosis and microangiopathy

Allam R *et al* has previously reported that extracellular histones mediate its cytotoxic effects in a TLR2/4-dependent manner in tubular epithelial cells⁹. Currently, it is unknown whether glomerular toxicity of extracellular histones occurs in a TLR2/4-dependent manner. To answer this question we have setup *ex-vivo* and *in-vivo* experiments using glomeruli that were isolated from *Tlr2/4*-deficient mice.

4.4.1. Histones are cytotoxic to wild-type but not *Tlr2/4*-deficient glomeruli *ex-vivo*

To determine the cytotoxic effect of extracellular histones, we isolated glomeruli from wild-type (Figure 21, picture) and *Tlr2/4*-deficient mice and incubated the glomeruli with histones at a concentration of 50 $\mu\text{g/ml}$ *ex-vivo* for 12 hours. Following incubation, we performed a lactate dehydrogenase (LDH) assay to measure the cytotoxic effect of extracellular histones. We found that histone exposure of glomeruli isolated from wt mice resulted in a significant increase in the LDH levels confirming the cytotoxicity of histones on glomeruli (Figure 21, graph). Interestingly, the LDH levels were significantly reduced when glomeruli from *Tlr2/4*-deficient mice were treated with histones compared to glomeruli from wt mice (white bars). This indicated that the cytotoxic effect of extracellular histones on glomeruli occurred in a TLR2/4 dependent manner.

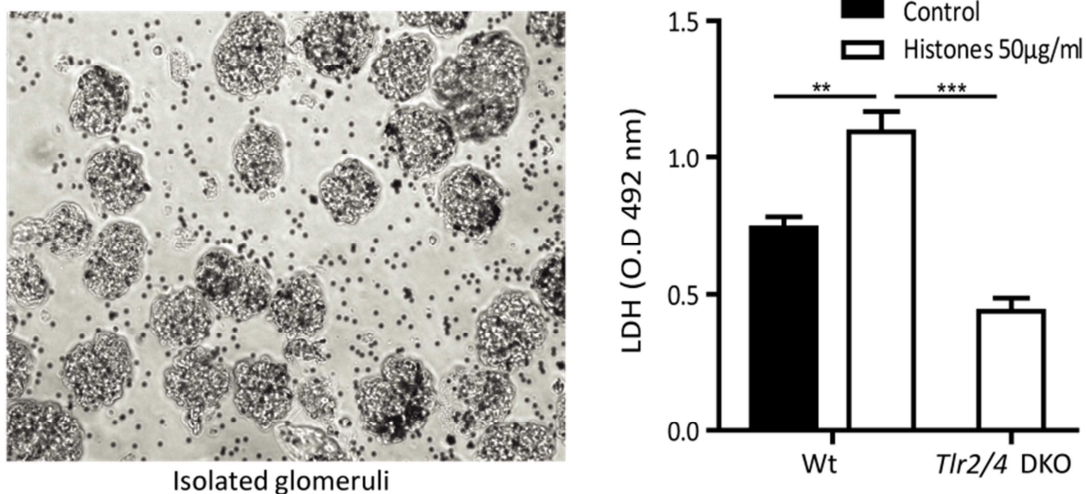


Figure: 21. (Left image) Representative image of isolated glomeruli from wild-type (wt) mice. (Right graph) Glomeruli were isolated from wt and *Tlr2/4*-deficient mice and incubated *ex-vivo* with histones (30 $\mu\text{g/ml}$). After 12 hours, LDH release in the supernatants was measured as a marker of glomerular

cell injury. Data represent mean OD \pm SEM of three experiments measured at a wavelength of 492 nm. ** = $P < 0.01$, *** = $P < 0.001$.

4.4.2. Extracellular histones stimulate inflammation in wild-type glomeruli ex-vivo

After showing that extracellular histones were cytotoxic to glomeruli isolated from wt mice, we wanted to investigate the pro-inflammatory effects of extracellular histones. Therefore, we exposed glomeruli that were isolated from both wt and *Tlr2/4*-deficient mice with histones (50 μ g/ml) and measured the mRNA values of pro-inflammatory cytokines via real time RT-PCR. As shown in Figure 10, glomeruli isolated from wt mice that were stimulated with histones significantly increased the mRNA expression of pro-inflammatory mediators such as TNF α (Figure 22A) and IL-6 (Figure 22B). In contrast, glomeruli from *Tlr2/4*-deficient mice, when exposed to histones, did not trigger the expression of IL-6 and TNF mRNA indicating that the pro-inflammatory effect of histones also occurred in a TLR2/4-dependent manner (Figure 22A and 22B).

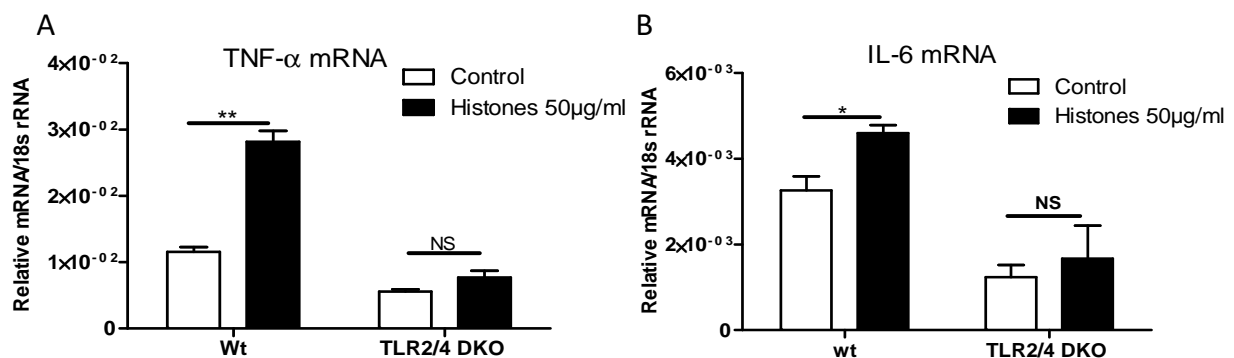


Figure: 22. Induction of cytokines in isolated glomeruli *ex-vivo* that were exposed to histones. Glomeruli were isolated from wild type (wt) and *Tlr2/4* double knockout mice, and exposed to histones (50 μ g/ml). After 12 hours, the mRNA levels of TNF- α (A) and IL-6 (B) were determined by real-time RT-PCR. Values are the mean \pm SEM of two independent experiments. * = $P < 0.05$, ** = $P < 0.01$.

4.4.3. Extracellular histones need involvement of TLR2/4 to show its toxic effects in-vivo

Finally, we wanted to look at the toxic effect of histones on glomeruli *in-vivo*. Reports have previously shown that an intravenous injection of histones can cause pulmonary microvascular injury, which is lethal in mice¹⁰. Therefore, we injected histones 10 mg/kg directly into the left renal artery in both wt and *Tlr2/4*-deficient mice that were anesthetized.

After 24 hours, kidneys were harvested and photon microscopy carried out to look at the structures of glomeruli. As shown in Figure 23A, treatment of histones *in-vivo* destroyed the structure of glomeruli (glomerular lesions) in wt mice that was well preserved in *Tlr2/4*-deficient mice. Unilateral histone injection caused glomerular lesions in wt mice that showed characteristics of minor endothelial fibrinogen positivity (Figure 23B), capillary obstruction and thrombotic microangiopathy (Figure 23C) and global glomerular necrosis (Figures 23D). Histone injection into the renal artery of *Tlr2/4*-deficient mice caused not only reduced glomerular lesions but also significantly less fibrinogen positivity (endothelial positivity, capillary obstruction and loop necrosis), as demonstrated in Figures 23E. These *in-vivo* results confirmed that extracellular histones induce glomerular injury occurs in a TLR2/4-dependent manner.

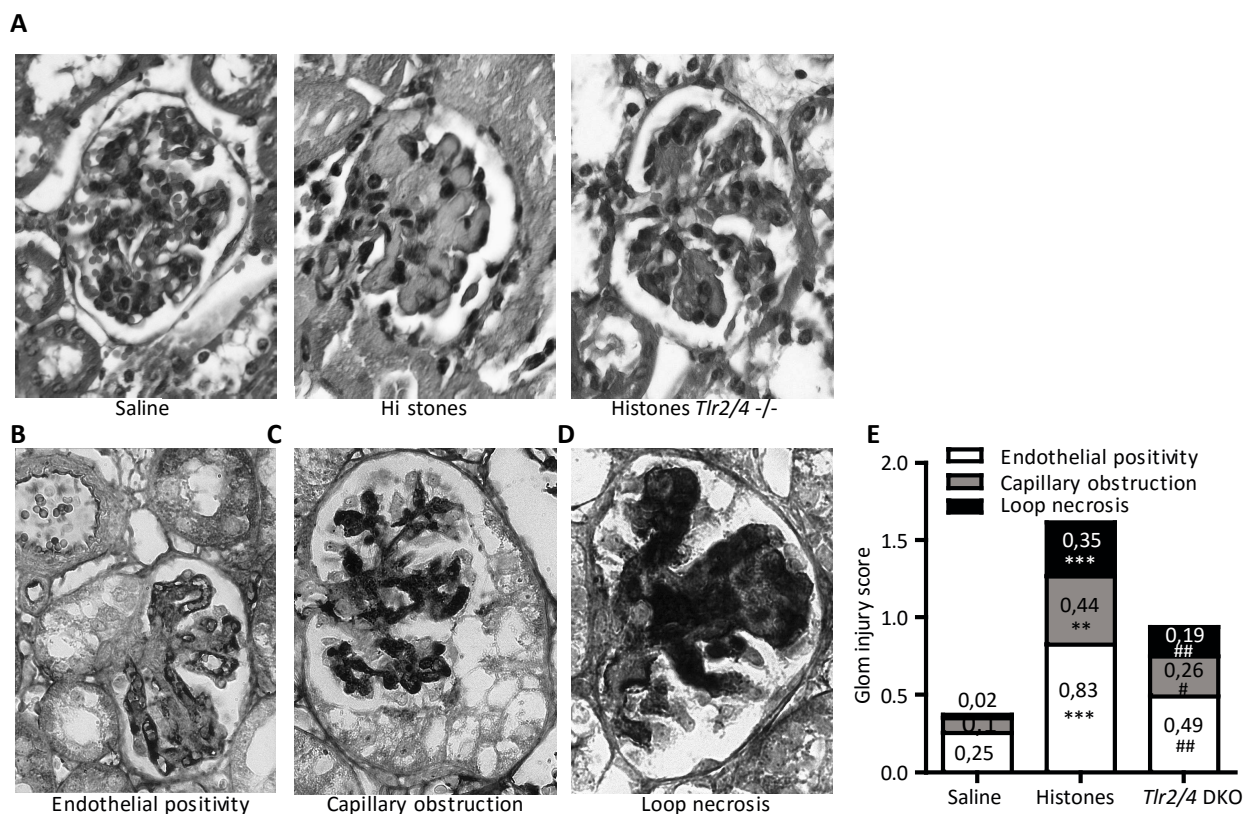


Figure: 23. (A) For intra-arterial histone injection the abdominal aorta was prepared and a micro-cannula was placed into the left renal artery to inject histones directly into the kidney. Images show hematoxylin-eosin staining of isolated glomeruli from saline and histone-treated wt mice as well as from histone-treated *Tlr2/4*-deficient mice. (B-D) Fibrinogen immunostaining of glomeruli isolated from wt mice displaying three different staining patterns: diffuse positivity of glomerular endothelial cells, entire luminal positivity indicating microthrombus formation, and global positivity of glomerular loop indicating loop necrosis. Original magnification x400. (E) Quantitative analysis of these lesions (glomeruli injury score). Values are the mean \pm SEM of two independent experiments. ** = $P < 0.01$, *** = $P < 0.001$.

4.5. Extracellular histones contribute to severe glomerulonephritis

4.5.1. Inhibition of NETs using Cl-amide *in-vivo* prevents glomerulonephritis

We hypothesized that extracellular histones released from NETs may also play an important role during the progression of severe GN¹⁷³. To address our theory, we blocked NET formation by using the peptidylarginine deiminase (PAD) inhibitor^{102,175,176} Cl-amide at the dose of 10mg/kg in an *in-vivo* model of severe GN. Mice were injected with heterologous sheep anti-rat GBM serum (100µl per mouse) to induce severe GN prior to a daily intraperitoneal (i.p.) injection of the PAD inhibitor (Cl-amide in 25 % DMSO). Control mice received only vehicle (25 % DMSO). After 7 days, mice were sacrificed and the glomeruli lesions of the treated kidneys analyzed for extracellular myeloperoxidase (MPO) and CD31 expression. As shown in Figure 12, treatment with the PAD inhibitor Cl-amidine prevented glomerular NET formation as evidenced by reduced MPO immunostaining (red) and quantitative measurement of the fluorescence area. In contrast, the blockade of glomerular NET formation preserved glomerular CD31+ endothelial cells, as demonstrated by a significant increase in the fluorescence intensity (Figure 24, green) and the fluorescent area (graph).

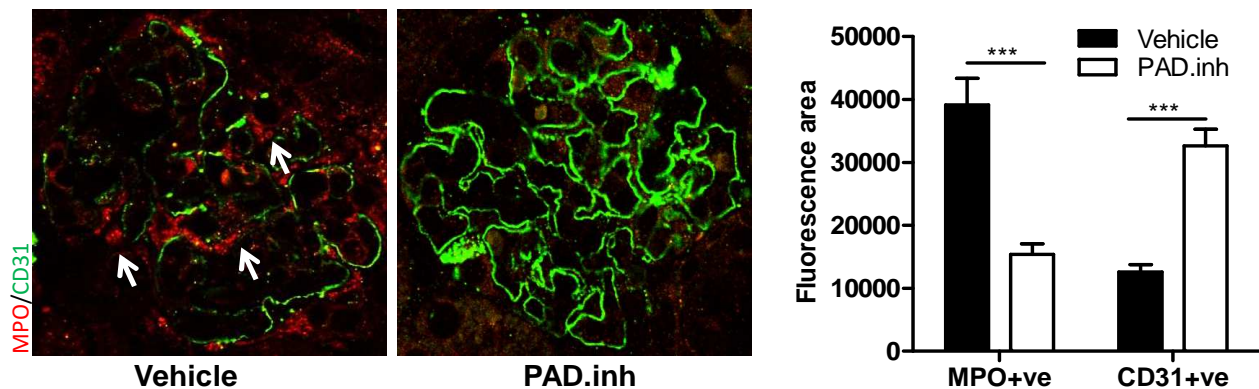


Figure: 24. (A) CD31 (green) and myeloperoxidase (MPO) (red) immunostaining representing NETs formation in the glomeruli in close association with the endothelial cells, vehicle group shows focal loss of endothelial cell positivity compare to treatment with the PAD inhibitor (PAD.inh). (B) Quantification of mean fluorescence area for MPO and CD31 positivity in glomeruli.

The previous data have shown the protective effect of the PAD inhibitor Cl-amide leading to a preserved endothelial microvasculature in the glomeruli during anti-GBM induced GN. We further measured the proteinuria in terms of the albumin to creatinine (A/C) ratio by ELISA. The results demonstrated that Cl-amide treatment significantly reduced the A/C ratio compare to the vehicle group (Figure 25A). This was also the case for the functional parameter including BUN levels (Figure 25B). Within this thesis we have shown that the main cause of proteinuria in the necrotizing GN model was due to the loss of podocytes within the glomeruli. Here, we wanted to evaluated this in more detail on histological sections using immunostaining of nephrin and WT-1 positive podocytes. Following Cl-amide treatment, we found a normal or maintained number of podocytes compare to the vehicle group (Figure 25C). PAS staining of sections were analyzed for glomerular morphology in healthy, segmental and global lesions in glomeruli. The results showed that Cl-amide treatment significantly increased the number of normal glomeruli and significantly decreased the global sclerotic lesions compare to the vehicle group (Figure 25D). Furthermore, one characteristic features of necrotizing GN are vibrant crescentic glomeruli that were significantly reduced upon Cl-amide treatment in comparison to the vehicle group (Figure 25E).

The infiltration of inflammatory cell represents another complication of necrotizing GN. To look at the infiltration of inflammatory cells in the glomeruli, we used immunostaining to identify Mac-2⁺ macrophages. The data showed that Cl-amide treatment significantly reduced the number of infiltrating macrophages in the glomeruli compare to the vehicle group (Figure 25F). These findings were further confirmed by flow cytometry analysis of single cell kidney suspension using a combination of fluorescent surface antibodies. The obtained results demonstrated that treatment with the PAD inhibitor significantly reduced the number of activated inflammatory cells including CD11c⁺ MHCII⁺ double positive dendritic cells, F4/80⁺ MHCII⁺ positive macrophages and total CD11c⁺ CD11b⁺ cells and CD3⁺ CD4⁻ CD8⁻ T cells in the kidney (Figure 25G). These findings indicated that blocking NETosis using the PAD inhibitor Cl-amide during a necrotizing form of GN not only protected the endothelial microvasculature but also abrogated the key features of GN including inflammatory cell recruitment.

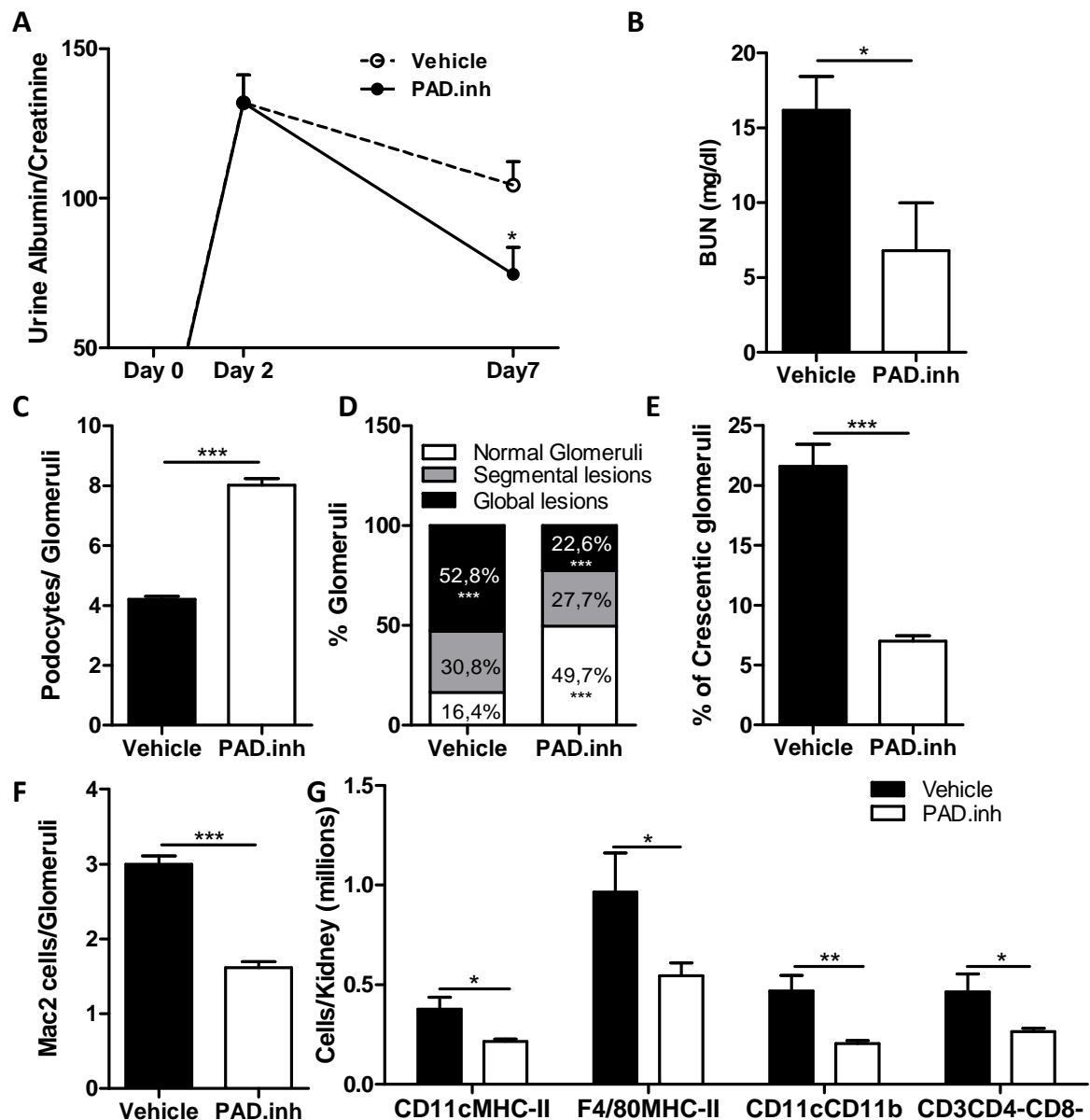


Figure: 25. In an *in-vivo* model of antiserum-induced GN, treatment with the Cl-amide (PAD.inh) following antiserum injection attenuated the disease burden. (A and B) Levels of proteinuria (A) and BUN (B) measured in the urine on day 7. (C) Podocytes were quantified as nephrin/WT-1+ cells on renal sections on day 7. (D and E) PAS staining to determine the percentage of glomeruli (D) and crescentic glomeruli (E). (F) Number of Macrophages per glomeruli determined by immunostaining using a Mac-2 antibody. (G) Flow cytometry analysis of kidney suspension. Data represent mean \pm SEM from five to six mice per group. * = $P < 0.05$, ** = $P < 0.01$, *** = $P < 0.001$.

4.5.2. Anti-Histone IgG treatment prevents complication of GN

We have previously shown that anti-histone IgG treatment can prevent the cytotoxic effect of histones on glomeruli *in-vitro*. To test whether these findings can be translated into an *in-vivo* model of GN, first we injected mice intravenously with 100 μ l GBM antiserum that was either raised in sheep or in mice to induce necrotizing types of GN. After 7 days, histology staining showed that only sheep IgG deposits were found in the glomeruli but not mouse IgG (Figure 26) demonstrating that excess autologous anti-sheep IgG did not stimulate the immune response to induce its own effect in the progression of GN. Furthermore, in these experiments we excluded possible non-specific actions of sheep-IgG and have shown that the disease pathology is mainly caused by direct killing or necrotizing action of sheep anti-GBM serum on different glomerular cells leading to the pathological conditions without any autoimmune or autologous reaction against the sheep antiserum during the disease.

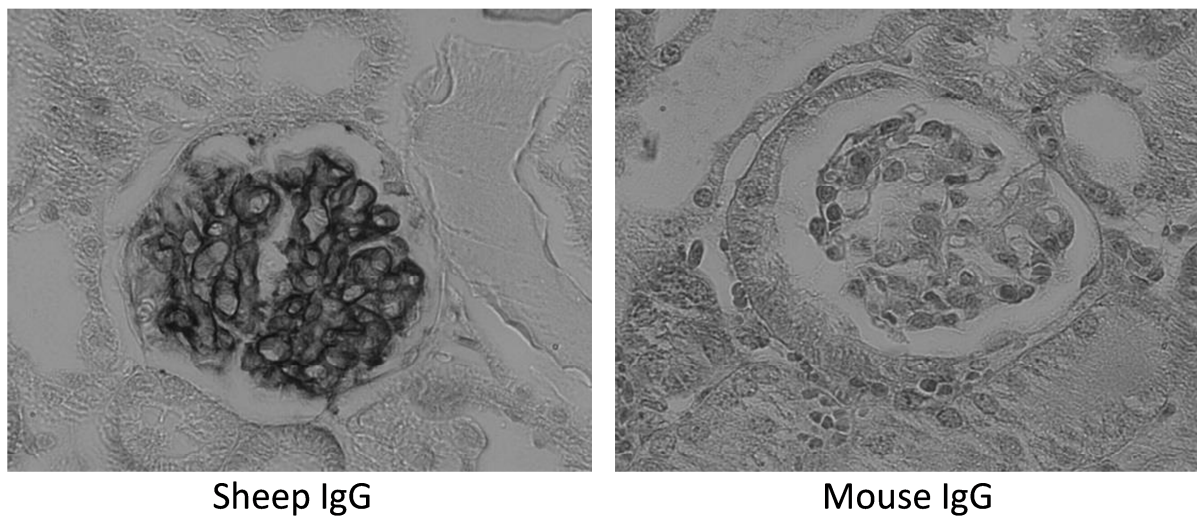


Figure: 26. Day 7 after injection of anti-GBM serum the kidneys were positively stained for sheep IgG, whereas mouse IgG was negative excluding the autologous sheep IgG response.

Next, mice were injected i.p. with 20 mg/kg anti-histone IgG or with 20 mg/kg control IgG 24 hours prior (prophylactic treatment) to the intravenous injection of 100 μ l GBM antiserum that was raised in sheep. The treatment with anti-histone IgG or control IgG was continued on alternative days up to 7 days after sheep GBM antiserum injection. During the experiment, urine and blood was collected to analyze functional parameters. After 7 days of antiserum injection, mice were sacrificed and kidneys removed for histology, FACS and qRT-PCR analysis. As shown in Figure 27A, treatment with anti-histone IgG significantly reduced the BUN levels following GBM antiserum injections compared to the control IgG treatment group. Anti-histone IgG not only increased the number of healthy glomeruli but also significantly reduced the percentage of global glomeruli as demonstrated by PAS histological staining of sections (Figure 27B-27C). The decrease in the severity of GN following anti-histone IgG treatment was further confirmed by the significant reduction in the percentage of crescentic glomeruli with less severe lesions on 7 days after antiserum injection in comparison to the control IgG treated group (Figure 27D).

To investigate the effect of NET related histone blockade by the anti-histone IgG treatment, histological sections were stained for NET-related MPO staining and endothelial CD31 markers to look at the effect on the maintenance of glomerular microvasculature. A focal loss of endothelial CD31 positivity, a marker of glomerular vascular injury, was observed in glomeruli isolated from control IgG treated mice (Figure 27E). However, anti-histone IgG did not affect extracellular positivity of MPO but maintained CD31⁺ vasculature indicating a protective effect on NET-related vascular injury. These results were further strengthened by quantifying the area of MPO⁺ and CD31⁺ showing that anti-histone IgG significantly increased the number of CD31 positivity compared to control IgG, whereas the MPO positivity remained unaffected (Figure 27F). Consistent with our *in-vitro* data, the *in-vivo* data now showed that anti-histone IgG treatment prevented the disease pathogenesis of sheep GBM antiserum-induced severe GN and clearly implied the importance of anti-histone IgG regarding the maintenance of the glomerular microvasculature and the number of podocytes present within the glomeruli.

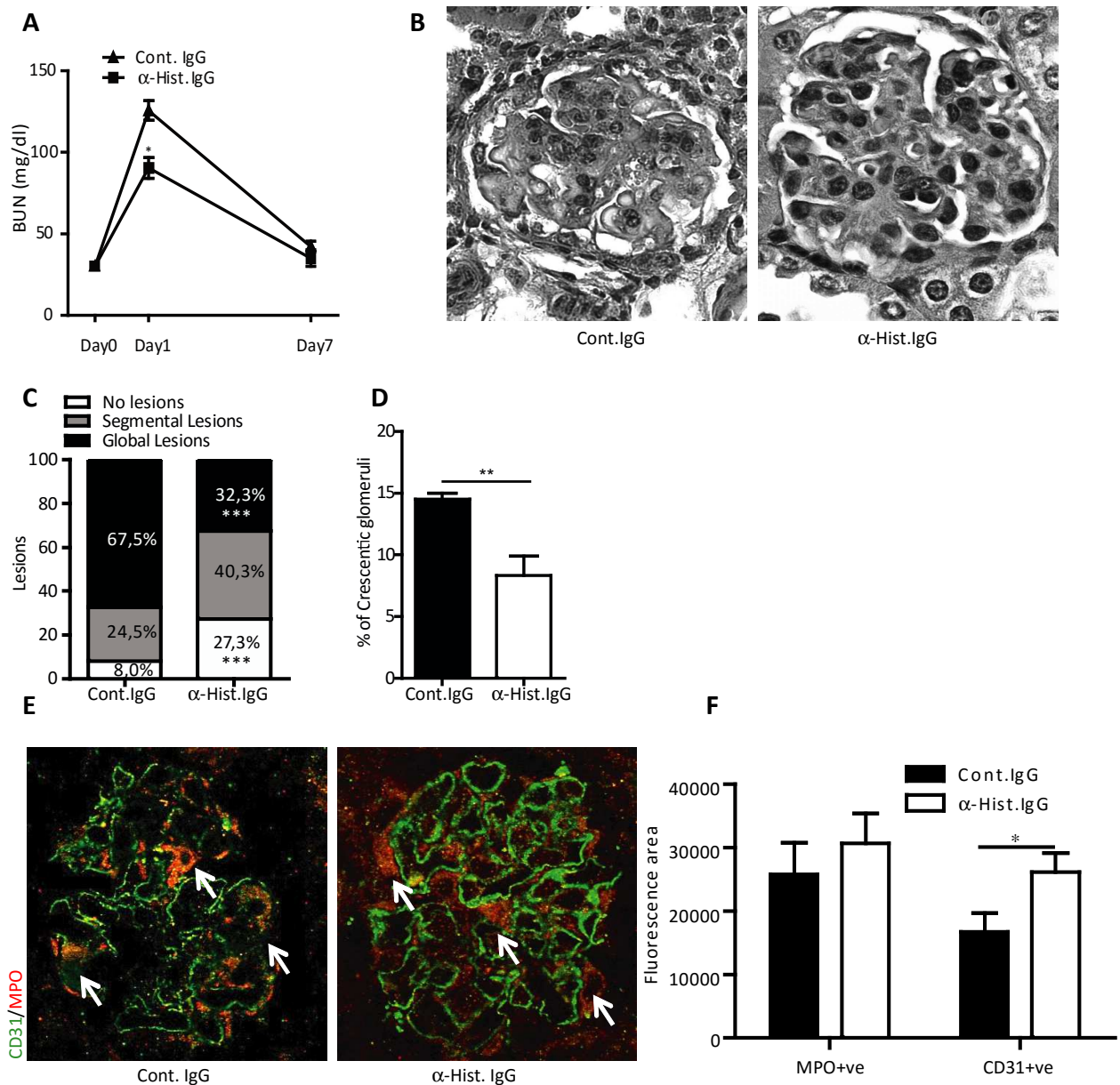


Figure: 27. Neutralizing of histones protects severe GN. (A) Blood urea nitrogen (BUN) levels were determined 1 and 7 days after intravenous injection of GBM antiserum. Mice were either treated with control IgG or anti-histone IgG prior to the injection with antiserum. (B) Representative HE staining of glomeruli are shown at an original magnification of 400x. (C and D) Morphometrical analysis of segmental and global glomerular lesions (left) and of glomeruli with crescents (right) as described in methods (section 3.8.1). (E) CD31 and MPO immunostaining representing NETs formation in the glomeruli close association with the endothelial cells, control IgG group shows focal loss of endothelial cell positivity compare to anti-histone IgG group. (F) Quantification of the mean fluorescence area for MPO and CD31 positivity in glomeruli. Data are means \pm SEM from five to six mice in each group. * = $P < 0.05$, ** = $P < 0.01$, *** = $P < 0.001$ versus control IgG.

4.5.3. Neutralizing histones protects the glomerular filtration barrier in glomerulonephritis

Because histones were shown to be toxic in glomerular endothelial cells and podocytes *in-vitro*, we assessed the effect of anti-histone IgG treatment on the glomerular capillary ultrastructure during severe GN *in-vivo* via transmission electron microscopy. As illustrated in Figure 28, mice that received only control IgG treatment showed severe glomerular damage with fibrin deposits replacing large glomerular segments (fibrinoid necrosis). The capillary loops showed extensive GBM splitting and thinning, prominent endothelial cell nuclei, massive subendothelial edema with closure of the endothelial fenestrae, and obliteration of the capillary lumina (Figure 28, upper panel, left). Subendothelial transudates (leaked serum proteins) and luminal platelets and neutrophils were also noted (Figure 28, upper panel, right). Severe podocyte injury with diffuse foot process effacement, reactive cytoplasmic changes and detachment from the GBM were apparent (Figure 28, both pictures upper panel). In contrast, glomeruli from mice injected with anti-histone IgG showed restored endothelial fenestrations, flat appearing endothelial cells and preserved podocytes with intact foot processes (Figure 28, lower panel).

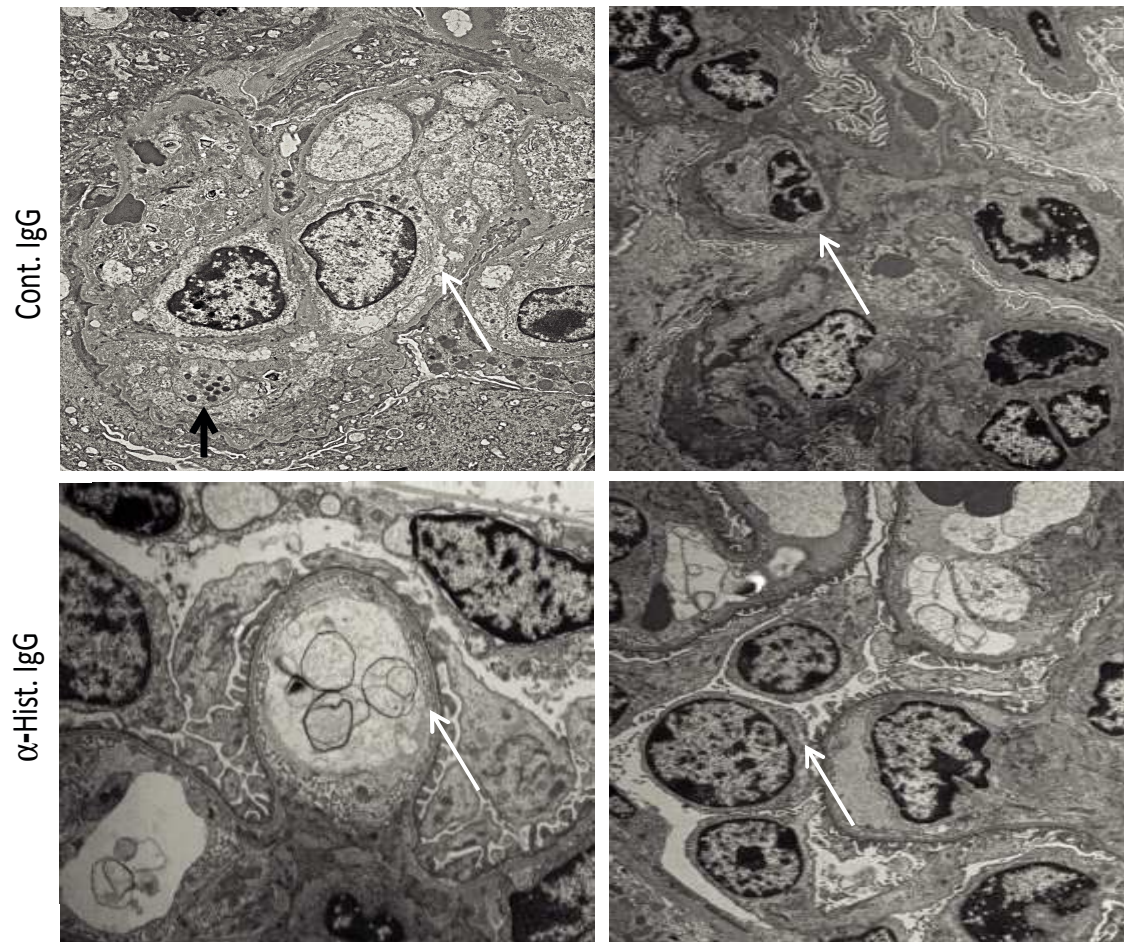


Figure: 28. Transmission electron microscopy of antiserum-induced GN revealed extensive glomerular injury with fibrinoid necrosis (upper left), endothelial cell swelling, luminal thrombosis, and intraluminal granulocytes (upper middle and right). Podocytes show foot process effacement (all upper images). Pre-emptive treatment with anti-histone IgG decreased most of these abnormalities in particular the endothelial cell and podocyte ultrastructure (lower images).

4.5.4. Anti-Histone IgG treatment maintains podocytes intact

A hallmark of glomerular diseases is an increase in proteinuria. This is mainly due to the loss of podocytes. To further investigate the cytotoxic effect of histones on *in-vitro* cultured podocytes, we stimulated the cultured monolayer of differentiated podocytes with histones in the absence or presence of anti-histone IgG. After 24 hours, we measured the detached podocytes by counting the floating (detached) podocytes manually in the culture supernatants. We found that addition of histones was leading to a significant increase in the percentage of detached podocytes in the control IgG group (Figure 29, black bars). In the presence of anti-histone IgG, the percentage of detached podocytes significantly decreased indicating the killing action of histones on cultured podocytes (Figure 29, white bars).

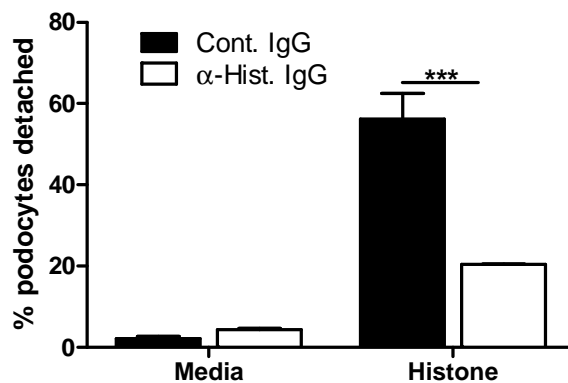
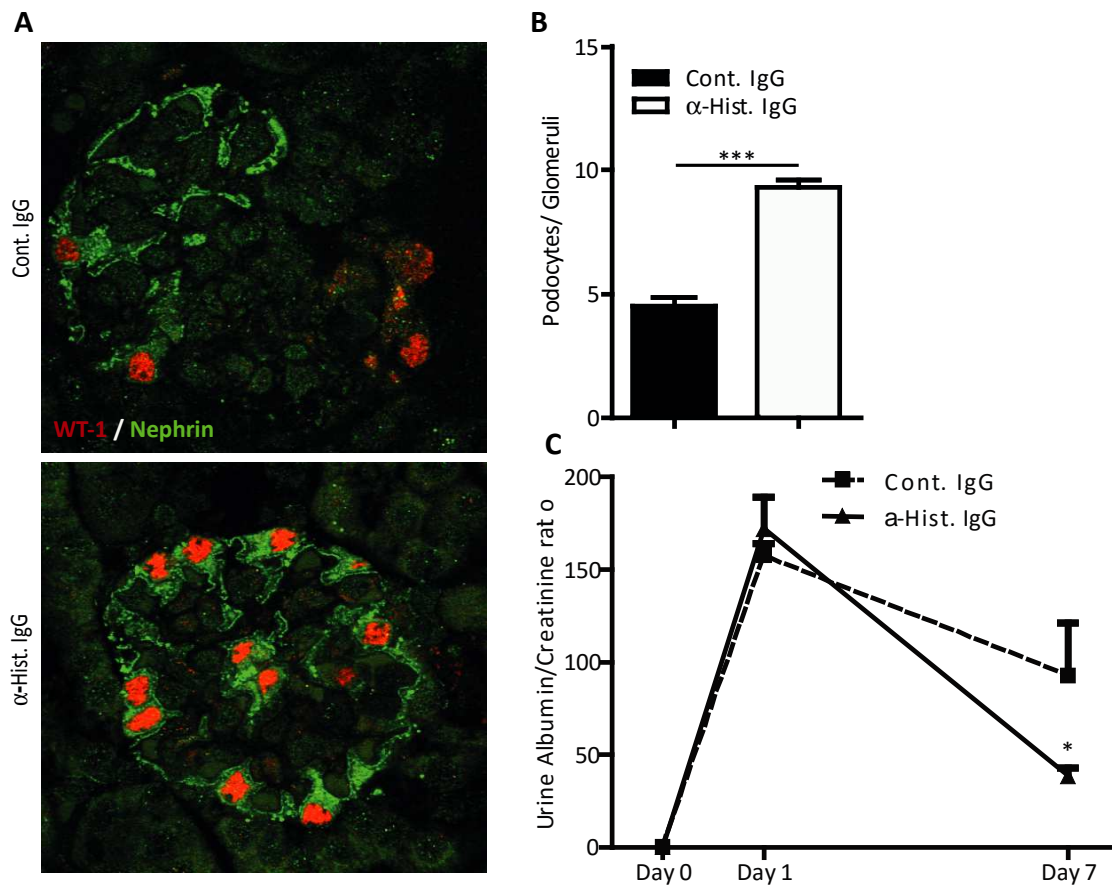


Figure: 29. Anti-histone IgG and podocyte detachment *in-vitro*. Murine podocytes were exposed to histones with or without anti-histone IgG. Data show the mean percentage \pm SEM of podocytes that were detached from the culture dish within 24 hours. *** = $P < 0.001$ versus control IgG.

Next, to confirm the effect of histone neutralization on podocyte counts in our *in-vivo* antiserum-induced GN model, we have used a co-immunostaining of WT-1 and nephrin to locate the podocytes in the glomerular turf. WT-1 (red) and nephrin (green) co-immunostaining revealed that anti-histone IgG largely prevented podocyte loss in antiserum-induced GN (Figure 30A), which was consistent with an increased number of WT-1/nephrin+ podocytes compared to control IgG (Figure 30B). On day 7, we also noticed a significant reduction of the albuminuria following injection with anti-histone IgG in GBM antiserum-

treated mice, which was not observed on day 1 (Figure 30C). These results demonstrated that extracellular histones induced severe GN by causing glomerular vascular injury and podocyte loss. Furthermore, anti-histone IgG also showed a significant decrease in the proteinuria compare to the control group, which further confirms the maintenance of podocytes and endothelial barriers in anti-histone IgG treated mice.



Figures: 30. (A) Immunostaining for WT-1 (red) and nephrin (green) was used to quantify podocytes. (B) The number of nephrin/WT-1+ podocytes following anti-histone IgG treatment on day 7 during antiserum-induced GN. (C) Urinary albumin/creatinine ratio was determined on day 1 and day 7 after antiserum injection. Data represent mean \pm SEM from five to six mice per group. * = $P < 0.05$, *** = $P < 0.001$ versus control IgG.

We further analyzed the urinary albumin/creatinine ratios and the number of podocytes by immunostaining for nephrin and WT-1 in PAD inhibitor-treated mice. The blockade of NETosis using the PAD inhibitor resulted in a decrease in the albumin/creatinine ratio but in an increase in the number of podocytes similar to that observed with anti-histone IgG (Figure 31A and 31B)

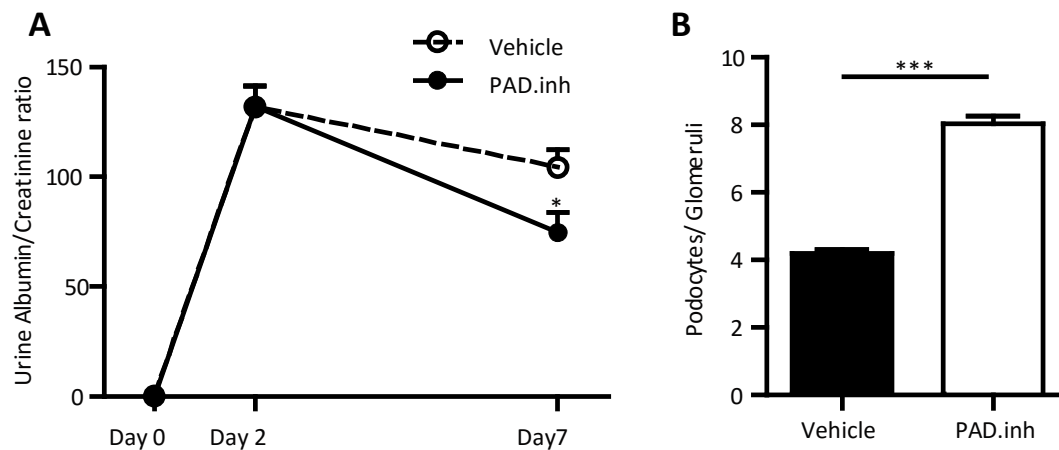


Figure: 31. (A) Urinary albumin/creatinine ratio and (B) number of podocytes after blocking NETs with the PAD inhibitor. Data represent mean \pm SEM from five to six mice of each group. * = $P < 0.05$, *** = $P < 0.001$ versus vehicle group.

4.5.5. Extracellular histones drive glomerular leukocyte recruitment and activation

Infiltrating leukocytes are a key source of extracellular histones during severe GN²⁵ and exert important effector functions including the production of chemokines during the pathogenesis of GN¹⁷⁷. One such chemokine is Chemokine (C-X-C motif) ligand 2 (CXCL2), a small molecule belonging to the CXC chemokine family that is also known as macrophage inflammatory protein-2 (MIP-2). CXCL2 is mainly secreted by monocytes and macrophages, and functions as a chemoattractant for polymorph nuclear leukocytes (neutrophils) and hematopoietic stem cells¹⁷⁸⁻¹⁸⁰. To investigate whether GEnC also express CXCL2, cultured GEnC were stimulated *in-vitro* with GBM antiserum at a concentration of 30 μ l/ml for 6 hours and mRNA isolated from those samples were analyzed for the expression of CXCL-2 by qRT-PCR. The results showed that stimulation of glomerular endothelial cells with GBM antiserum triggered the expression of CXCL2 (Figure 32) indicating that CXCL2 may well be the major chemokine for neutrophil infiltration into the glomeruli and further pathogenic effects.

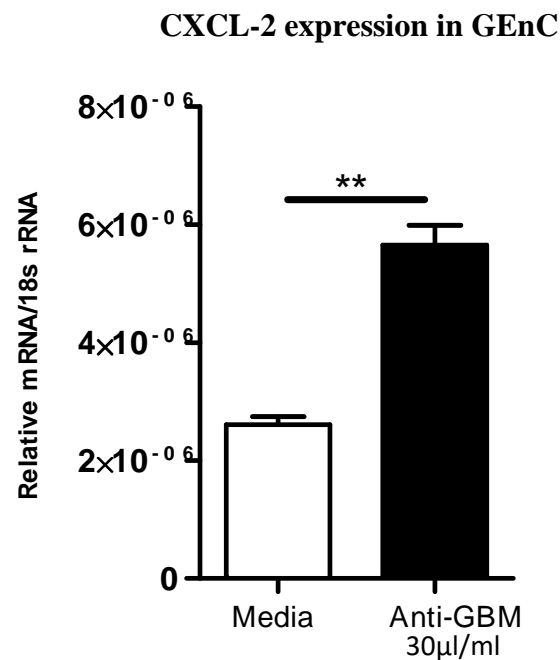


Figure: 32. CXCL2 mRNA expression in glomerular endothelial cells. Exposure of GEnC to glomerular basement membrane (GBM) antiserum (30µl/ml) induced the expression of MIP-2/CXCL2 mRNA, as determined by qRT-PCR. Data are the mean \pm SEM from three independent experiments. ** = $P < 0.01$ (Student's t-test).

Finally, we investigated the effect of leukocyte infiltration in the *in-vivo* setting of severe GN. Immunostaining and manually counting of the number of neutrophils and macrophages per glomeruli showed that anti-histone IgG treatment *in-vivo* significantly reduced the numbers of glomerular neutrophils (Ly-6B.2) and macrophages (Mac-2) during severe GN (Figure 33A). Furthermore, flow cytometry analysis of renal cell suspensions was used to unravel the distinct renal mononuclear phagocyte populations during severe GN. As shown in Figure 33B, we have identified 5 distinct cell populations, whereby the F4/80+ cells, F4/80+ MHCII+ cells and CD11b+ CD103+ cells were predominantly present in the kidney. Upon treatment with anti-histone IgG, the number of all cell populations was significantly reduced (Figure 33B).

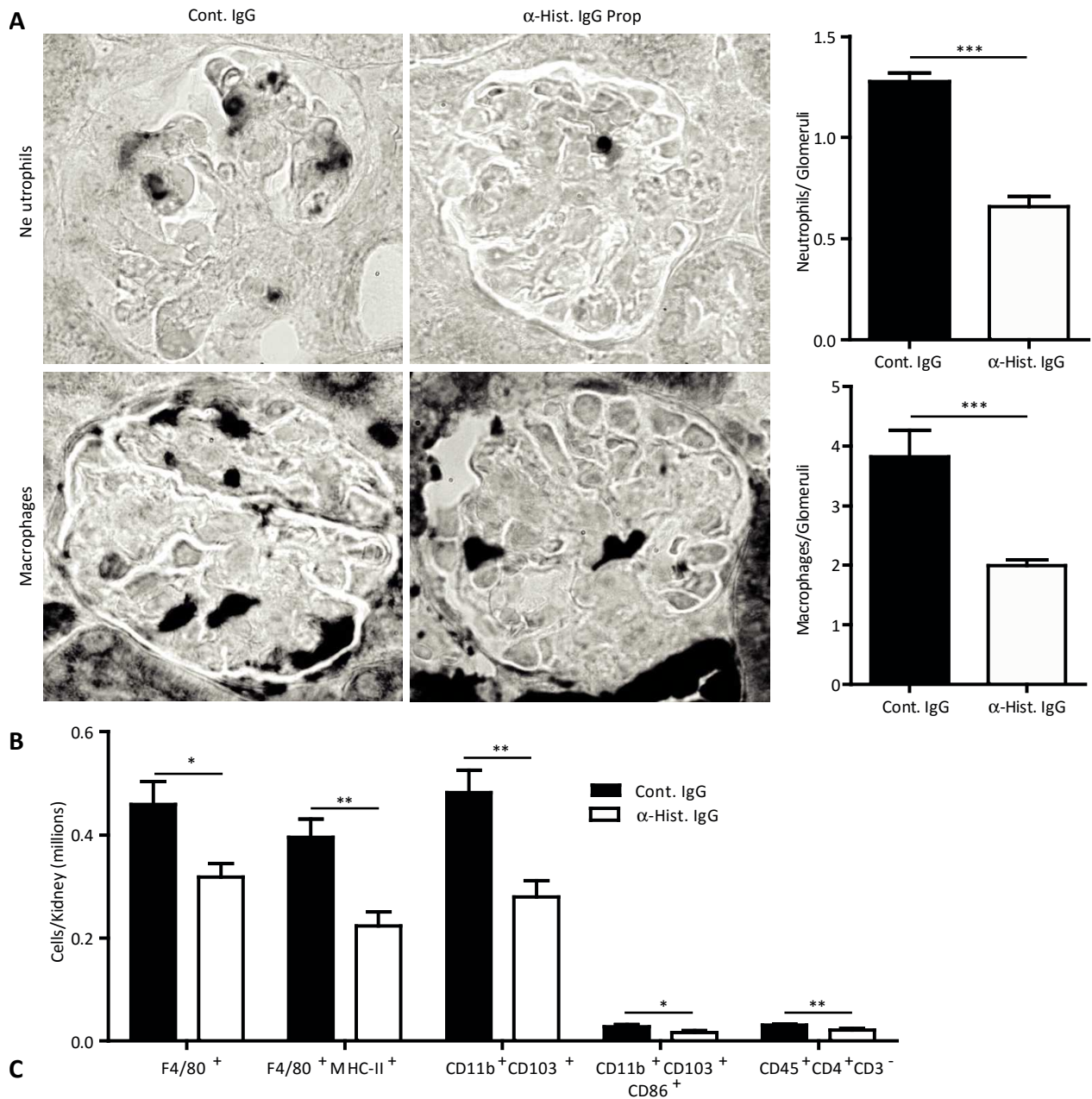


Figure: 33. Leukocyte recruitment and activation during glomerulonephritis. (A) Glomerular neutrophil (Ly-6B.2) and macrophage (Mac-2) infiltrates were quantified by immunostaining. Representative images are shown at an original magnification of 400x. (B) Leukocyte activation was quantified by flow cytometry of renal cell suspensions harvested 7 days after antiserum injection. Data represent mean \pm SEM from five to six mice of each group. * = $P < 0.05$, ** = $P < 0.01$, *** = $P < 0.001$.

In an *in-vitro* experiment we also showed that histones are able to induce the upregulation of activation markers such as MHCII, CD40, CD80, and CD86 in cultured bone marrow-derived dendritic cells (BMDCs) in a dose-dependent manner that were significantly reduced following anti-histone IgG administration (Figure 34). Taken together, the *in-vitro* and *in-vivo* data in this section demonstrated that extracellular histones triggered glomerular leukocyte recruitment and activation that can be blocked with anti-histone IgG.

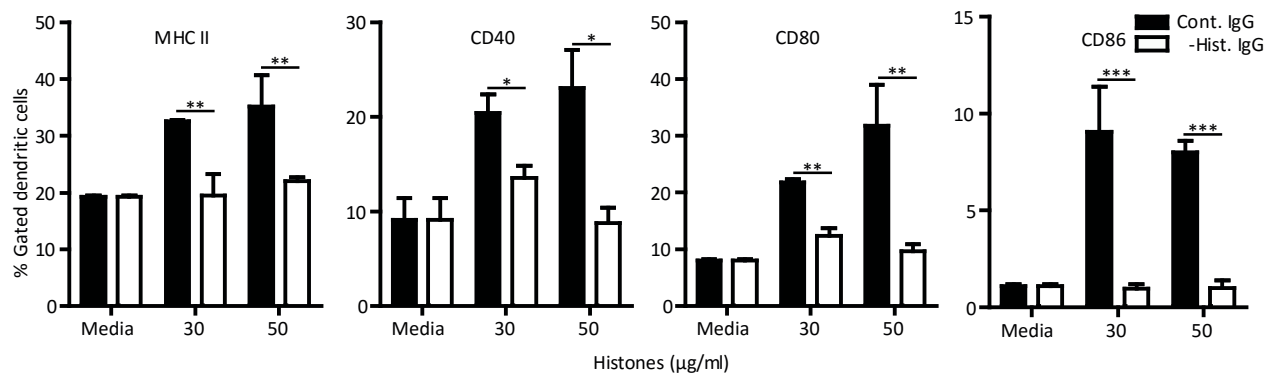


Figure: 34. Cultured bone marrow-derived dendritic cells were exposed to increasing doses of histones as indicated. After 24 hours, flow cytometry was used to determine the percentage of cells that expressed the activation markers MHCII, CD40, CD80 and CD86. Data are means \pm SEM from three independent experiments. * = $P < 0.05$, ** = $P < 0.01$, *** = $P < 0.001$.

4.5.6. Extracellular histones trigger intraglomerular TNF- α release and thrombosis

Activated mononuclear phagocytes have been shown to be an important source of pro-inflammatory cytokine production during glomerular disease. Among these, TNF- α particularly contributes to the loss of podocytes, proteinuria, and glomerulosclerosis¹⁸¹. To investigate whether histones can trigger the production of TNF- α in mononuclear phagocytes, we cultured J774 macrophages and bone marrow derived dendritic cells (BMDCs) in the presence of different concentrations of histones *in-vitro* and measured the secreted level of TNF- α via ELISA. As shown in Figure 35A, histone-stimulated J774 macrophages and BMDCs produced TNF- α that was completely inhibited following addition of anti-histone IgG. We next assessed the glomerular TNF- α expression *in-vivo* on day 7 after antiserum injection. Immunostaining displayed a robust TNF- α positivity within the glomerular tuft that was not only expressed by the infiltrating cells but also present in the inner and outer aspect of the glomerular capillaries (Figure 35B). Interestingly, anti-histone IgG treatment significantly reduced the glomerular TNF- α positivity, which was consistent with the corresponding renal mRNA expression levels (Figure 35C). TNF- α is not only an inducer of NETosis but can also trigger the prothrombotic activity of (glomerular) endothelial cells and intravascular fibrin formation¹⁸²⁻¹⁸⁴. In our GN model, the glomerular capillaries were expressing global fibrinogen that was significantly decreased with anti-histone IgG (Figure 35D). This was also the case for the fibrinogen mRNA levels in the presence of anti-histone IgG (Figure 35E). These results highlighted the importance of extracellular histones in triggering intraglomerular TNF- α production and microthrombi formation within the glomerular capillaries.

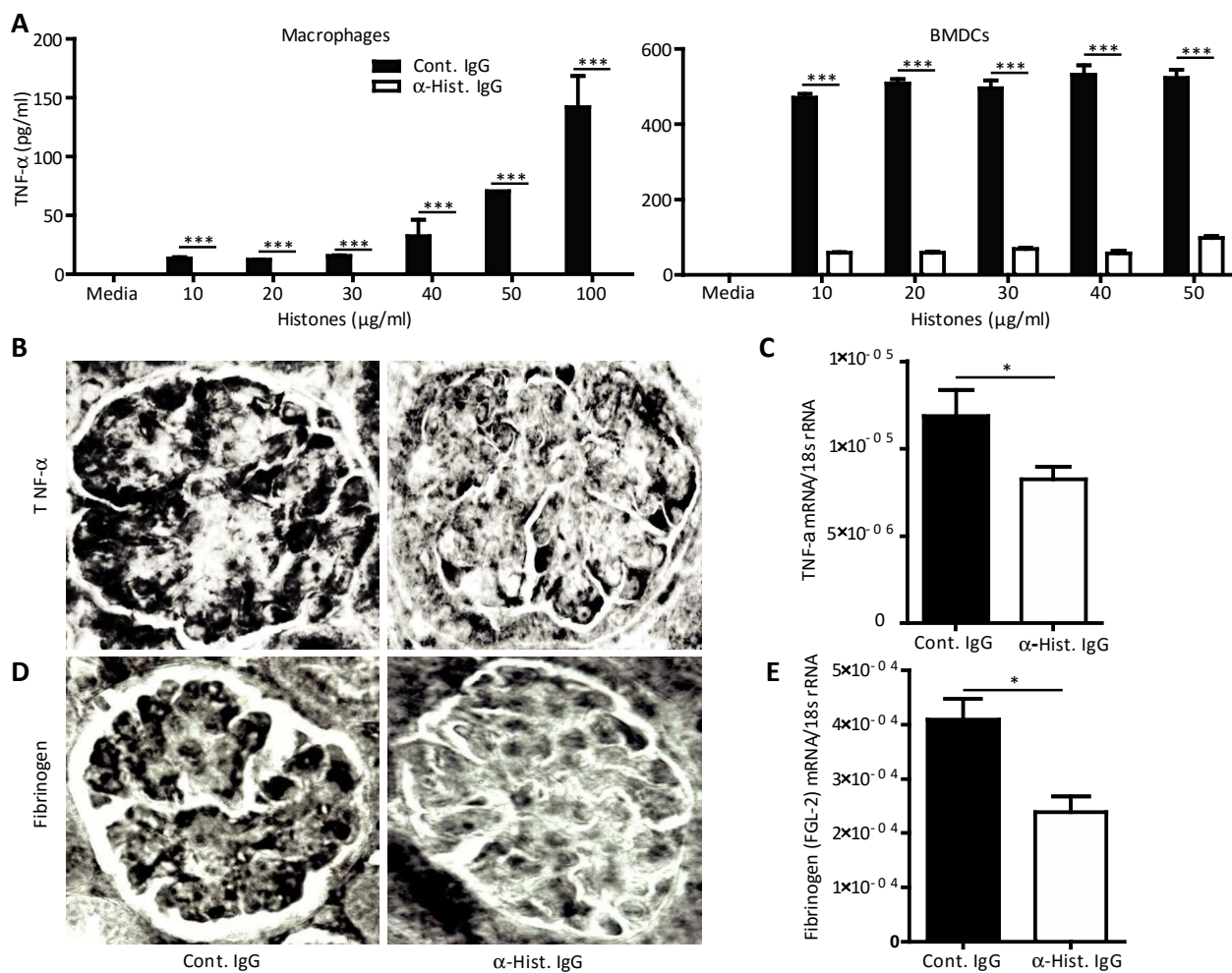
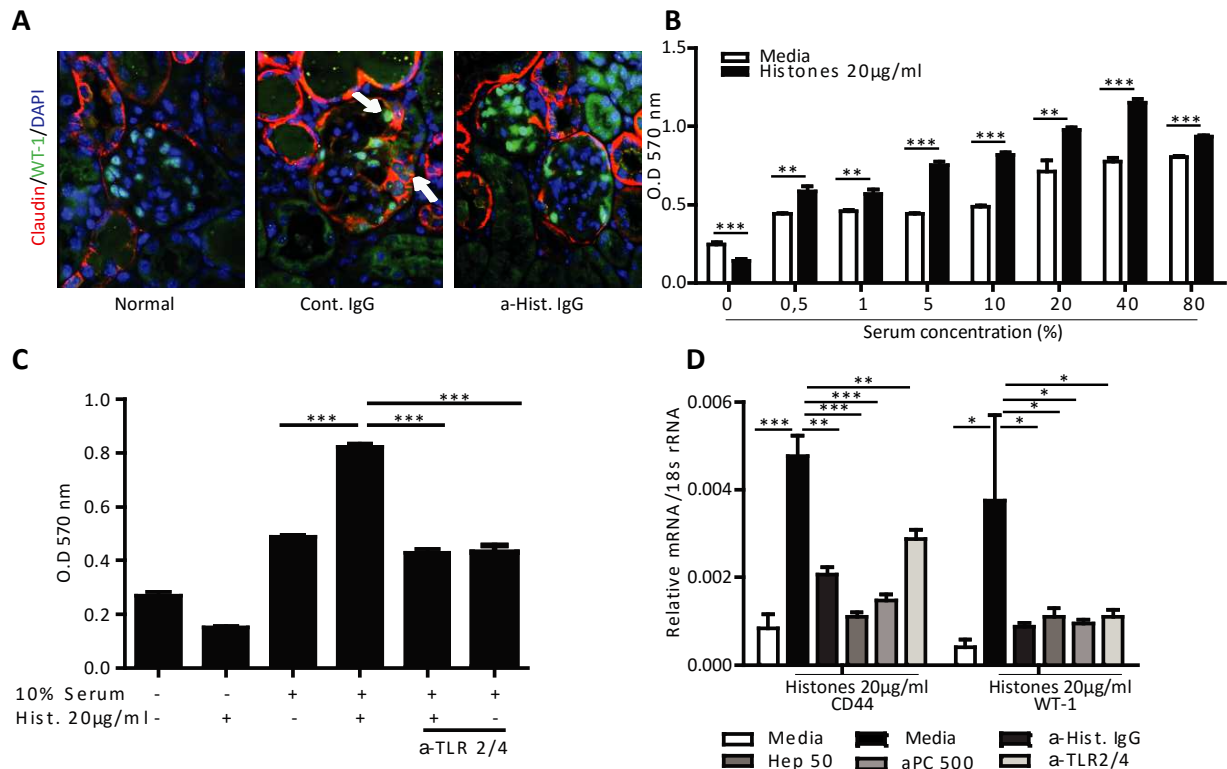


Figure: 35. Histones activate TNF- α production. (A) J774 macrophages and bone marrow dendritic cells (BMDCs) were cultured in the presence of different concentrations of histones with or without anti-histone IgG and secreted TNF- α levels determined by ELISA. Data are means \pm SEM from three independent experiments. *** = $P < 0.001$ by two-way ANOVA with Bonferroni's post test. (B and D) TNF- α and fibrinogen immunostaining on renal sections from both treatment groups taken on day 7 after antiserum injection. Representative images are shown at an original magnification of 400x. (C and E): Real time RT-PCR for TNF- α and fibrinogen mRNA on renal tissue on day 7 after antiserum injection. Data are means \pm SEM from at least five to six mice in each group. * = $P < 0.05$.

4.5.7. Extracellular histones activate parietal epithelial cells via TLR2/4

Mitogenic plasma proteins that are leaking from the injured glomerular capillaries can cause PEC hyperplasia and glomerular crescent formation^{171,172,185}. To investigate whether released DAMPs and leaked serum proteins as a result of endothelial damage and during the GN are responsible for the activation of PECs and crescent formation, PECs were first fluorescently stained with claudin-1 and the activation marker WT-1. As shown in Figure 36A, PECs were identified as claudin-1/WT-1 positive during antiserum-induced GN glomerular crescents^{186,187}. However, in the presence of anti-histone IgG, PECs were less positive for WT-1 indicating that histones can induce the activation of PECs. Secondly, we performed *in-vitro* experiments, where cultured and fully differentiated PECs were stimulated with a low dose of histones (20µg/ml) in the presence of different concentration of serum. The data showed that PECs significantly increased their proliferative capacity when treated with histones in the presence of different concentrations of serum (Figure 36B) that was significantly abolished following addition of anti-histone IgG or anti-TLR2/4 antibodies (Figure 36C). Thirdly, the blockade of TLR2/4 reduced histone-induced mRNA expression of activation markers like CD44 and WT-1 in PECs (Figure 36D). Besides the effect of anti-histone IgG and anti-TLR2/4 antibodies to block the toxic effect of extracellular histone, the same capability was attributed to heparin and recombinant activated protein C (aPC)^{10,140}. As such, the protective effect on PEC activation was confirmed by heparin, activated protein C (aPC), anti-TLR2/4 as well as anti-histone IgG treatment (Figure 36D).

Finally, heparin and aPC were shown to be able to suppress the cytotoxic actions of histones on glomerular endothelial cells in the same way like anti-histone IgG did (Figure 37A-37B). Thus, extracellular histones can activate PECs in a TLR2/4-dependent manner, a process that may act synergistically with other triggers of PEC hyperplasia during crescent formation and that can be blocked by anti-histone IgG, aPC or heparin.



Figures: 36. (A) Renal sections were stained with claudin-1 (red, marker for parietal epithelial cells/PECs and some tubular cells), WT-1 (green, marker for podocytes and activated PECs), and DAPI (blue, DNA marker) in the absence or presence of anti-histone IgG during severe GN crescents. Original magnification: x200. (B) Cell viability (MTT assay) was determined by cultured PECs in the presence of different serum concentrations together with a low concentration (20µg/ml) of histones that without serum reduces PEC viability. (C) PECs viability was measured by MTT assay following treatment with anti-TLR2 and anti-TLR4 antibodies and anti-histone IgG to neutralize the histone effect on PEC growth. Data are mean OD \pm SEM of three experiments measured at a wavelength of 570 nm. (D) RT-PCR analysis of PECs stimulated with histones and various neutralizing compounds (anti-histone IgG, 50µg/ml heparin, 500nM activated protein C, 1ng/ml anti-TLR2 or -4). Note that all these interventions blocked histone-induced CD44 and WT-1 mRNA expression. Data are means \pm SEM of three experiments. * = $P < 0.05$, ** = $P < 0.01$, *** = $P < 0.001$.

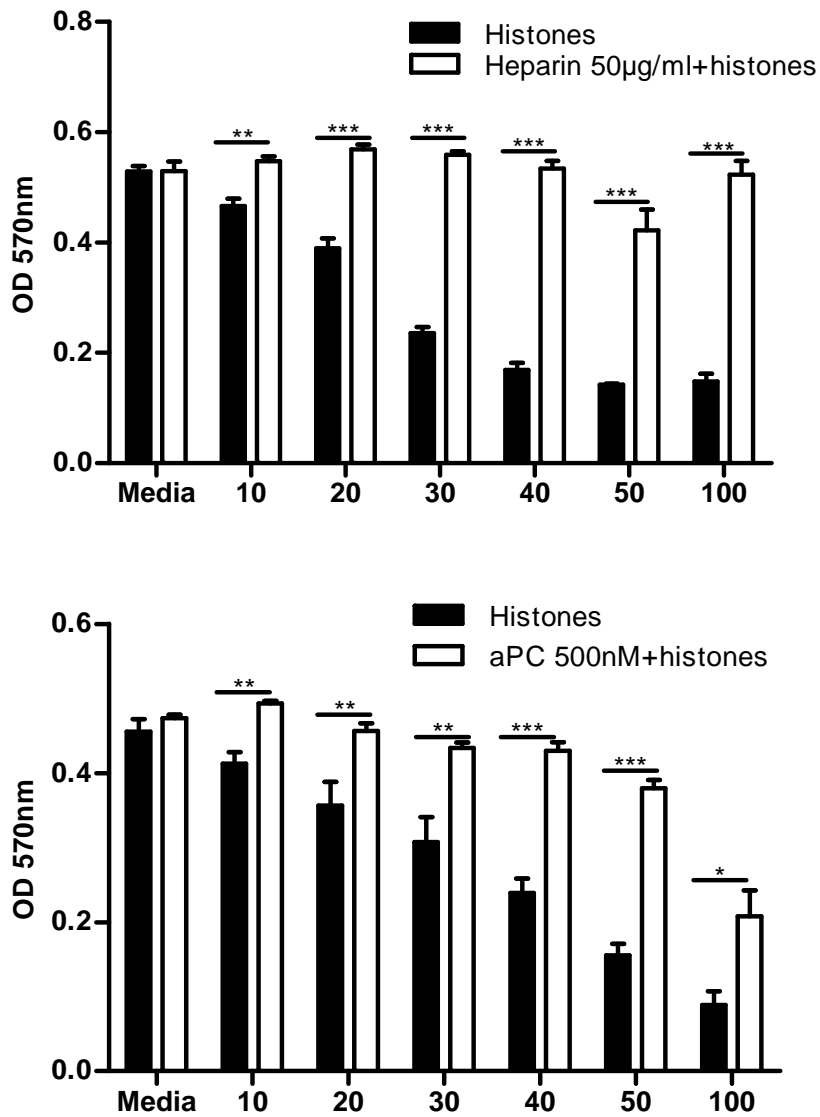


Figure: 37. Heparin and activated protein C block histone toxicity on glomerular endothelial cells. Glomerular endothelial cells were exposed to increasing doses of histones with or without heparin (A) or aPC (B) as indicated and PEC viability determined via MTT assay. Data represent mean OD \pm SEM of three MTT assay experiments measured at a wavelength of 492 nm. * = $P < 0.05$, ** = $P < 0.01$, *** = $P < 0.001$.

4.6. Delayed onset of histone neutralization still improves severe glomerulonephritis

The results within this thesis have shown that pre-emptive histone neutralization contributes to the amelioration of the pathogenesis of severe GN. This has led us to the question: Could histone neutralization be a potential therapeutic approach for treating already established severe GN?

We used the aforementioned three therapeutic interventions including anti-histone IgG, heparin, and aPC due to their capability to completely block histone toxicity on glomeruli *ex-vivo* (section 4.3.1 and 4.6). To investigate the therapeutic effect of the histone blocking agents (anti-histone IgG, heparin and aPC), we stimulated first isolated glomeruli with histones at a concentration of 50 µg/ml 24 hours prior to the treatment with agents and performed the lactate dehydrogenase (LDH) release assay to check the cytotoxic effect of histone on isolated glomeruli. As shown in Figure 38A, all histone blocking agents significantly reduced the LDH release compared to the control IgG or vehicle group.

To further test the effect of histone neutralization therapeutically, a number of *in-vivo* experiments were performed, whereby 100 µl of GBM antiserum was injected 24 hours prior to treatment with anti-histone IgG, heparin, and aPC. On day 2, increased proteinuria and elevated BUN levels were observed in all groups independent of the therapeutic intervention with histone blocking agents (Figures 38B and 38C). However, on day 7 after establishing GN, all treatment approaches significantly reduced plasma creatinine levels, proteinuria, and podocyte loss compared to control IgG (Figures 38B-D). Furthermore, the therapeutic blockade of histones not only significantly reduced the percentage of glomeruli with global lesions or halted damage (Figure 39A-B) but also the percentages of glomerular crescents by 80% (Figure 39C) and the percentage of hpf of cast deposition, which features secondary tubular injury (Figure 39D).

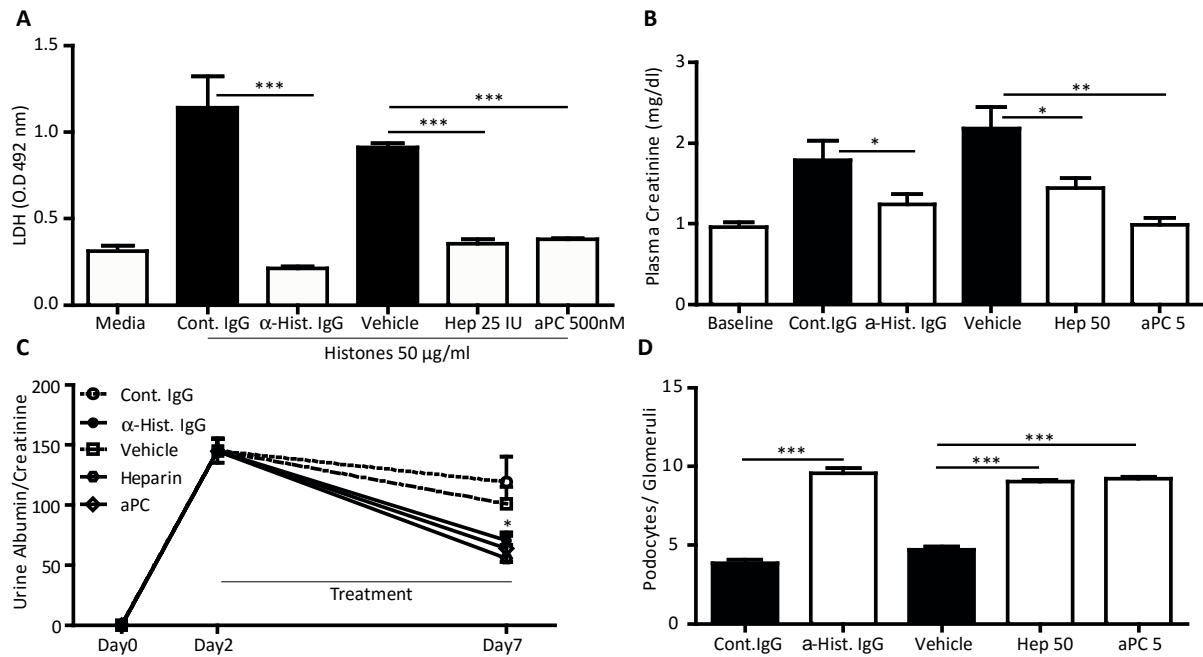


Figure: 38. Delayed histone blockade still improves glomerulonephritis. (A) Glomeruli were isolated from wild type mice and incubated with histones in the presence or absence of anti-histone IgG, heparin or aPC. LDH release was measured in the supernatants as a marker of glomerular cell injury. (B) In the model of antiserum-induced GN, anti-histone IgG, heparin or recombinant aPC were injected 24 hours following disease onset and the urinary albumin/creatinine ratio was determined. (C) Plasma creatinine levels determined on day 7 and albuminuria also on day 2. (D) Podocytes were quantified as nephrin/WT-1+ cells on renal sections on day 7. Data represent the means \pm SEM of three experiments. * = $P < 0.05$, ** = $P < 0.01$, *** = $P < 0.001$.

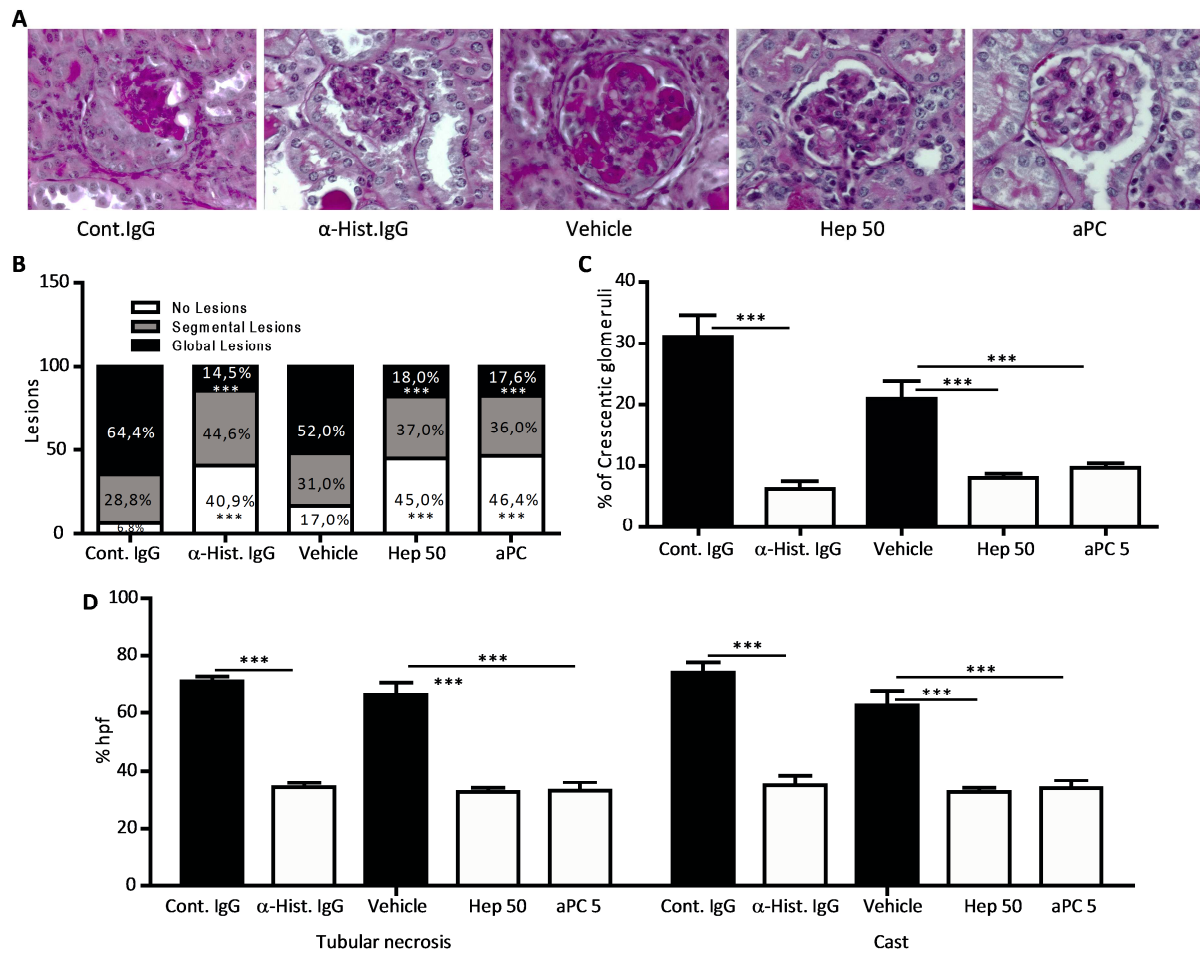


Figure: 39. (A) Periodic acid-Schiff staining (B) Glomerular lesions (C) and the percentage of crescentic glomeruli (D) and hpf as tubular injury score measured on day 7. Data represent the means \pm SEM of three experiments. * = $P < 0.05$, ** = $P < 0.01$, *** = $P < 0.001$.

Next, we determined the number of infiltrating neutrophils and macrophages within the glomeruli by histology as well as looked at the percentage of immune cells in GN-induced mice. As demonstrated in Figure 40A and 40B, less neutrophils and macrophages infiltrated the glomeruli following treatment with the histone blocking agent anti-histone IgG, heparin or aPC. Flow cytometry analysis of kidneys from anti-histone IgG, heparin or aPC-treated GN mice showed a significant reduction in the percentage of all intrarenal leukocyte subpopulations including neutrophils, macrophages, dendritic and T cells as well as their status of activation compared to control IgG-treated mice (Figure 41A and 41B).

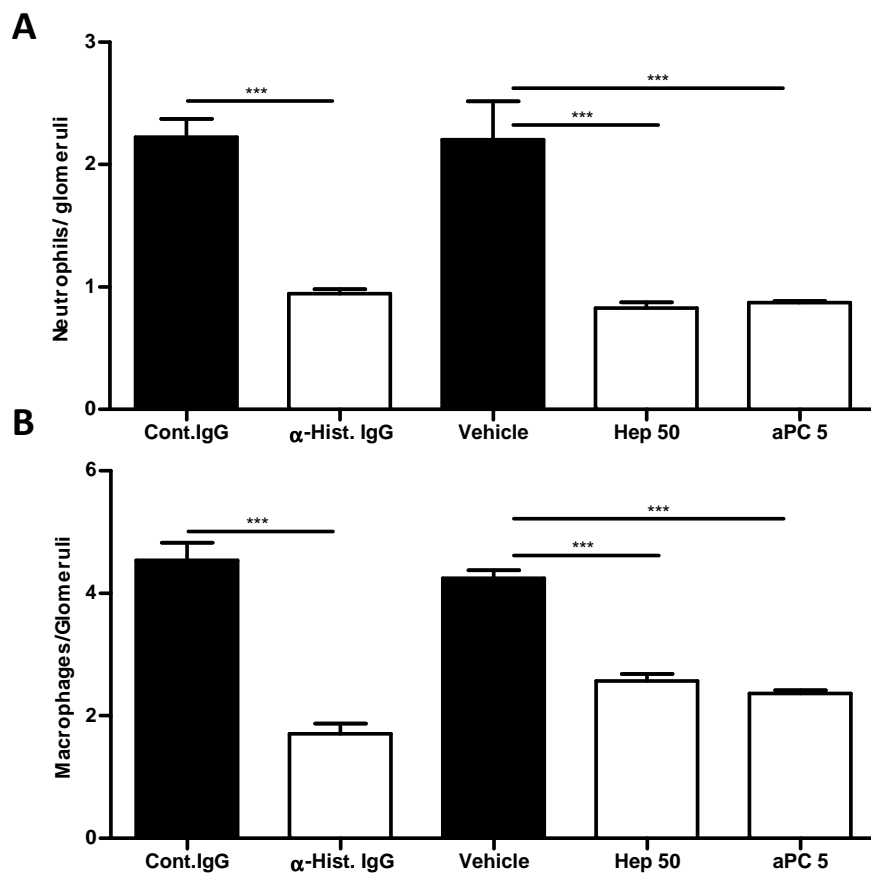


Figure: 40. Therapeutic histone blockade and renal leukocytes. Renal sections were obtained on day 7 and stained for neutrophils (A) and Mac2 (macrophages, B). Data represent mean glomerular cell counts \pm SEM of 5-6 mice in each group. * = $P < 0.05$, ** = $P < 0.01$, *** = $P < 0.001$ versus control IgG or vehicle.

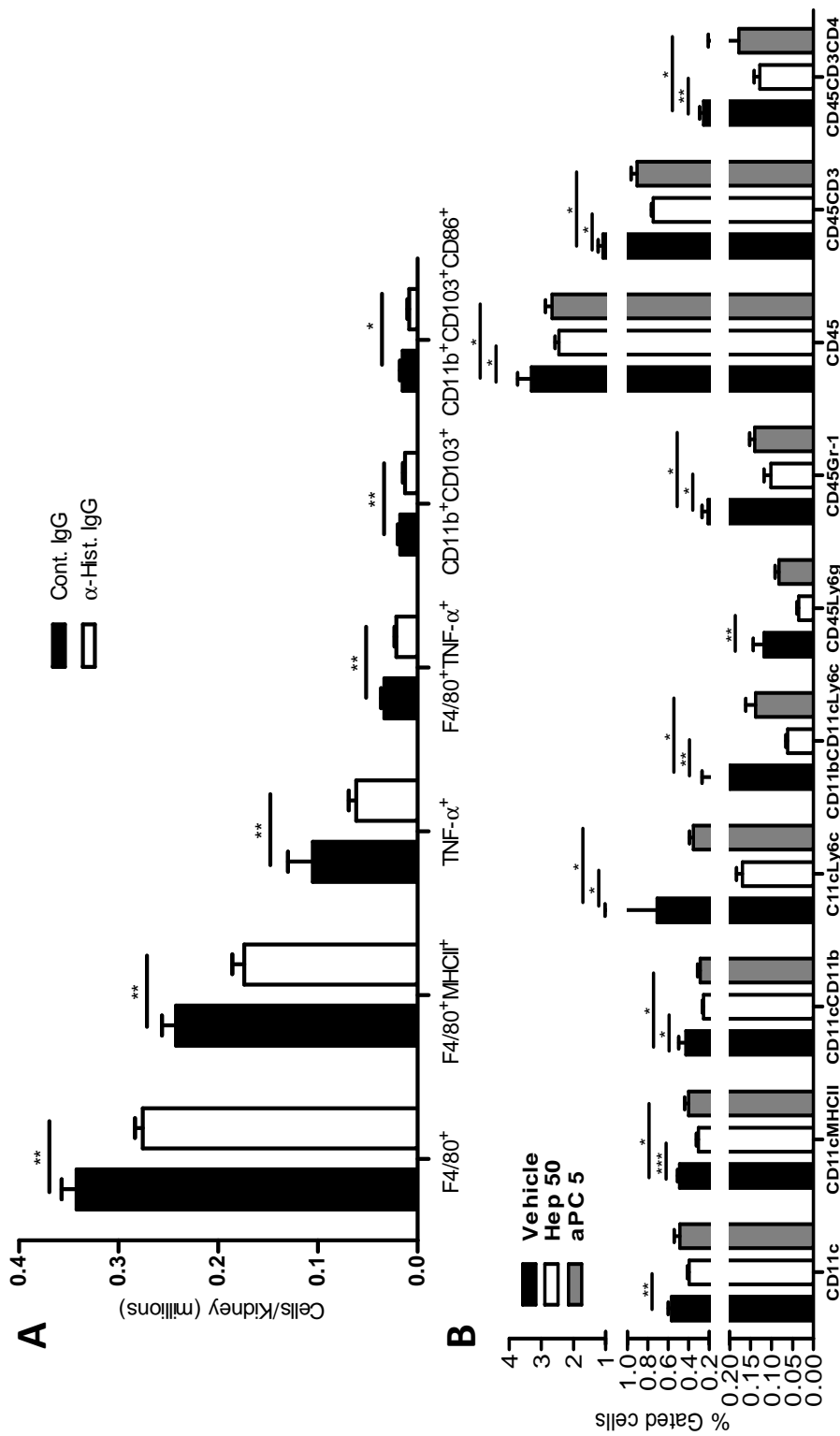


Figure: 41. (A and B) Flow cytometry data of various leukocyte subsets from kidneys of anti-histone IgG, heparin or aPC treated GN mice. * = $P < 0.05$, ** = $P < 0.01$, *** = $P < 0.001$ versus control IgG or vehicle.

4.7. Delayed onset of histone neutralization using combination of histone blocking agents improves severe glomerulonephritis but had no additive effects

Finally, we investigated the effect of histone neutralization using a combination therapy of the previously used histone blocking agent anti-histone IgG, heparin and aPC in a GBM antiserum induced severe GN model. Although combination therapy using all three agents resulted in a reduction in the urinary albumin/creatinine ratio and creatinine levels (Figure 42 upper and lower), it did not further decrease proteinuria and creatinine levels compared to the individual treatments. Taken together, therapeutic histone blockade with anti-histone IgG, heparin or aPC and in combination protected from renal dysfunction and structural injury during severe GN.

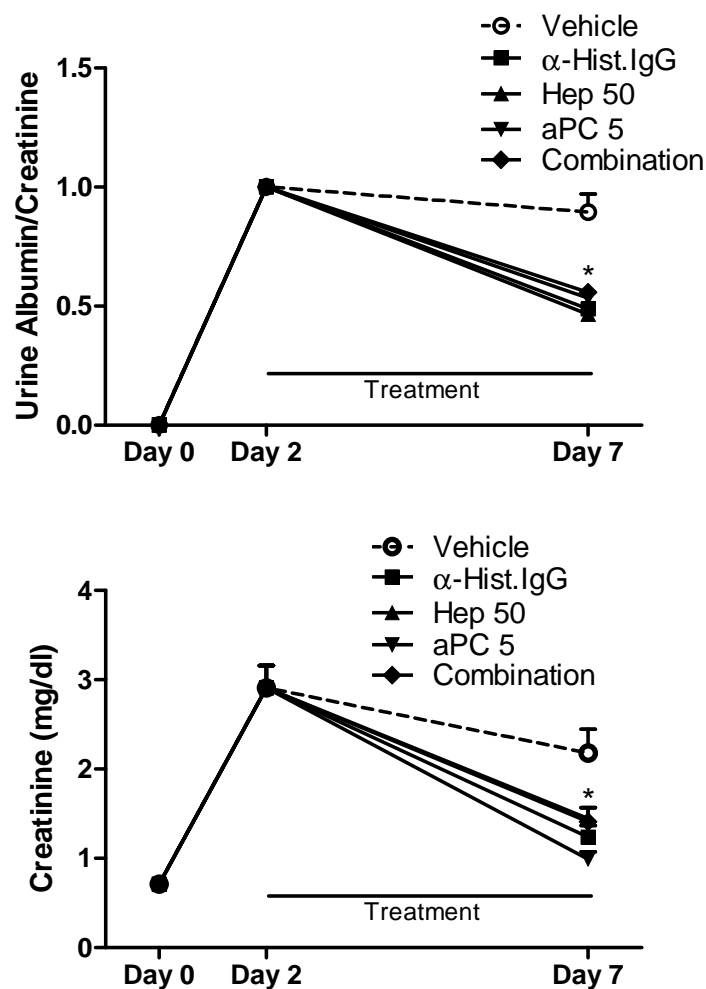


Figure: 42. (A) Effect of different treatments and combination of anti-histone IgG, heparin and aPC on proteinuria of anti-GBM induced glomerulonephritis on day 7 and (B) the creatinine levels. * = $P < 0.05$.

5. Discussion

There have been many studies that have explored the involvement of DAMPs in association with GN. This thesis provides further insights into the novel pathomechanisms involved in the progression of GN and CKD, in particular the source, release and toxic effects of extracellular histones and the beneficial outcomes of blocking released extracellular histones using anti-histone IgG and histone neutralizing agents like heparin and aPC during the pathogenesis and progression of necrotizing and crescentic GN.

The foremost questions we wanted to answer by this research are: Do dying glomerular cells and NETting neutrophils release extracellular histones? Are they contributing to the development of crescentic GN? Dying glomerular cells and NETs formation within the glomerulus have been shown to release cellular components, which act as DAMPs to elicit cytotoxic and immunostimulatory effects on glomerular cells leading to the progression of crescentic GN^{22,25}. The data presented in this thesis also confirm that extracellular histones released from dying glomerular cells and NETs exhibited cytotoxic and immunostimulatory effects causing the development of crescentic GN. Furthermore, neutralizing extracellular histones was effective during both treatment approaches, prophylactically and therapeutically indicating that histone neutralizing agents have the potential to serve as therapeutics during severe GN.

As mentioned above, NETosis is a regulated form of neutrophil death and was first discovered in 2004 in the context of being a neutrophil-specific mechanism required for killing of extracellular bacteria⁶³. Reports have shown that NETosis is not only an antibacterial host defense mechanism but can also occur during sterile inflammation because NETosis can be triggered via pro-inflammatory cytokines such as TNF- α . Our *in-vitro* studies showed that a sublethal dose of TNF- α is sufficient to trigger NETosis-driven injury in glomerular endothelial cells, as illustrated in Figure 43B. The ability of NETs to kill glomerular endothelial cells was solely dependent on the presence of histones generated within the NETs structure. This killing effect of NETs could be reversed by the addition of anti-histone IgG antibody (Figure 43C). Interestingly, blocking NETs *in-vivo* using the PAD inhibitor Cl-amide, which blocks the citrullination of histone H3, prevented NETs formation

by neutrophils and resulted in the protection of mice from developing GN. This is consistent with previous findings in a mouse model of lupus nephritis¹⁸⁸.

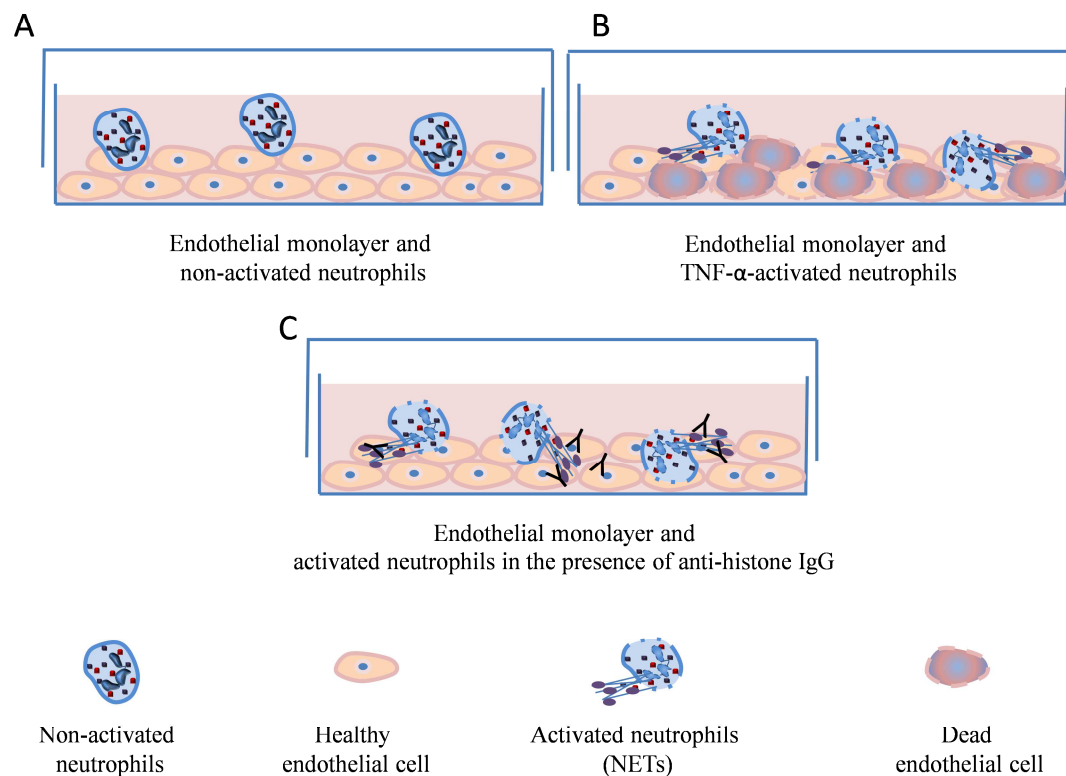


Figure: 43. Diagram representing the formation of NETs in-vitro and killing action of NETs when neutrophils get activated in the presence of $\text{TNF-}\alpha$. A) Normal endothelial monolayer with unstimulated neutrophils. B) Endothelial monolayer co-cultured with NETs forming neutrophils following stimulation with $\text{TNF-}\alpha$. C) Endothelial monolayer with $\text{TNF-}\alpha$ -activated neutrophils in the presence of anti-histone IgG.

NETosis causes the release of many aggressive proteases, oxygen radicals and potentially DAMPs into the extracellular space that drive vascular injury in the glomerulus. For example, DAMPs can activate TLRs and other pattern recognition receptors of the innate immune system leading to sterile inflammation. Our data now demonstrate an essential role for DAMPs in particular extracellular histones. Extracellular histones have been reported to contribute to endothelial dysfunction, organ failure and death during sepsis as a result of

microvascular endothelial cell injury in the lung¹⁰. Reports have further explored the thrombogenic potential of extracellular histones that exert their action via direct activation of endothelial cells and platelets^{91,93,101,113,139,147}. Similarly, in experimental infection and sepsis models, NETosis is most likely the source of extracellular histones, whereas in mechanical trauma, toxic liver injury, cerebral stroke and post-ischemic renal tubular necrosis histones are also released from dying tissue cells^{9,53}.

The data herein show that injection of extracellular histones *in-vivo* into healthy mice through the renal artery clearly triggered the killing action of histones in glomerular cells, which resulted in the progression of glomerulosclerosis. This was the case for anti-GBM-induced glomerulosclerosis, as illustrated in Figure 30. The mechanisms involved in histone toxicity are not entirely understood. However, there is evidence indicating that histones exert their killing activity due to their strong basic charge, a TLR-independent form of cytotoxicity⁹⁰. While the basic charge of histones is required within the nucleus to neutralize acidic residues of the DNA, the basic charge outside the cell has the capacity to damage the cell membrane⁹⁰. Reports have shown that the polyanion heparin can block this charge effect of histones, which may well explain its antagonistic effect on histone toxicity *in-vitro* and *in-vivo*. However, we and others discovered that histones elicit also DAMP-like immunostimulatory activity by activating TLR2, TLR4, and the NLRP3 inflammasome in dendritic cells and possibly other immune cell types^{9,93,94,98,121}. This represents another pathway of how extracellular histones trigger sterile inflammation. Because TLR2 and TLR4 (but not NLRP3) are known to induce glomerular injury in the heterologous anti-GBM GN model and are expressed inside the glomerulus in human ANCA vasculitis, we further explored the association of the histone-TLR2/4 axis^{22,168,189-191}. The data herein show that *Tlr2/4*-deficient glomeruli were protected from histone-induced injury *ex-vivo* and *in-vivo* implying that histone-related glomerular injury occurs in a TLR2/4-dependent DAMP manner. However, in the presence of serum the cytotoxic effect of histones on PECs can be reversed leading instead to PEC proliferation, which was entirely TLR2/4 dependent. Although PEC necrosis can be followed by excessive PEC recovery leading to PEC hyperplasia and crescent formation¹⁹², concomitant plasma leakage and histone release provide additional mitogenic stimuli during severe GN¹⁸⁵ (Figure 44).

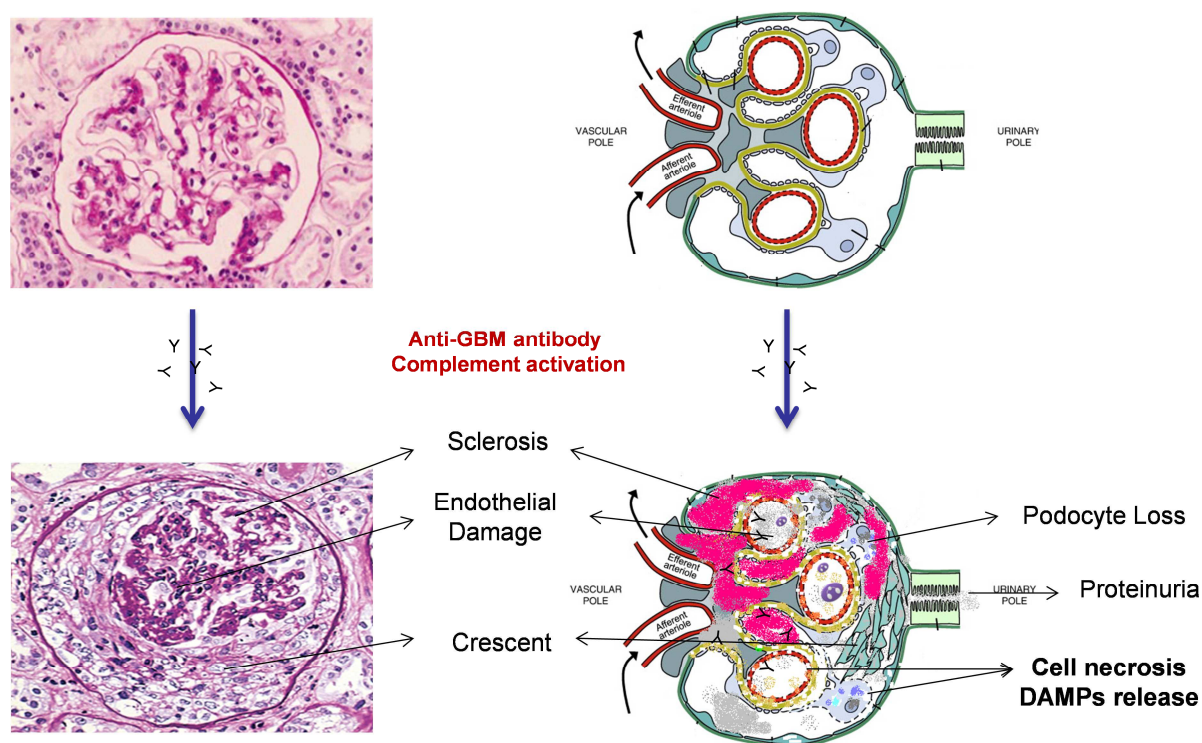


Figure: 44. Schematic representation of normal glomeruli and sclerotic glomeruli with capillary necrosis, hyperproliferation of PECs leading to crescents and podocytes detachment and death that further aggravates to proteinuria.

To explore the potential efficacy of histone blockade during severe GN, we applied three different treatment agents of histone inactivation. The experimental therapeutic approaches of histone neutralization were based on pre-emptive or post-induced GN using anti-histone IgG. Both therapeutic approaches with anti-histone IgG had a protective effect on the GN pathogenesis in accordance with reduced glomerular injury, proteinuria, and serum creatinine levels. A similar effect on the pathogenesis of GN by blocking histones was observed following heparin treatment, which was consistent with previously published findings in GN models¹⁹³. Furthermore, we have also demonstrated that heparin can inhibit the direct toxic effects of histones on glomerular endothelial cells, which is in line with reports investigating other cell types^{57,93,139,140,147}. Previously, aPC has been reported to be able to degrade extracellular histones¹⁰. Like anti-histone IgG and heparin, aPC was equally effective in abrogating extracellular histone toxicity *in-vitro* and severe GN *in-vivo*. The fact that combination therapy of all three agents did not show any additive effect supports the concept

that their protective effect on GN occurs via histone neutralization and not via unrelated mechanisms.

The anti-GBM induced severe GN model mimics the human GN conditions. However, the main limitations of this study are that the anti-GBM model is an artificial condition to induce GN by using antiserum against the collagen present in the GBM membrane and that the pathogenesis is short and severe with a high number of heterologous antibodies, which have direct killing effect on glomerular cells unlike in human GN. The disease severity might differ between the dose and batch of the serum used. Further studies are required to confirm the histone neutralization in human disease condition to make an effective treatment of blocking histones during GN in humans.

Taken together, NETosis releases histones into the extracellular space where they exert their toxic effects on glomerular endothelial cells and podocytes. Extracellular histone-induced glomerular injury depends on signaling through both receptors TLR2 and 4. In contrast, histone neutralization either by anti-histone IgG, recombinant aPC or heparin abrogates the pathogenesis of GBM antiserum-induced severe GN in both the pre-emptive and post-established model. In summary, extracellular histones represent a novel therapeutic target in severe GN.

6. Conclusion

The research presented within this thesis focused on the functional role of extracellular and NETs-related histones during the pathogenesis of severe GN and provides new insights into a potential anti-histone therapy in targeting histones to prevent severe GN and CKD.

The findings of the current study have multiple implications that are listed as followed and summarized in Figure 43:

- Extracellular histones released from dying cells and NETs contribute to glomerular cells death, mainly in GEnC.
- Extracellular histones are pro-inflammatory and activate dendritic cells and macrophages to release inflammatory cytokines.
- Extracellular histones show its toxic effects by activating TLR2/4 receptors.
- Extracellular histones activate PECs both *in-vitro* and *in-vivo* leading to crescent formation.
- Blockade of NETs by using a PAD inhibitor ameliorates all aspects of GBM antiserum-induced glomerulosclerosis.
- Pre-emptive as well as delayed onset of histone neutralization either by anti-histone IgG, recombinant aPC or heparin abrogates all aspects of GBM antiserum-induced severe GN.

Taken together, our research highlights the importance of extracellular histones as crucial mediators of severe GN.

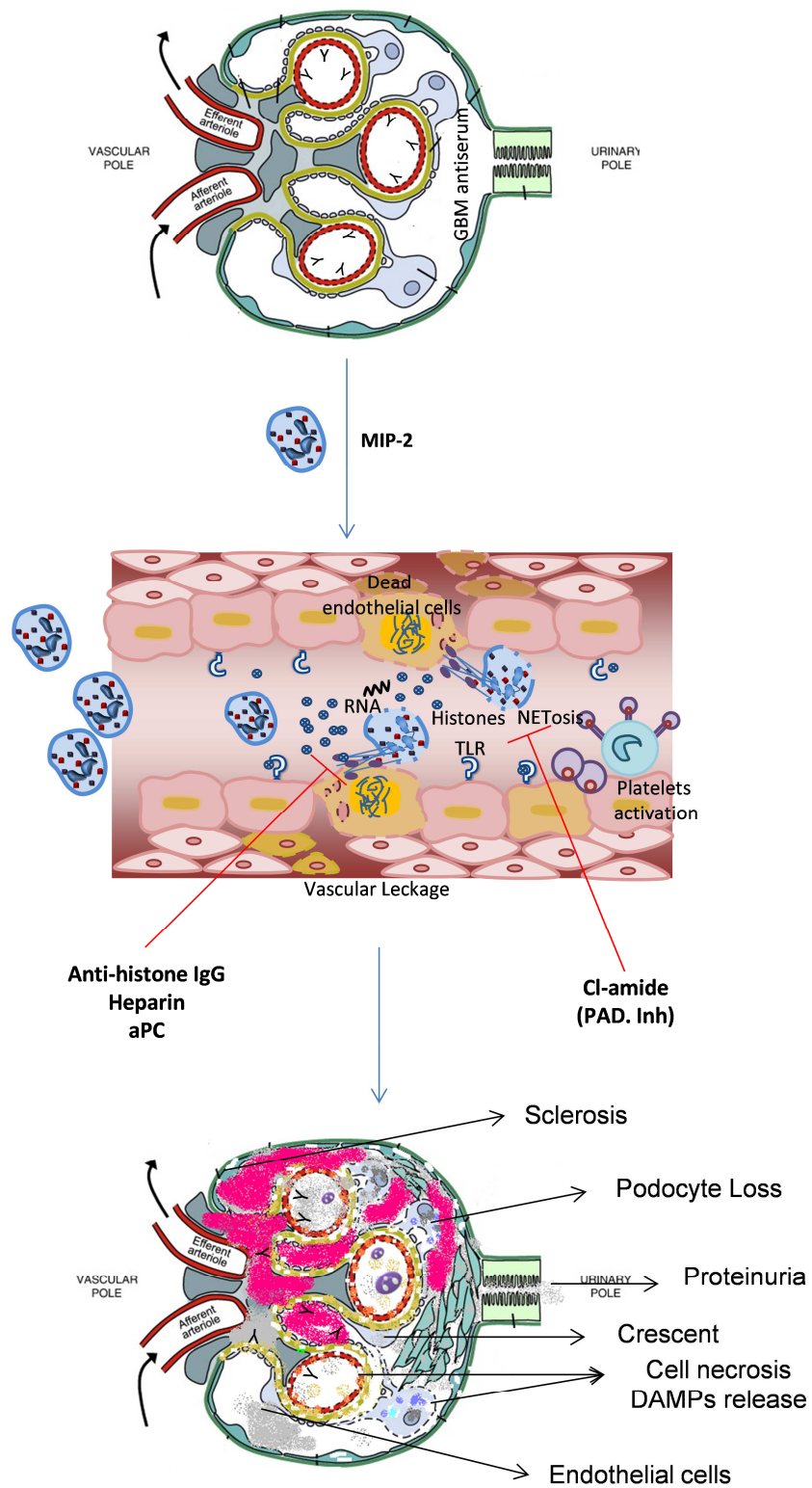


Figure: 45. Schematic representation of mechanism involved in the pathogenesis of glomerulonephritis and involvement of extracellular histones release from dying glomerular cells and NETing neutrophils.

7. *Future Direction*

It has been reported that histones show their cytotoxicity due to the strong positive charge present on their surface, but not much information is currently available regarding the specific cell death pathways. Future studies could be undertaken to determine the mechanism by which histones show their cytotoxicity. It would also be interesting to know whether histones exert cytotoxic effect via special regulated necrosis pathways or by simple apoptosis of cells.

Histones have been demonstrated to be involved in the pathogenicity of GN by killing endothelial cells and other glomerular cells. It would be interesting to study the effect of different cell death inhibitors in the GBM antiserum-induced GN, for example using inhibitors for necroptosis, ferroptosis or Cyclophilin D-mediated necrosis.

GBM antiserum-induced GN resulted in the infiltration of macrophages and blocking of histones reduced both infiltrating cells and cytokine production during the disease. Here it would be of interest to investigate the role of histone neutralization and differentiation of macrophages into an anti-inflammatory M2-like macrophage phenotype or a wound healing/fibrotic-like macrophage phenotype and to look at the functional role of these macrophage phenotypes during GBM antiserum-induced GN.

In our GBM antiserum-induced GN in-vivo model, we have reported heparin as a therapeutic histone neutralizing agent and showed a good protection of the disease progression in regards to reducing proteinuria, BUN levels and decreasing inflammation. Therefore, it would be of great importance to study the effect of heparin in patients who have severe GN to show its valuable clinical efficacy.

8. References

1. Medzhitov, R. Origin and physiological roles of inflammation. *Nature* **454**, 428-435 (2008).
2. Chen, G.Y. & Nunez, G. Sterile inflammation: sensing and reacting to damage. *Nature reviews. Immunology* **10**, 826-837 (2010).
3. Matzinger, P. Tolerance, danger, and the extended family. *Annual review of immunology* **12**, 991-1045 (1994).
4. Matzinger, P. The danger model: a renewed sense of self. *Science* **296**, 301-305 (2002).
5. Matzinger, P. Friendly and dangerous signals: is the tissue in control? *Nature immunology* **8**, 11-13 (2007).
6. Zhang, Q., *et al.* Circulating mitochondrial DAMPs cause inflammatory responses to injury. *Nature* **464**, 104-107 (2010).
7. Mbitikon-Kobo, F.M., *et al.* Characterization of a CD44/CD122int memory CD8 T cell subset generated under sterile inflammatory conditions. *Journal of immunology* **182**, 3846-3854 (2009).
8. Lu, C.Y., Hartono, J., Senitko, M. & Chen, J. The inflammatory response to ischemic acute kidney injury: a result of the 'right stuff' in the 'wrong place'? *Current opinion in nephrology and hypertension* **16**, 83-89 (2007).
9. Allam, R., *et al.* Histones from dying renal cells aggravate kidney injury via TLR2 and TLR4. *Journal of the American Society of Nephrology : JASN* **23**, 1375-1388 (2012).
10. Xu, J., *et al.* Extracellular histones are major mediators of death in sepsis. *Nat Med* **15**, 1318-1321 (2009).
11. Leelahavanichkul, A., *et al.* Chronic kidney disease worsens sepsis and sepsis-induced acute kidney injury by releasing High Mobility Group Box Protein-1. *Kidney international* **80**, 1198-1211 (2011).
12. Rabadi, M.M., Ghaly, T., Goligorsky, M.S. & Ratliff, B.B. HMGB1 in renal ischemic injury. *American journal of physiology. Renal physiology* **303**, F873-885 (2012).
13. Wang, H., *et al.* HMG-1 as a late mediator of endotoxin lethality in mice. *Science* **285**, 248-251 (1999).
14. Wu, H., *et al.* HMGB1 contributes to kidney ischemia reperfusion injury. *Journal of the American Society of Nephrology : JASN* **21**, 1878-1890 (2010).

15. Arumugam, T.V., *et al.* Toll-like receptors in ischemia-reperfusion injury. *Shock* **32**, 4-16 (2009).
16. Schaefer, L., *et al.* The matrix component biglycan is proinflammatory and signals through Toll-like receptors 4 and 2 in macrophages. *The Journal of clinical investigation* **115**, 2223-2233 (2005).
17. Merline, R., *et al.* Signaling by the matrix proteoglycan decorin controls inflammation and cancer through PDCD4 and MicroRNA-21. *Science signaling* **4**, ra75 (2011).
18. Treutiger, C.J., *et al.* High mobility group 1 B-box mediates activation of human endothelium. *Journal of internal medicine* **254**, 375-385 (2003).
19. Mkaddem, S.B., *et al.* Heat shock protein gp96 interacts with protein phosphatase 5 and controls toll-like receptor 2 (TLR2)-mediated activation of extracellular signal-regulated kinase (ERK) 1/2 in post-hypoxic kidney cells. *The Journal of biological chemistry* **284**, 12541-12549 (2009).
20. Harrison, E.M., *et al.* Heat shock protein 90-binding agents protect renal cells from oxidative stress and reduce kidney ischemia-reperfusion injury. *American journal of physiology. Renal physiology* **295**, F397-405 (2008).
21. Patschan, D., Patschan, S., Gobe, G.G., Chintala, S. & Goligorsky, M.S. Uric acid heralds ischemic tissue injury to mobilize endothelial progenitor cells. *Journal of the American Society of Nephrology : JASN* **18**, 1516-1524 (2007).
22. Lichtnekert, J., *et al.* Trif is not required for immune complex glomerulonephritis: dying cells activate mesangial cells via Tlr2/Myd88 rather than Tlr3/Trif. *American journal of physiology. Renal physiology* **296**, F867-874 (2009).
23. Zickert, A., *et al.* Renal expression and serum levels of high mobility group box 1 protein in lupus nephritis. *Arthritis research & therapy* **14**, R36 (2012).
24. Bruchfeld, A., *et al.* High-mobility group box-1 protein (HMGB1) is increased in antineutrophilic cytoplasmic antibody (ANCA)-associated vasculitis with renal manifestations. *Molecular medicine* **17**, 29-35 (2011).
25. Kessenbrock, K., *et al.* Netting neutrophils in autoimmune small-vessel vasculitis. *Nature medicine* **15**, 623-625 (2009).
26. Chen, K., *et al.* ATP-P2X4 signaling mediates NLRP3 inflammasome activation: a novel pathway of diabetic nephropathy. *The international journal of biochemistry & cell biology* **45**, 932-943 (2013).
27. Lin, M., *et al.* The TLR4 antagonist CRX-526 protects against advanced diabetic nephropathy. *Kidney international* **83**, 887-900 (2013).

28. Zhou, R., Tardivel, A., Thorens, B., Choi, I. & Tschopp, J. Thioredoxin-interacting protein links oxidative stress to inflammasome activation. *Nature immunology* **11**, 136-140 (2010).
29. Schaefer, L., *et al.* Small proteoglycans in human diabetic nephropathy: discrepancy between glomerular expression and protein accumulation of decorin, biglycan, lumican, and fibromodulin. *FASEB journal : official publication of the Federation of American Societies for Experimental Biology* **15**, 559-561 (2001).
30. Merline, R., *et al.* Decorin deficiency in diabetic mice: aggravation of nephropathy due to overexpression of profibrotic factors, enhanced apoptosis and mononuclear cell infiltration. *Journal of physiology and pharmacology : an official journal of the Polish Physiological Society* **60 Suppl 4**, 5-13 (2009).
31. Thompson, J., *et al.* Renal accumulation of biglycan and lipid retention accelerates diabetic nephropathy. *The American journal of pathology* **179**, 1179-1187 (2011).
32. Yan, S.F., Ramasamy, R. & Schmidt, A.M. Receptor for AGE (RAGE) and its ligands-cast into leading roles in diabetes and the inflammatory response. *Journal of molecular medicine* **87**, 235-247 (2009).
33. Bierhaus, A., *et al.* Understanding RAGE, the receptor for advanced glycation end products. *Journal of molecular medicine* **83**, 876-886 (2005).
34. Bohlender, J.M., Franke, S., Stein, G. & Wolf, G. Advanced glycation end products and the kidney. *American journal of physiology. Renal physiology* **289**, F645-659 (2005).
35. Heidland, A., Sebekova, K. & Schinzel, R. Advanced glycation end products and the progressive course of renal disease. *American journal of kidney diseases : the official journal of the National Kidney Foundation* **38**, S100-106 (2001).
36. Myint, K.M., *et al.* RAGE control of diabetic nephropathy in a mouse model: effects of RAGE gene disruption and administration of low-molecular weight heparin. *Diabetes* **55**, 2510-2522 (2006).
37. D'Agati, V., Yan, S.F., Ramasamy, R. & Schmidt, A.M. RAGE, glomerulosclerosis and proteinuria: roles in podocytes and endothelial cells. *Trends in endocrinology and metabolism: TEM* **21**, 50-56 (2010).
38. Yamamoto, Y., *et al.* Development and prevention of advanced diabetic nephropathy in RAGE-overexpressing mice. *The Journal of clinical investigation* **108**, 261-268 (2001).

39. Wendt, T.M., *et al.* RAGE drives the development of glomerulosclerosis and implicates podocyte activation in the pathogenesis of diabetic nephropathy. *The American journal of pathology* **162**, 1123-1137 (2003).
40. Lech, M. & Anders, H.J. The pathogenesis of lupus nephritis. *Journal of the American Society of Nephrology : JASN* **24**, 1357-1366 (2013).
41. Marshak-Rothstein, A. & Rifkin, I.R. Immunologically active autoantigens: the role of toll-like receptors in the development of chronic inflammatory disease. *Annual review of immunology* **25**, 419-441 (2007).
42. Migliorini, A. & Anders, H.J. A novel pathogenetic concept-antiviral immunity in lupus nephritis. *Nature reviews. Nephrology* **8**, 183-189 (2012).
43. Migliorini, A., *et al.* The antiviral cytokines IFN-alpha and IFN-beta modulate parietal epithelial cells and promote podocyte loss: implications for IFN toxicity, viral glomerulonephritis, and glomerular regeneration. *The American journal of pathology* **183**, 431-440 (2013).
44. Patole, P.S., *et al.* G-rich DNA suppresses systemic lupus. *Journal of the American Society of Nephrology : JASN* **16**, 3273-3280 (2005).
45. Pawar, R.D., *et al.* Ligands to nucleic acid-specific toll-like receptors and the onset of lupus nephritis. *Journal of the American Society of Nephrology : JASN* **17**, 3365-3373 (2006).
46. Pawar, R.D., *et al.* Toll-like receptor-7 modulates immune complex glomerulonephritis. *Journal of the American Society of Nephrology : JASN* **17**, 141-149 (2006).
47. Moreth, K., *et al.* The proteoglycan biglycan regulates expression of the B cell chemoattractant CXCL13 and aggravates murine lupus nephritis. *The Journal of clinical investigation* **120**, 4251-4272 (2010).
48. Pan, H.F., Wu, G.C., Li, W.P., Li, X.P. & Ye, D.Q. High Mobility Group Box 1: a potential therapeutic target for systemic lupus erythematosus. *Molecular biology reports* **37**, 1191-1195 (2010).
49. Urbonaviciute, V., *et al.* Induction of inflammatory and immune responses by HMGB1-nucleosome complexes: implications for the pathogenesis of SLE. *The Journal of experimental medicine* **205**, 3007-3018 (2008).
50. Jiang, W. & Pisetsky, D.S. Expression of high mobility group protein 1 in the sera of patients and mice with systemic lupus erythematosus. *Ann Rheum Dis* **67**, 727-728 (2008).

51. Qing, X., *et al.* Pathogenic anti-DNA antibodies modulate gene expression in mesangial cells: involvement of HMGB1 in anti-DNA antibody-induced renal injury. *Immunology letters* **121**, 61-73 (2008).
52. Iwata, Y., *et al.* Dendritic cells contribute to autoimmune kidney injury in MRL-Fas^{lpr} mice. *The Journal of rheumatology* **36**, 306-314 (2009).
53. Allam, R., Kumar, S.V., Darisipudi, M.N. & Anders, H.J. Extracellular histones in tissue injury and inflammation. *Journal of molecular medicine* **92**, 465-472 (2014).
54. Felsenfeld, G. & Groudine, M. Controlling the double helix. *Nature* **421**, 448-453 (2003).
55. Grunstein, M. Histone acetylation in chromatin structure and transcription. *Nature* **389**, 349-352 (1997).
56. Helin, K. & Dhanak, D. Chromatin proteins and modifications as drug targets. *Nature* **502**, 480-488 (2013).
57. Hirsch, J.G. Bactericidal action of histone. *The Journal of experimental medicine* **108**, 925-944 (1958).
58. Galluzzi, L., *et al.* Molecular definitions of cell death subroutines: recommendations of the Nomenclature Committee on Cell Death 2012. *Cell death and differentiation* **19**, 107-120 (2012).
59. Hotchkiss, R.S., Strasser, A., McDunn, J.E. & Swanson, P.E. Cell death. *The New England journal of medicine* **361**, 1570-1583 (2009).
60. Wickman, G.R., *et al.* Blebs produced by actin-myosin contraction during apoptosis release damage-associated molecular pattern proteins before secondary necrosis occurs. *Cell death and differentiation* **20**, 1293-1305 (2013).
61. Kono, H. & Rock, K.L. How dying cells alert the immune system to danger. *Nature reviews. Immunology* **8**, 279-289 (2008).
62. Vanden Berghe, T., Linkermann, A., Jouan-Lanhouet, S., Walczak, H. & Vandenabeele, P. Regulated necrosis: the expanding network of non-apoptotic cell death pathways. *Nature reviews. Molecular cell biology* **15**, 135-147 (2014).
63. Brinkmann, V., *et al.* Neutrophil extracellular traps kill bacteria. *Science* **303**, 1532-1535 (2004).
64. Douida, D.N., Yip, L., Khan, M.A., Grasemann, H. & Palaniyar, N. Akt is essential to induce NADPH-dependent NETosis and to switch the neutrophil death to apoptosis. *Blood* **123**, 597-600 (2014).

65. Yipp, B.G., *et al.* Infection-induced NETosis is a dynamic process involving neutrophil multitasking in vivo. *Nature medicine* **18**, 1386-1393 (2012).
66. Clark, S.R., *et al.* Platelet TLR4 activates neutrophil extracellular traps to ensnare bacteria in septic blood. *Nature medicine* **13**, 463-469 (2007).
67. Fink, S.L. & Cookson, B.T. Caspase-1-dependent pore formation during pyroptosis leads to osmotic lysis of infected host macrophages. *Cellular microbiology* **8**, 1812-1825 (2006).
68. Bergsbaken, T., Fink, S.L. & Cookson, B.T. Pyroptosis: host cell death and inflammation. *Nature reviews. Microbiology* **7**, 99-109 (2009).
69. Case, C.L., *et al.* Caspase-11 stimulates rapid flagellin-independent pyroptosis in response to *Legionella pneumophila*. *Proceedings of the National Academy of Sciences of the United States of America* **110**, 1851-1856 (2013).
70. Doitsh, G., *et al.* Cell death by pyroptosis drives CD4 T-cell depletion in HIV-1 infection. *Nature* **505**, 509-514 (2014).
71. Monroe, K.M., *et al.* IFI16 DNA sensor is required for death of lymphoid CD4 T cells abortively infected with HIV. *Science* **343**, 428-432 (2014).
72. Brennan, M.A. & Cookson, B.T. Salmonella induces macrophage death by caspase-1-dependent necrosis. *Molecular microbiology* **38**, 31-40 (2000).
73. Sun, G.W., Lu, J., Pervaiz, S., Cao, W.P. & Gan, Y.H. Caspase-1 dependent macrophage death induced by *Burkholderia pseudomallei*. *Cellular microbiology* **7**, 1447-1458 (2005).
74. Chen, Y., Smith, M.R., Thirumalai, K. & Zychlinsky, A. A bacterial invasin induces macrophage apoptosis by binding directly to ICE. *The EMBO journal* **15**, 3853-3860 (1996).
75. Bergsbaken, T. & Cookson, B.T. Macrophage activation redirects yersinia-infected host cell death from apoptosis to caspase-1-dependent pyroptosis. *PLoS pathogens* **3**, e161 (2007).
76. Linkermann, A. & Green, D.R. Necroptosis. *The New England journal of medicine* **370**, 455-465 (2014).
77. Miao, B. & Degterev, A. Methods to analyze cellular necroptosis. *Methods in molecular biology* **559**, 79-93 (2009).
78. McComb, S., *et al.* cIAP1 and cIAP2 limit macrophage necroptosis by inhibiting Rip1 and Rip3 activation. *Cell death and differentiation* **19**, 1791-1801 (2012).

79. Baines, C.P., *et al.* Loss of cyclophilin D reveals a critical role for mitochondrial permeability transition in cell death. *Nature* **434**, 658-662 (2005).
80. Linkermann, A., *et al.* Two independent pathways of regulated necrosis mediate ischemia-reperfusion injury. *Proceedings of the National Academy of Sciences of the United States of America* **110**, 12024-12029 (2013).
81. Nakagawa, T., *et al.* Cyclophilin D-dependent mitochondrial permeability transition regulates some necrotic but not apoptotic cell death. *Nature* **434**, 652-658 (2005).
82. Dixon, S.J., *et al.* Ferroptosis: an iron-dependent form of nonapoptotic cell death. *Cell* **149**, 1060-1072 (2012).
83. Yang, W.S., *et al.* Regulation of ferroptotic cancer cell death by GPX4. *Cell* **156**, 317-331 (2014).
84. Thomasova, D., *et al.* Murine Double Minute-2 Prevents p53-Overactivation-Related Cell Death (Podoptosis) of Podocytes. *Journal of the American Society of Nephrology : JASN* (2014).
85. Lee, D.Y., *et al.* Histone H4 is a major component of the antimicrobial action of human sebocytes. *The Journal of investigative dermatology* **129**, 2489-2496 (2009).
86. Wang, Y., *et al.* Differential microbicidal effects of human histone proteins H2A and H2B on *Leishmania* promastigotes and amastigotes. *Infection and immunity* **79**, 1124-1133 (2011).
87. Rose, F.R., *et al.* Potential role of epithelial cell-derived histone H1 proteins in innate antimicrobial defense in the human gastrointestinal tract. *Infection and immunity* **66**, 3255-3263 (1998).
88. Chen, R., Kang, R., Fan, X.G. & Tang, D. Release and activity of histone in diseases. *Cell death & disease* **5**, e1370 (2014).
89. Kutcher, M.E., *et al.* Extracellular histone release in response to traumatic injury: implications for a compensatory role of activated protein C. *The journal of trauma and acute care surgery* **73**, 1389-1394 (2012).
90. Gillrie, M.R., *et al.* *Plasmodium falciparum* histones induce endothelial proinflammatory response and barrier dysfunction. *The American journal of pathology* **180**, 1028-1039 (2012).
91. Saffarzadeh, M., *et al.* Neutrophil extracellular traps directly induce epithelial and endothelial cell death: a predominant role of histones. *PloS one* **7**, e32366 (2012).
92. Gilthorpe, J.D., *et al.* Extracellular histone H1 is neurotoxic and drives a pro-inflammatory response in microglia. *F1000Research* **2**, 148 (2013).

93. Semeraro, F., *et al.* Extracellular histones promote thrombin generation through platelet-dependent mechanisms: involvement of platelet TLR2 and TLR4. *Blood* **118**, 1952-1961 (2011).
94. Xu, J., Zhang, X., Monestier, M., Esmon, N.L. & Esmon, C.T. Extracellular histones are mediators of death through TLR2 and TLR4 in mouse fatal liver injury. *Journal of immunology* **187**, 2626-2631 (2011).
95. Rock, K.L., Latz, E., Ontiveros, F. & Kono, H. The sterile inflammatory response. *Annual review of immunology* **28**, 321-342 (2010).
96. Huang, H., *et al.* Endogenous histones function as alarmins in sterile inflammatory liver injury through Toll-like receptor 9 in mice. *Hepatology* **54**, 999-1008 (2011).
97. Schroder, K. & Tschopp, J. The inflammasomes. *Cell* **140**, 821-832 (2010).
98. Allam, R., Darisipudi, M.N., Tschopp, J. & Anders, H.J. Histones trigger sterile inflammation by activating the NLRP3 inflammasome. *European journal of immunology* **43**, 3336-3342 (2013).
99. Darisipudi, M.N., *et al.* Uromodulin triggers IL-1beta-dependent innate immunity via the NLRP3 inflammasome. *Journal of the American Society of Nephrology : JASN* **23**, 1783-1789 (2012).
100. Martinon, F., Petrilli, V., Mayor, A., Tardivel, A. & Tschopp, J. Gout-associated uric acid crystals activate the NALP3 inflammasome. *Nature* **440**, 237-241 (2006).
101. Fuchs, T.A., Bhandari, A.A. & Wagner, D.D. Histones induce rapid and profound thrombocytopenia in mice. *Blood* **118**, 3708-3714 (2011).
102. Martinod, K., *et al.* Neutrophil histone modification by peptidylarginine deiminase 4 is critical for deep vein thrombosis in mice. *Proceedings of the National Academy of Sciences of the United States of America* **110**, 8674-8679 (2013).
103. Lam, F.W., *et al.* Histone induced platelet aggregation is inhibited by normal albumin. *Thrombosis research* **132**, 69-76 (2013).
104. Carestia, A., *et al.* Functional responses and molecular mechanisms involved in histone-mediated platelet activation. *Thrombosis and haemostasis* **110**, 1035-1045 (2013).
105. Luger, K., Mader, A.W., Richmond, R.K., Sargent, D.F. & Richmond, T.J. Crystal structure of the nucleosome core particle at 2.8 Å resolution. *Nature* **389**, 251-260 (1997).
106. Von, H. Stabilization of DNA Structure by Histones against Thermal Denaturation. *Experientia* **21**, 90-91 (1965).

107. Mortensen, E.S., Fenton, K.A. & Rekvig, O.P. Lupus nephritis: the central role of nucleosomes revealed. *The American journal of pathology* **172**, 275-283 (2008).
108. Hakkim, A., *et al.* Impairment of neutrophil extracellular trap degradation is associated with lupus nephritis. *Proceedings of the National Academy of Sciences of the United States of America* **107**, 9813-9818 (2010).
109. Mortensen, E.S. & Rekvig, O.P. Nephritogenic potential of anti-DNA antibodies against necrotic nucleosomes. *Journal of the American Society of Nephrology : JASN* **20**, 696-704 (2009).
110. Balicki, D. & Beutler, E. Histone H2A significantly enhances in vitro DNA transfection. *Molecular medicine* **3**, 782-787 (1997).
111. Wildhagen, K.C., *et al.* Non-anticoagulant heparin prevents histone-mediated cytotoxicity in vitro and improves survival in sepsis. *Blood* (2013).
112. Allam, R., Darisipudi, M.N., Tschopp, J. & Anders, H.J. Histones trigger sterile inflammation by activating the NLRP3 inflammasome. *Eur J Immunol* (2013).
113. Abrams, S.T., *et al.* Circulating histones are mediators of trauma-associated lung injury. *American journal of respiratory and critical care medicine* **187**, 160-169 (2013).
114. Johansson, P.I., Windelov, N.A., Rasmussen, L.S., Sorensen, A.M. & Ostrowski, S.R. Blood levels of histone-complexed DNA fragments are associated with coagulopathy, inflammation and endothelial damage early after trauma. *J Emerg Trauma Shock* **6**, 171-175 (2013).
115. Nakahara, M., *et al.* Recombinant thrombomodulin protects mice against histone-induced lethal thromboembolism. *PloS one* **8**, e75961 (2013).
116. De Meyer, S.F., Suidan, G.L., Fuchs, T.A., Monestier, M. & Wagner, D.D. Extracellular chromatin is an important mediator of ischemic stroke in mice. *Arteriosclerosis, thrombosis, and vascular biology* **32**, 1884-1891 (2012).
117. Pemberton, A.D. & Brown, J.K. In vitro interactions of extracellular histones with LDL suggest a potential pro-atherogenic role. *PLoS One* **5**, e9884 (2010).
118. Bosmann, M., *et al.* Extracellular histones are essential effectors of C5aR- and C5L2-mediated tissue damage and inflammation in acute lung injury. *FASEB journal : official publication of the Federation of American Societies for Experimental Biology* **27**, 5010-5021 (2013).

119. Barrero, C.A., *et al.* Histone 3.3 participates in a self-sustaining cascade of apoptosis that contributes to the progression of chronic obstructive pulmonary disease. *American journal of respiratory and critical care medicine* **188**, 673-683 (2013).
120. Huang, H., *et al.* Endogenous histones function as alarmins in sterile inflammatory liver injury through toll-like receptor 9. *Hepatology* (2011).
121. Huang, H., *et al.* Histones activate the NLRP3 inflammasome in Kupffer cells during sterile inflammatory liver injury. *Journal of immunology* **191**, 2665-2679 (2013).
122. Rosin, D.L. & Okusa, M.D. Dying cells and extracellular histones in AKI: beyond a NET effect? *Journal of the American Society of Nephrology : JASN* **23**, 1275-1277 (2012).
123. Dwivedi, N., *et al.* Felty's syndrome autoantibodies bind to deiminated histones and neutrophil extracellular chromatin traps. *Arthritis and rheumatism* **64**, 982-992 (2012).
124. Pratesi, F., *et al.* Antibodies from patients with rheumatoid arthritis target citrullinated histone 4 contained in neutrophils extracellular traps. *Ann Rheum Dis* (2013).
125. Monach, P.A., *et al.* A broad screen for targets of immune complexes decorating arthritic joints highlights deposition of nucleosomes in rheumatoid arthritis. *Proceedings of the National Academy of Sciences of the United States of America* **106**, 15867-15872 (2009).
126. Dwivedi, N. & Radic, M. Citrullination of autoantigens implicates NETosis in the induction of autoimmunity. *Ann Rheum Dis* (2013).
127. Fuchs, T.A., *et al.* Neutrophils release extracellular DNA traps during storage of red blood cell units. *Transfusion* **53**, 3210-3216 (2013).
128. Schimmel, M., *et al.* Nucleosomes and neutrophil activation in sickle cell disease painful crisis. *Haematologica* **98**, 1797-1803 (2013).
129. Shin, S.H., Joo, H.W., Kim, M.K., Kim, J.C. & Sung, Y.K. Extracellular histones inhibit hair shaft elongation in cultured human hair follicles and promote regression of hair follicles in mice. *Exp Dermatol* **21**, 956-958 (2012).
130. Wen, Z., *et al.* Circulating histones exacerbate inflammation in mice with acute liver failure. *Journal of cellular biochemistry* **114**, 2384-2391 (2013).
131. Bosch, X. Systemic lupus erythematosus and the neutrophil. *The New England journal of medicine* **365**, 758-760 (2011).
132. Lande, R., *et al.* Neutrophils activate plasmacytoid dendritic cells by releasing self-DNA-peptide complexes in systemic lupus erythematosus. *Science translational medicine* **3**, 73ra19 (2011).

133. Villanueva, E., *et al.* Netting neutrophils induce endothelial damage, infiltrate tissues, and expose immunostimulatory molecules in systemic lupus erythematosus. *Journal of immunology* **187**, 538-552 (2011).
134. Stummvoll, G.H., *et al.* Characterisation of cellular and humoral autoimmune responses to histone H1 and core histones in human systemic lupus erythematosis. *Ann Rheum Dis* **68**, 110-116 (2009).
135. Pratesi, F., *et al.* Antibodies from patients with rheumatoid arthritis target citrullinated histone 4 contained in neutrophils extracellular traps. *Ann Rheum Dis* **73**, 1414-1422 (2014).
136. Dwivedi, N. & Radic, M. Citrullination of autoantigens implicates NETosis in the induction of autoimmunity. *Ann Rheum Dis* **73**, 483-491 (2014).
137. Mastronardi, F.G., *et al.* Increased citrullination of histone H3 in multiple sclerosis brain and animal models of demyelination: a role for tumor necrosis factor-induced peptidylarginine deiminase 4 translocation. *The Journal of neuroscience : the official journal of the Society for Neuroscience* **26**, 11387-11396 (2006).
138. Cadrillier, A., *et al.* Platelets induce neutrophil extracellular traps in transfusion-related acute lung injury. *The Journal of clinical investigation* **122**, 2661-2671 (2012).
139. Fuchs, T.A., *et al.* Extracellular DNA traps promote thrombosis. *Proceedings of the National Academy of Sciences of the United States of America* **107**, 15880-15885 (2010).
140. Wildhagen, K.C., *et al.* Nonanticoagulant heparin prevents histone-mediated cytotoxicity in vitro and improves survival in sepsis. *Blood* **123**, 1098-1101 (2014).
141. Monestier, M., Fasy, T.M., Losman, M.J., Novick, K.E. & Muller, S. Structure and binding properties of monoclonal antibodies to core histones from autoimmune mice. *Molecular immunology* **30**, 1069-1075 (1993).
142. Nicolaes, G.A. & Dahlback, B. Congenital and acquired activated protein C resistance. *Seminars in vascular medicine* **3**, 33-46 (2003).
143. in *Venous Thromboembolic Diseases: The Management of Venous Thromboembolic Diseases and the Role of Thrombophilia Testing* (London, 2012).
144. de Kort, E.H., *et al.* Long-term subcutaneous protein C replacement in neonatal severe protein C deficiency. *Pediatrics* **127**, e1338-1342 (2011).
145. Minhas, N., Xue, M., Fukudome, K. & Jackson, C.J. Activated protein C utilizes the angiopoietin/Tie2 axis to promote endothelial barrier function. *FASEB journal* :

- official publication of the Federation of American Societies for Experimental Biology* **24**, 873-881 (2010).
146. Bouwens, E.A., Stavenuiter, F. & Mosnier, L.O. Mechanisms of anticoagulant and cytoprotective actions of the protein C pathway. *Journal of thrombosis and haemostasis : JTH* **11 Suppl 1**, 242-253 (2013).
147. Ammollo, C.T., Semeraro, F., Xu, J., Esmon, N.L. & Esmon, C.T. Extracellular histones increase plasma thrombin generation by impairing thrombomodulin-dependent protein C activation. *Journal of thrombosis and haemostasis : JTH* **9**, 1795-1803 (2011).
148. Zeerleder, S., *et al.* Circulating nucleosomes and severity of illness in children suffering from meningococcal sepsis treated with protein C. *Critical care medicine* **40**, 3224-3229 (2012).
149. Ranieri, V.M., *et al.* Drotrecogin alfa (activated) in adults with septic shock. *The New England journal of medicine* **366**, 2055-2064 (2012).
150. Alcantara, F.F., Iglehart, D.J. & Ochs, R.L. Heparin in plasma samples causes nonspecific binding to histones on Western blots. *Journal of immunological methods* **226**, 11-18 (1999).
151. Zhao, D., *et al.* Heparin rescues sepsis-associated acute lung injury and lethality through the suppression of inflammatory responses. *Inflammation* **35**, 1825-1832 (2012).
152. Cox, C.S., Jr., *et al.* Heparin improves oxygenation and minimizes barotrauma after severe smoke inhalation in an ovine model. *Surgery, gynecology & obstetrics* **176**, 339-349 (1993).
153. Murakami, K., *et al.* High-dose heparin fails to improve acute lung injury following smoke inhalation in sheep. *Clinical science* **104**, 349-356 (2003).
154. Couser, W.G. Basic and translational concepts of immune-mediated glomerular diseases. *Journal of the American Society of Nephrology : JASN* **23**, 381-399 (2012).
155. Schreiber, A., Luft, F.C. & Kettritz, R. Phagocyte NADPH Oxidase Restrains the Inflammasome in ANCA-Induced GN. *Journal of the American Society of Nephrology : JASN* (2014).
156. Sangaletti, S., *et al.* Neutrophil extracellular traps mediate transfer of cytoplasmic neutrophil antigens to myeloid dendritic cells toward ANCA induction and associated autoimmunity. *Blood* **120**, 3007-3018 (2012).

157. Jennette, J.C. & Falk, R.J. Pathogenesis of antineutrophil cytoplasmic autoantibody-mediated disease. *Nature reviews. Rheumatology* **10**, 463-473 (2014).
158. Kolaczowska, E. & Kubes, P. Neutrophil recruitment and function in health and inflammation. *Nature reviews. Immunology* **13**, 159-175 (2013).
159. Schauer, C., *et al.* Aggregated neutrophil extracellular traps limit inflammation by degrading cytokines and chemokines. *Nature medicine* **20**, 511-517 (2014).
160. Remijsen, Q., *et al.* Dying for a cause: NETosis, mechanisms behind an antimicrobial cell death modality. *Cell death and differentiation* **18**, 581-588 (2011).
161. Bhandari, V., *et al.* Hyperoxia causes angiopoietin 2-mediated acute lung injury and necrotic cell death. *Nature medicine* **12**, 1286-1293 (2006).
162. Wilhelm, D.L. Mechanisms responsible for increased vascular permeability in acute inflammation. *Agents and actions* **3**, 297-306 (1973).
163. Okamoto, H. Molecular architecture of the Goodpasture autoantigen. *The New England journal of medicine* **363**, 1770; author reply 1771 (2010).
164. Pedchenko, V., *et al.* Molecular architecture of the Goodpasture autoantigen in anti-GBM nephritis. *The New England journal of medicine* **363**, 343-354 (2010).
165. Khandelwal, M., *et al.* Recurrence of anti-GBM disease 8 years after renal transplantation. *Nephrology, dialysis, transplantation : official publication of the European Dialysis and Transplant Association - European Renal Association* **19**, 491-494 (2004).
166. Tang, W., *et al.* Anti-glomerular basement membrane antibody disease is an uncommon cause of end-stage renal disease. *Kidney international* **83**, 503-510 (2013).
167. Kluth, D.C. & Rees, A.J. Anti-glomerular basement membrane disease. *Journal of the American Society of Nephrology : JASN* **10**, 2446-2453 (1999).
168. Lichtnekert, J., *et al.* Anti-GBM glomerulonephritis involves IL-1 but is independent of NLRP3/ASC inflammasome-mediated activation of caspase-1. *PloS one* **6**, e26778 (2011).
169. Vielhauer, V., Stavrakis, G. & Mayadas, T.N. Renal cell-expressed TNF receptor 2, not receptor 1, is essential for the development of glomerulonephritis. *The Journal of clinical investigation* **115**, 1199-1209 (2005).
170. Tang, W.W., Qi, M. & Warren, J.S. Monocyte chemoattractant protein 1 mediates glomerular macrophage infiltration in anti-GBM Ab GN. *Kidney international* **50**, 665-671 (1996).

171. Smeets, B., *et al.* Renal progenitor cells contribute to hyperplastic lesions of podocytopathies and crescentic glomerulonephritis. *Journal of the American Society of Nephrology : JASN* **20**, 2593-2603 (2009).
172. Smeets, B., *et al.* Tracing the origin of glomerular extracapillary lesions from parietal epithelial cells. *Journal of the American Society of Nephrology : JASN* **20**, 2604-2615 (2009).
173. Nakazawa, D., Tomaru, U., Yamamoto, C., Jodo, S. & Ishizu, A. Abundant neutrophil extracellular traps in thrombus of patient with microscopic polyangiitis. *Frontiers in immunology* **3**, 333 (2012).
174. Branzk, N. & Papayannopoulos, V. Molecular mechanisms regulating NETosis in infection and disease. *Seminars in immunopathology* **35**, 513-530 (2013).
175. Willis, V.C., *et al.* N-alpha-benzoyl-N5-(2-chloro-1-iminoethyl)-L-ornithine amide, a protein arginine deiminase inhibitor, reduces the severity of murine collagen-induced arthritis. *Journal of immunology* **186**, 4396-4404 (2011).
176. Rohrbach, A.S., Slade, D.J., Thompson, P.R. & Mowen, K.A. Activation of PAD4 in NET formation. *Frontiers in immunology* **3**, 360 (2012).
177. Kurts, C., Panzer, U., Anders, H.J. & Rees, A.J. The immune system and kidney disease: basic concepts and clinical implications. *Nature reviews. Immunology* **13**, 738-753 (2013).
178. Wolpe, S.D., *et al.* Identification and characterization of macrophage inflammatory protein 2. *Proceedings of the National Academy of Sciences of the United States of America* **86**, 612-616 (1989).
179. Iida, N. & Grotendorst, G.R. Cloning and sequencing of a new gro transcript from activated human monocytes: expression in leukocytes and wound tissue. *Molecular and cellular biology* **10**, 5596-5599 (1990).
180. Pelus, L.M. & Fukuda, S. Peripheral blood stem cell mobilization: the CXCR2 ligand GRObeta rapidly mobilizes hematopoietic stem cells with enhanced engraftment properties. *Experimental hematology* **34**, 1010-1020 (2006).
181. Ryu, M., Mulay, S.R., Miosge, N., Gross, O. & Anders, H.J. Tumour necrosis factor-alpha drives Alport glomerulosclerosis in mice by promoting podocyte apoptosis. *The Journal of pathology* **226**, 120-131 (2012).
182. Nawroth, P., *et al.* Tumor necrosis factor/cachectin-induced intravascular fibrin formation in meth A fibrosarcomas. *The Journal of experimental medicine* **168**, 637-647 (1988).

183. Hertig, A. & Rondeau, E. Role of the coagulation/fibrinolysis system in fibrin-associated glomerular injury. *Journal of the American Society of Nephrology : JASN* **15**, 844-853 (2004).
184. Engelmann, B. & Massberg, S. Thrombosis as an intravascular effector of innate immunity. *Nature reviews. Immunology* **13**, 34-45 (2013).
185. Ryu, M., *et al.* Plasma leakage through glomerular basement membrane ruptures triggers the proliferation of parietal epithelial cells and crescent formation in non-inflammatory glomerular injury. *The Journal of pathology* **228**, 482-494 (2012).
186. Shankland, S.J., Anders, H.J. & Romagnani, P. Glomerular parietal epithelial cells in kidney physiology, pathology, and repair. *Current opinion in nephrology and hypertension* **22**, 302-309 (2013).
187. Zhang, J., *et al.* Retinoids augment the expression of podocyte proteins by glomerular parietal epithelial cells in experimental glomerular disease. *Nephron. Experimental nephrology* **121**, e23-37 (2012).
188. Knight, J.S., *et al.* Peptidylarginine deiminase inhibition is immunomodulatory and vasculoprotective in murine lupus. *The Journal of clinical investigation* **123**, 2981-2993 (2013).
189. Brown, H.J., Lock, H.R., Sacks, S.H. & Robson, M.G. TLR2 stimulation of intrinsic renal cells in the induction of immune-mediated glomerulonephritis. *Journal of immunology* **177**, 1925-1931 (2006).
190. Brown, H.J., *et al.* Toll-like receptor 4 ligation on intrinsic renal cells contributes to the induction of antibody-mediated glomerulonephritis via CXCL1 and CXCL2. *Journal of the American Society of Nephrology : JASN* **18**, 1732-1739 (2007).
191. Wang, H., Gou, S.J., Zhao, M.H. & Chen, M. The expression of Toll-like receptors 2, 4 and 9 in kidneys of patients with anti-neutrophil cytoplasmic antibody (ANCA)-associated vasculitis. *Clinical and experimental immunology* **177**, 603-610 (2014).
192. Sicking, E.M., *et al.* Subtotal ablation of parietal epithelial cells induces crescent formation. *Journal of the American Society of Nephrology : JASN* **23**, 629-640 (2012).
193. Floege, J., Eng, E., Young, B.A., Couser, W.G. & Johnson, R.J. Heparin suppresses mesangial cell proliferation and matrix expansion in experimental mesangioproliferative glomerulonephritis. *Kidney international* **43**, 369-380 (1993).

9. Abbreviations

AKI	Acute kidney injury	PAMPs	Pathogen-associated molecular patterns
ANCA	Anti-neutrophil cytoplasmic antibody	PAS	Periodic acid Schiff staining
aPC	Activated protein C	PECs	Parietal Epithelial Cells
BUN	Blood urea nitrogen	PRRs	pattern recognition receptors
DAMPs	Damage-associated molecular patterns	RAGE	Receptor for advanced glycation end-products
DCs	Dendritic cells	RNA	Ribonucleic acid
DN	Diabetic nephropathy	ROS	Reactive oxygen species
DNAA	Deoxyribonucleic acid	RPGN	Rapidly-progressive glomerulonephritis
ELISA	Enzyme linked immunosorbent assay	SLE	Systemic lupus erythematosus
GBM	Glomerular basement membrane	TLRs	Toll like receptors
GEnC	Glomerular endothelial cells	TNF	Tumor necrosis factor
GN	Glomerulonephritis		
HMGB1	High mobility group box-1		
HSP	Heat shock proteins		
IFN- γ	Interferon-gamma		
IL	Interleukins		
LRRs	leucine-rich repeats		
MPO	Myeloperoxidase		
NET	Neutrophils extracellular traps		
NLR	Nod-like receptor		
NLRP3	NOD-like receptor family, pyrin domain containing 3)		
O.D.	Optical density		

10. Appendix**Composition of buffers used**FACS buffer :

Sterile DPBS	500 ml
Na Azide	500 mg (0.1 %)
BSA	1 g (0.2 %)

10X HBSS (Hank's Balanced Saline Solution) with Ca, Mg:

For 1000 ml

KCl	4 g
KH_2PO_4	0.6 g
NaCl	80 g
$\text{Na}_2\text{HPO}_4 \cdot 2\text{H}_2\text{O}$	0.621 g
NaHCO_3	3.5 g
CaCl_2	1.4 g (or $\text{CaCl}_2 \cdot 2\text{H}_2\text{O}$ 1.854 g)
$\text{MgCl}_2 \cdot 6\text{H}_2\text{O}$	1 g
$\text{MgSO}_4 \cdot 7\text{H}_2\text{O}$	1 g
D-Glucose	10 g

Dissolve in 900 ml of distilled water and adjust to pH 7.4 with 1N HCl or 1N NaOH.
Make up the volume with distilled water to 1000 ml.

10X HBSS (Hank's Balanced Saline Solution) without Ca, Mg:

For 1000 ml

KCl	4 g
KH_2PO_4	0.6 g
NaCl	80 g
$\text{Na}_2\text{HPO}_4 \cdot 2\text{H}_2\text{O}$	0.621 g

Dissolve in 1000 ml and autoclave.

DNase stock solution (1 mg/ml):

DNase (type III) 15000 U/6 mg (Sigma D5025)

To prepared 1 mg/ml solution:

Add 6 ml of 50 % (w/v) Glycerol in 20 mM Tris-HCl (pH 7.5), 1 mM MgCl₂.

Can be kept at -20 °C for several weeks.

Caution: Solution is stable only for 1 week at 4 °C.

50 % Glycerol in 20 mM Tris-HCl (pH 7.5), 1 mM MgCl₂:

a. 0.48 g of Tris-HCl in 100 ml of distilled water, adjust pH to 7.4 (= 40 mM)

b. 50 ml of Glycerol 100 % + 50 ml of 40 mM Tris-HCl (20 mM)

c. Add 100 ul of 1M MgCl₂ solution.

Collagenase / DNase solution:

1 mg/ml Collagenase, 0.1 mg/ml DNase in 1X HBSS (with Ca, Mg)

For 10 ml:

Collagenase (type I) (Sigma C0130) 10 mg

1 mg/ml DNase stock solution 1 ml

HBSS (with Ca, Mg) 9 ml

To be preheated in 37 °C water bath before use.

Caution: Prepare freshly every time (Stable only for few days)

Collagenase solution:

1 mg/ml Collagenase in 1X HBSS (with Ca, Mg)

For 10 ml:

Collagenase (type I) 10 mg

HBSS (with Ca, Mg) 10 ml

To be preheated in 37 °C water bath before use.

Caution: Prepare freshly every time (Stable only for few days)

EDTA 2 mM:

EDTA 7.44 mg in 10 ml HBSS (without Ca, Mg)

To be preheated in 37 °C water bath before use.

Citrate buffer 10X:

110 mM Sodiumcitrate in ddH₂O
with 2N NaOH to pH 6

PBS:

2.74 M NaCl
54 mM KCl
30 mM KH₂PO₄
130 mM Na₂HPO₄
in ddH₂O

Adjust pH to 7.5 with HCl

TBS (10x):

Tris	24.23g
NaCl	80.06g
Conc. HCL	around 17.5ml

Make up volume to 1000ml (pH 7.6)

Eidesstattliche Versicherung

VANKAYALA RAMAIAH, SANTHOSH KUMAR

Name, Vorname

Ich erkläre hiermit an Eides statt,

dass ich die vorliegende Dissertation mit dem Thema

EXTRACELLULAR HISTONES CAUSE VASCULAR NECROSIS IN SEVERE GLOMERULONEPHRITIS

selbständig verfasst, mich außer der angegebenen keiner weiteren Hilfsmittel bedient und alle Erkenntnisse, die aus dem Schrifttum ganz oder annähernd übernommen sind, als solche kenntlich gemacht und nach ihrer Herkunft unter Bezeichnung der Fundstelle einzeln nachgewiesen habe.

Ich erkläre des Weiteren, dass die hier vorgelegte Dissertation nicht in gleicher oder in ähnlicher Form bei einer anderen Stelle zur Erlangung eines akademischen Grades eingereicht wurde.

Munich, 18.02.2015

Ort, Datum

Santhosh Kumar VR

Unterschrift Doktorandin/Doktor